SYNTHESIS AND ANTIOXIDANT ACTIVITY

OF PRENYLATED XANTHONES DERIVED

FROM 1,3,6-TRIHYDROXYXANTHONE

CHAN SIEW LING

BACHELOR OF SCIENCE (HONS.) CHEMISTRY

FACULTY OF SCIENCE

UNIVERSITI TUNKU ABDUL RAHMAN

MAY 2013

CHAN SIEW LING

B.Sc. (Hons.) Chemistry

2013

SYNTHESIS AND ANTIOXIDANT ACTIVITY

OF PRENYLATED XANTHONES DERIVED

FROM 1,3,6-TRIHYDROXYXANTHONE

By

CHAN SIEW LING

A Project Report Submitted to the Department of Chemical Science,

Faculty of Science,

Universiti Tunku Abdul Rahman

in Partial Fulfillment of the Requirement for the

Degree of Bachelor of Science (Hons.) Chemistry

May 2013

ABSTRACT

SYNTHESIS AND ANTIOXIDANT ACTIVITY
OF PRENYLATED XANTHONES DERIVED
FROM 1,3,6-TRIHYDROXYXANTHONE

Chan Siew Ling

In this study, a xanthonic block 1,3,6-trihydroxyxanthone (**15**) and two new prenylated xanthones, namely 1-hydroxy-2-(3-methylbut-2-en-1-yl)-3,6-bis((3-methylbut-2-en-1-yl)oxy)-9*H*-xanthen-9-one (**50**) and 2,2,4,4-tetrakis(3-methylbut-2-en-1-yl)-6-((3-methylbut-2-en-1-yl)oxy)-1*H*-xanthene-1,3,9 (2*H,4H)*-trione (**51**) were successfully synthesized. The structure of the compounds was established by means of IR, UV-Vis, MS, and NMR (^{1}H, ^{13}C, HMQC, and HMBC) techniques.

The xanthonic block was synthesized via Grover, Shah and Shah reaction in the presence of Eaton's reagent which was subsequently used as starting material for direct prenylation by using potassium carbonate in *t*- butyl alcohol.

Antioxidant properties of the compounds were evaluated by using DPPH radical scavenging assay, and the results indicated that 1,3,6-trihydroxyxanthone (**15**) exhibited weak antioxidant effect with IC_{50} value of 167 μg/mL, whereby the two prenylated derivatives, compounds **50** and **51** gave no significant activities.

ABSTRAK

Dalam kajian ini, satu blok xanthone iaitu 1,3,6-trihidroksixanthone (**15**) dan dua prenilasi xanthone yang baru, iaitu 1-hidroksi-2-(3-metil-but-2-enil)-3,6-bis(metil-but-2-eniloksi)-9*H*-xanthen-9-one (**50**), dan 2,2,4,4-tetrakis(3-metil-but-2-enil)-6-(3-metil-but-2-eniloksi)-1*H*-xanthen-1,3,9(2*H*,4*H*)-trione (**51**) telah berjaya dihasilkan dan dikenalpastikan. Struktur sebatian-sebatian tersebut telah dikenalpasti dengan menggunakan kaedah spektroskopi, iaitu IR, UV-Vis,, MS dan NMR (^{1}H, ^{13}C, HMQC, and HMBC).

Blok xanthone telah disintesis melalui reaksi Grover, Shah, dan Shah dengan menggunakan reagen Eaton. Hasil sintesis tersebut telah digunakan sebagai bahan permulaan untuk kerja prenilasi dalam larutan *t-* butil alkohol dengan menggunakan kalium karbonat.

Semua xanthone yang dihasilkan telah diuji aktiviti antioksidan masing-masing dengan menggunakan kaedah DPPH dan didapati hanya 1,3,6-trihidroksixanthone (**15**) menunjukkan aktiviti yang lemah manakala dua prenilasi xanthone **50** dan **51** tidak memberikan aktiviti antioksidan yang efektif.

ACKNOWLEDGEMENT

First and foremost, I would like to express my sincere gratitude to Assistant Professor Dr. Lim Chan Kiang for his guidance, advice, patience and unselfish as well as unfailing support as my dissertation supervisor. I have gained a lot of extra knowledge during the research period.

Special thanks to my senior, Lai Chooi Kuan and my teammates, Tung Chui Hoong and Kheo Chee Hoe, for their unconditional guidance and help. It has been a pleasant experience to share scientific discussion and problem solving with them.

Last but not least, my gratitude goes to my parents and friends for their invaluable support and encouragement that help me to go through hardships throughout the course of this project. Without all of them, my dissertation and research would not be accomplished successfully.

DECLARATION

I hereby declare that the project report is based on my original work except for quotations and citations which have been duly acknowledged. I also declare that it has not been previously or concurrently submitted for any other degree at UTAR or other institutions.

_____

(CHAN SIEW LING)

APPROVAL SHEET

This project report entitled "**SYNTHESIS AND ANTIOXIDANT ACTIVITY OF PRENYLATED XANTHONES DERIVED FROM 1,3,6-TRIHYDROXYXANTHONE**" was prepared by CHAN SIEW LING and submitted in partial fulfillment of the requirements for the degree of Bachelor of Science (Hons.) in Chemistry at Universiti Tunku Abdul Rahman.

Approved by:

_____   Date: _____

(Dr. Lim Chan Kiang)

Supervisor

Department of Chemical Science

Faculty of Science

Universiti Tunku Abdul Rahman

FACULTY OF SCIENCE

UNIVERSITI TUNKU ABDUL RAHMAN

Date: _____

PERMISSION SHEET

It is hereby certified that **CHAN SIEW LING** (ID No: **09ADB03483**) has completed this report entitled "**SYNTHESIS AND ANTIOXIDANT ACTIVITY OF PRENYLATED XANTHONES DERIVED FROM 1,3,6-TRIHYDROXYXANTHONE**" supervised by Assistant Professor Dr. Lim Chan Kiang from the Department of Chemical Science, Faculty of Science.

I hereby give permission to my supervisor to write and prepare manuscript of these research findings for publishing in any form, if I do not prepare it within six (6) month time from this date, provided that my name is included as one of the authors for this article. The arrangement of the name depends on my supervisor.

Yours truly,

_____

(CHAN SIEW LING)

TABLE OF CONTENTS

LIST OF TABLES

LIST OF FIGURES

LIST OF ABBREVIATIONS

α	Alpha
δ	Chemical shift in ppm
^{o}C	Degree Celsius
^{1}H	Proton
^{13}C	Carbon-13
cm	Centimetre
μL	Microlitre
μm	Micromitre
%	Percent sign
λ_{max}	Wavelength maxima in nm
A_0	Absorbance of negative control in DPPH assay
A_1	Absorbance of test compound in DPPH assay
Ace	Acetone
$AlCl_3$	Aluminium chloride
AIBN	Azobisisobutyronitrile
Aq.	Aqueous
C	Carbon
CCl_4	Carbon tetrachloride
C-prenylated	Carboprenylated
CH_3SO_3H	Methanesulfonic acid
CO_2	Carbon dioxide
CoA	Coenzyme A
Cu	Copper

dd	Doublet of doublet
d	Doublet
DCM	Dichloromethane
DMF	Dimethylformamide
DMSO	Dimethyl sulfoxide
DNA	Deoxyribonucleic acid
DPPH	2,2-diphenyl-1-picrylhydrazyl
EA	Ethyl acetate
et. al.	et alii (and others)
$FeCl_3$	Iron (III) chloride
g	Gram
G. mangostana	*Garcinia mangostana*
GSS	Grover, Shah and Shah
h	Hour
H	Hydrogen
H_2O	Water
HBF_4	Fluoroboric acid
HCl	Hydrochloric acid
Hex	Hexane
HMBC	Heteronuclear Multiple Bond Coherence
HMQC	Heteronuclear Multiple Quantum Coherence
HRESIMS	High Resolution Electrospray Ionization Mass Spectrometry
HSCoA	Coenzyme A
IBX	2-Iodoxybenzoic acid
IC_{50}	50% Inhibitory Concentration
IR	Infrared

J	Coupling constant in Hz
KBr	Potassium bromide
K_2CO_3	Potassium carbonate
KOH	Potassium hydroxide
MAOS	Microwave-assisted organic synthesis
Me	Methyl
mg	Milligram
MHz	Megahertz
ml	Millilitre
min	Minute
mmol	Milimole
mol	Mole
MW	Microwave
MS	Mass Spectrometry
NBS	N-Bromosuccinimide
nBuLi	n-Butyllithium
nm	nanometer
NMR	Nuclear Magnetic Resonance
2D-NMR	Two dimensional Nuclear Magnetic Resonance
o	*Ortho*
O-prenylated	Oxyprenylated
P_2O_5	Phosphorus pentoxide
PPA	Polyphosphoric acid
ppm	Parts per million
$POCl_3$	Phosphorus oxychloride
r.t.	Room temperature

R_f	Retention factor
ROS	Reactive oxygen species
s	Singlet
SAR	Structure-activity relationship
sBuLi	Sec-butyllithium
t	Triplet
THF	Tetrahydrofuran
TLC	Thin Layer Chromatography
TMS	Tetramethylsilane
UV-Vis	Ultraviolet-Visible
$ZnCl_2$	Zinc chloride

CHAPTER 1

INTRODUCTION

1.1 Introduction to Xanthones

Xanthone (**1**) is a type of chemical compounds which can be found naturally from living organisms or via chemial synthesis. In Greek word, "xanthos" means yellow and it becomes the origin name for this yellow organic heterolytic compound. In 2004 IUPAC provisional recommendations, xanthone is scientifically known as 9*H*-xanthen-9-one with its given molecular formula of $C_{13}H_8O_2$.

Xanthone is typically a tricyclic aromatic ring system, which consists of two benzene rings fused to a pyron-4-one ring to form dibenzo-γ-pyrone as basic skeleton (Esteves, Santos, Brito, Silva and Caveleiro, 2011). The two benzene rings are identical in terms of their molecular symmetry where both C-1(C-8) and C-4(C-5) are acidic sites due to the withdrawing effect of the electronegative oxygen atoms (Odrowaz-Sypbiewski, Tsoungas, Varvounis and Cordopatis, 2009). The carbon numbering is often numbered according to biosynthetic convention. Thus, xanthone skeleton is numbered with carbons 1 - 4 being assigned as acetate-derived ring and carbons 5 - 8 being assigned as

shikimate-derived ring, whereas the other carbon atoms are numbered as 4a, 8a, 9, 9a, and 10a for the sake of elucidation purposes.

Due to its conjugated ring systems, xanthone is essentially planar in the solid state with small deviation in some cases due to substituent effects (Gales and Damas, 2005). Besides, the two aromatic rings connected by a carbonyl group and an oxygen bridge give fused ring system, which limits the xanthone framework toward free rotation. Hence, there is an increase in the rigidity of the framework, and capacity to resist a higher temperature while maintaining its integrity (Gales and Damas, 2005).
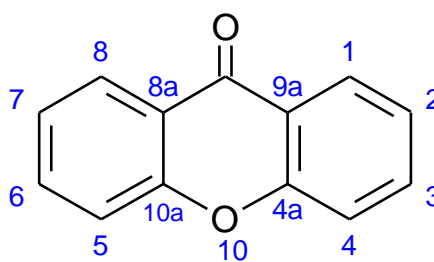
(1)

Figure 1.1: The basic skeletal structure of xanthone

1.2 Background of Xanthones

Xanthones were first discovered when scientists started to carry out studies on the health benefits and antioxidant potency of mangosteen based on its traditional medical uses by the indigenous peoples (Shifko, 2010). In the

middle of 19th century, the first xanthone derivative (mangostin) was isolated from the fruit hulls of *G. mangostana* by Dr. W. Schmid, a German chemist. He coined the word xanthone (Greek word for yellow) to name the new chemical class due to the bright yellow colour of mangostin extract (Rai and Chikindas, 2011). In fact, "naked" xanthone skeleton cannot be found naturally. In 1860, the first synthetic xanthone was obtained by Kolbe and Lautermann by the use of phosphorus oxychloride in sodium salicylate via condensation of phenol and salicylic acid (Hepworth, 1924).

Lesch and Bräes (2004) described the xanthone moiety as 'privileged structure' (El-seedi, et al., 2009), since the ring systems are susceptible to substitution of hydroxyl, methoxyl, prenyl groups at different positions on the benzene which leads to a large variety of analogues (Demirkiran, 2007).

Xanthones were commonly used as folk remedies in Southeast Asia. In 1983, scientists discovered that some xanthones were found to demonstrate anti-viral, anti-bacteria, anti-fungal, and anti-parasitic effects. In later years, scientists also discovered garcinone E. to be *in vitroly* outperformed and was listed as the top six potential cancer chemotherapy agent (Farrell, 2006). Until today, more than 2400 scientific papers were published in PubMed with relation to clinical and pharmacological studies, and synthesis and isolation of new xanthone derivatives.

1.3 Distribution of Xanthones

Xanthone is a secondary plant metabolite that can be obtained naturally from higher plants family, fungal, and bacteria kingdoms. In fact, majority of them have been found in just two families of higher plants – *Guttiferae* and *Gentianaceae.* In 1961, Roberts submitted a comprehensive review reporting that fungi or lichen could be a potential source of xanthones besides higher plants. Apart from that, isolation of xanthones from fossil fuels was also reported, which possibly suggest the considerable stability of the xanthone core (Masters and Bräse, 2012).

Many researches were conducted in past two decades to extract and isolate natural xanthones, and around 200 xanthones were identified. Among the plant species, the purple fruit of *Garcinia mangostana L.* is well known for its rich xanthone content and so far more than 40 xanthones have been reported. The pericarp of mangosteen has been popularly used as medicine for skin infections, and wounds treatment in Southeast Asia (Zarena and Sankar, 2009). The major constituent reported in the pericarp is prenylated xanthone derivatives. Other than that, isoprenylated xanthone isolated from *Cudrania tricuspidata* root bark has also been reported for its use as important folk remedies for cancer treatment in Korea (Lee, et al., 2005) whereas *Cratoxylum cochinchinense* (Yellow Cow Wood) has been used as Chinese traditional medicine to treat fever, coughing, diarrhea, itching, ulcers, and abdominal complaints (Akrawi, Mohammed, Patonay, Villinger and Langer, 2012).

1.4 Classification of Xanthones

There are five major groups of xanthone derivatives: (1) simple oxygenated xanthones from mono- to hexaoxy- substituent, (2) xanthone glycosides (*O*-glycosides & *C*-glycosides) from lichen *Umbilicaria proboscidea* (Muggia, Schmitt and Grube, 2009), (3) prenylated and related xanthones from *Garcinia virgata* (Merza, et al., 2004), (4) xanthonolignoid, with a phenylpropane skeleton linked to an *ortho*-dihydroxyxanthone by a dioxane ring (Tanaka, Kashiwada, Kim, Sekiya and Ikeshiro, 2009), and (5) miscellaneous (Chun-Hui, Li, Zhen-ping, Feng and Jing, 2012).

Among five groups of xanthone derivatives, prenylated xanthones have been reported of having high therapeutic value in treatment of diseases (Castanheiro and Pinto, 2009). The presence of prenyl side chains is associated with enhanced biological functionality as compared with non-prenylated analogues (Castanheiro and Pinto, 2009). The phenolic nature of xanthone makes it a strong scavenger of free radical in biological system. According to Jiang, Dai and Li (2004), xanthone derivatives are commonly found in Chinese herbs such as *Swertia davida Franch* which are used in the treatment of inflammation, allergy, and hepatitis. Therefore, prenylated xanthones either extracted from natural sources or synthesized through chemical reactions have become a potential source of therapeutic agent for pharmacological studies.

1.5 Natural and Synthetic Xanthones

Xanthones are phytonutrient compounds which can be isolated from some particular plants, fungi, and lichen. Besides, they can also be synthesized through chemical reactions to obtain specifically modified structure of xanthone derivatives.

1.5.1 Biosynthesis of Xanthones

Review by Masters and Bräse (2012), indicated that xanthone biosynthesis occurs in fungi and lichens are distincted from that of higher plants. In fungi and lichens, the xanthone unit is wholly derived from a polyketide (**3**) which is resulted from head-to-tails linkage of acetate units (**2**) shown in Figure 1.2. C_{16} polyketide is biosynthesized through Claisen condensation of 8 units of acetate by polyketide synthases. Then, cyclization of carbon chain through aldol addition leads to the formation of the fused rings, anthraquinone (**4**), followed by oxidative cleavage to form benzophenone (**5**). The benzophenone intermediate (**5**) subsequently undergoes either (i) direct cyclization to form xanthone (**6**) or (ii) allylic rearrangement to give of polyhydrogenated xanthone (**7**).

In higher plants, the xanthone nucleus is formed via mixed biosynthesis pathway whereby the ring A (carbon 1 - 4) is acetate-derived while the ring B (carbon 5 - 8) is shikimate-derived. Masters and Bräse (2012) stated that from the study of xanthone biological synthesis in *Gentiana lutea*, polyhydroxyxanthone is synthesized from acetate and hydroxybenzoic acid as shown in Figure 1.3. 3-Hydroxybenzoic acid (**7**) derived from phenylalanine is coupled with 3 acetate units (**2**) to form shikimic acid derivative (**8**). Aromatation of shikimic acid derivative (**8**) leads to the formation of benzophenone intermediate (**9**). Due to its freely rotation at ring B, benzophenone (**9**) is then undergoing divergent oxidative phenolic coupling to form trihydroyxanthones (**10**, **11**) with different position of hydroxyl attached.
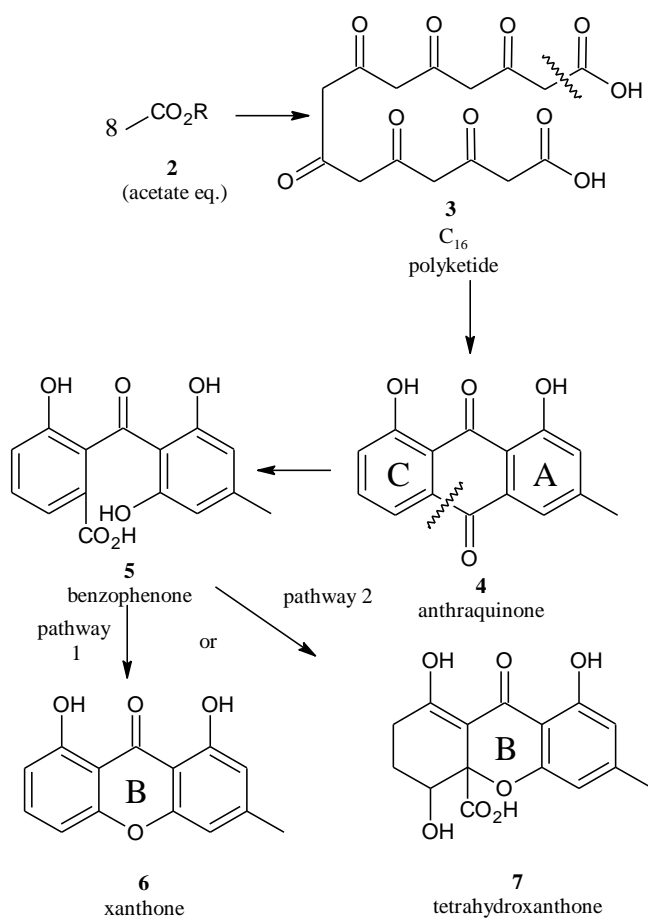
Figure 1.2: Xanthone synthesis in fungi and lichens

Figure 1.3: Xanthone synthesis in higher plants (*Gentiana lutea*)

`

1.5.2 Chemical Synthesis of Xanthones

There are some limitation in biosynthesis of xanthones, because extracts produce only limited types of xanthone derivatives in relatively small quantity. The success of Kolbe and Lautermann in synthesizing the first xanthone in

1860 (Hepworth, 1924) had opened new avenue to chemical synthesis of xanthone by using different reaction parameters and reagents. One of the benefits of chemical synthesis is that chemists are able to design and synthesize some desired xanthone structures that cannot be found in nature. Development of new and diverse xanthone derivatives which are difficult to be accomplished through biosynthesis due to the limitation of biosynthetic pathways can be achieved through chemical synthesis. In chemical synthesis, the percentage yield of product can be optimized by altering the parameters of synthesis. There are various methods which have been developed for xanthone synthesis and their detailed descriptions are elaborated in Chapter 2.

1.6 Objectives

The objectives of this study include:

- To synthesize 1,3,6-trihydroxyxanthone and its prenylated derivatives.

- To purify the synthetic compounds through column chromatography.

- To elucidate the isolated compounds by using various spectroscopic and spectrometric methods such as IR, UV-Vis, MS, and 1D- & 2D-NMR (^{1}H, ^{13}C, HMQC and HMBC).

- To evaluate antioxidant activities of synthetic xanthones via DPPH method.

CHAPTER 2

LITERATURE REVIEW

2.1 Synthesis Approaches of Xanthones

The very first method used for the synthesis of xanthone derivatives was introduced by Michael in 1833. This method involved the distillation of a mixture of phenol, salicylic acid and acetate anhydrides to produce hydroxyl-xanthone (Naidon, 2009) . However, this method gave poor yielding of product and the reaction was not under ambient condition. There was high possibility of side reactions to occur such as decarboxylation, and auto-condensation (Naidon, 2009).

2.1.1 Classical Methods of Xanthone Synthesis

There are three classical methods commonly used in the synthesis of xanthonic building blocks which are Grover, Shah, and Shah (GSS) reaction, synthesis via a benzophenone intermediate, and synthesis via diaryl ethers.

2.1.1.1 Grover, Shah, and Shah (GSS) Reaction

GSS reaction was introduced in 1954 by Grover, Shah, and Shah in the synthesis of 1,3,6-trihydroxyxanthones (**15**) as shown in Figure 2.1. The polyhydroxyxanthone (**15**) was conveniently obtained from reaction of 2,4-dihydroxybenzoic acid (**12**) and phloroglucinol (**13**) in the presence of zinc chloride and phosphorus oxychloride under a mild condition. Condensing agent such as phosphorus oxychloride coupled with zinc chloride has been proven for its effectiveness in the synthesis of hydroxyxanthone via cyclization of hydroxybenzophenone intermediate as compared with Nenki's reaction which used fused zinc chloride alone (Grover, Shah and Shah, 1955). However, there were some limitations in GSS reaction in which some benzophenone intermediates failed to undergo cyclization to give product. This synthesis produced relatively low yield (13%) as compared to other methods. (Naidon, 2009; Mengwasser, 2011)
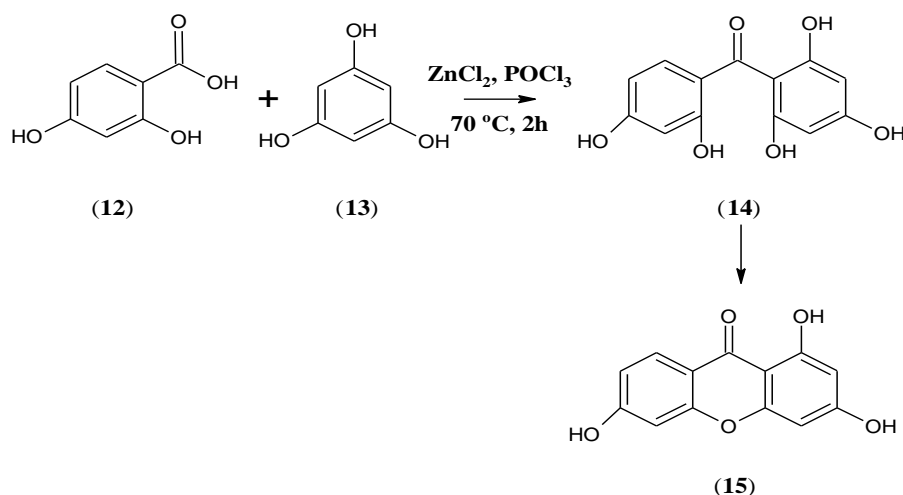
Figure 2.1: 1,3,6-Trihydroxyxanthone synthesized via Grover, Shah, and Shah (GSS) method

2.1.1.2 Synthesis via Benzophenone Intermediate

In year 1932, Quillinan and Scheinmann successfully synthesized numerous xanthone analogues which were difficult to be obtained through GSS reaction (Naidon, 2009; Mengwasser, 2011). The synthesis of 2-hydroxy-2'-methoxylbenzophenone (**18**) was reported to be more efficiently done through Friedel-Crafts acylation of substituted benzoyl chloride (**16**) with anisole (**17**) as shown in Figure 2.2. The reaction via elimination of methanol in the presence of alkaline medium gave xanthone (**1**) (Naidon, 2009). As reported by Pedro and his co-workers (2002), cyclization of benzophenone intermediate (**18**) was carried out through a dehydrative or oxidative process.
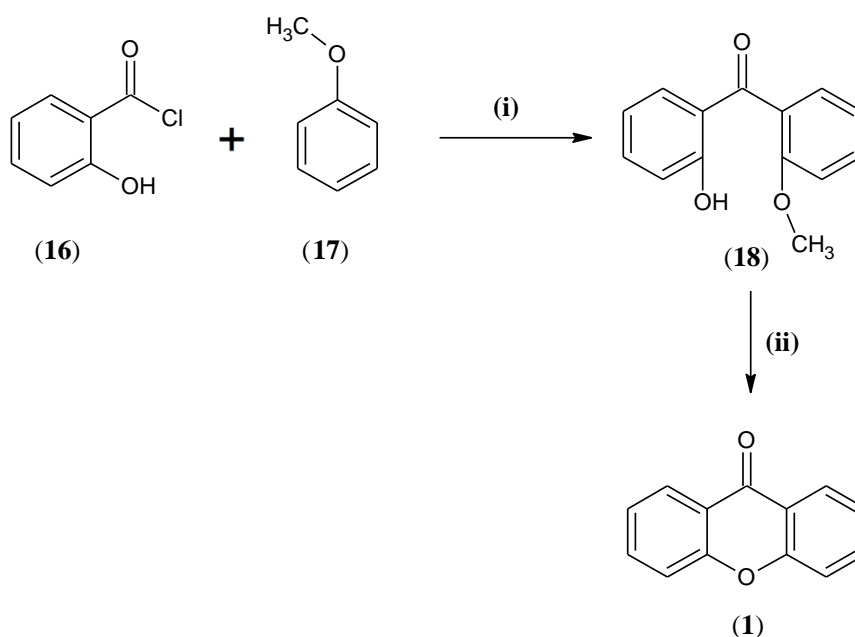
Figure 2.2 : Synthesis route for xanthone. Reagents and conditions:

(i) AlCl₃, dry ether, r.t., 1h; (ii) NaOH, methanol, reflux, 6h

2.1.1.3 Synthesis via Diaryl Ethers (Ullmann Coupling Reaction)

Ullmann coupling reaction was commonly used to synthesize diphenyl ether intermediate from phenol or phenolate (**20**) with *o*-halogenated benzoic acid (**19**) (Esteves, Santos, Brito, Silva and Caveleiro, 2011) as shown in Figure 2.3. The intermediate of 2-aryloxybenzoic acids (**21**) was then undergoing cylco-acylation to form methoxyxanthone (**22**) (Naidon, 2009; Mengwasser, 2011). However, the disadvantage of this method was a low yield of product obtained. The diaryl ether method carried out by Pedro and his co-workers (2002), involved the formation of xanthone middle ring through one-step conversion from biphenyl ether intermediate in the presence of acetyl chloride.
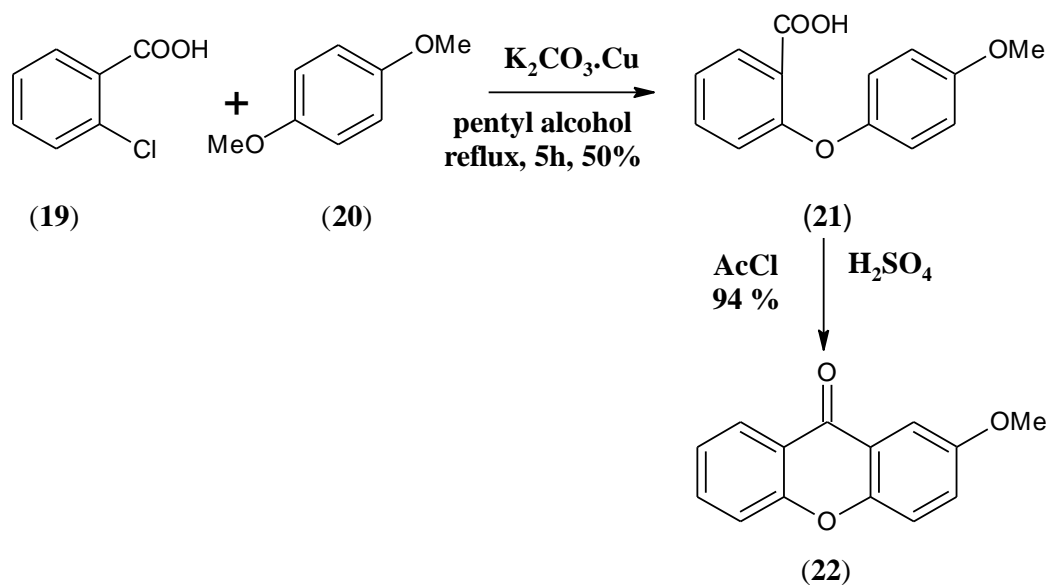
Figure 2.3: Ulmann ether synthesis of methoxyxanthone

2.1.2 New and Modified Methods

Although the classical methods to synthesize xanthone framework are still in use nowadays, new and modified methods have been developed in this decade to improve the product yield. The aims of the new methods are to reduce the steps in the synthesis and to put the reaction under a milder condition. Different experimental parameters are modified in order to boost up the yield of product.

2.1.2.1 Acyl Radical Cyclization

Kraus and Liu, 2012 introduced a new method in xanthone synthesis through acyl radical cyclization to form polyhydroxyxanthone. They reported that quinone (**25**) was synthesized via a coupling reaction of acetal (**23**) with bromoquinone (**24**) in the presence of K_2CO_3 in DMF followed by hydrolysis with aqueous HCl. Subsequent cyclization of quinone (**25**) gave xanthene-1,4,9-trione intermediate (**26**). Later, this intermediate (**26**) was catalytically reduced to form xanthone (**28**) in low yield. As an alternative, a higher yield was obtained by reacting the intermediate (**26**) in the presence of Zn to give hydroxybenzophenone (**27**) which was then heated in DMF at 180 °C for 16 hours to give xanthone (**28**) in a higher yield as shown in Figure 2.4 (Kraus and Liu, 2012) .
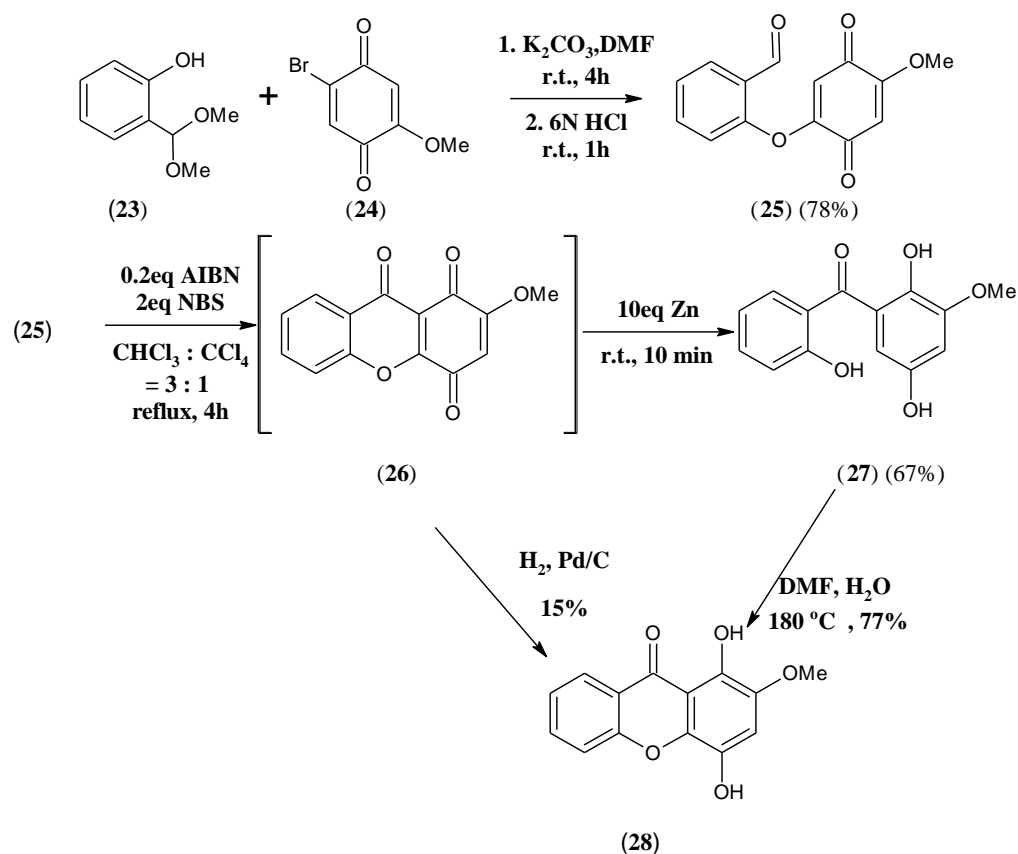
Figure 2.4: Synthesis of polyhydroxyxanthone through acyl radical cyclization of acetal and bromoquinone

2.1.2.2 Modified Grover, Shah and Shah (GSS) Reaction

In this modified method, Eaton's reagent, comprising of a mixture of phosphorus pentaoxide – methanesulfonic acid in the ratio of 1:10 by weight is used instead of phosphorus oxychloride – zinc chloride catalysis used in the conventional GSS (Eaton, Carlson and Lee, 1973; Sousa and Pinto, 2005). This modified method has been proven to give a better yield as the reagent provides a more effective route of synthesis (Yang, et al., 2012). According to Sousa

and Pinto (2005), Eaton's reagent which is known as acylation catalyst has been revealed to be an excellent condensing agent for the reaction of phloroglucinol (**29**) and 3-methylsalicylic acid (**30**), and provided high yield (90%) of xanthone (**31**) without detectable amount of benzophenone (**32**). Table 2.1 shows the comparison between conventional GSS reaction and modified GSS reaction.
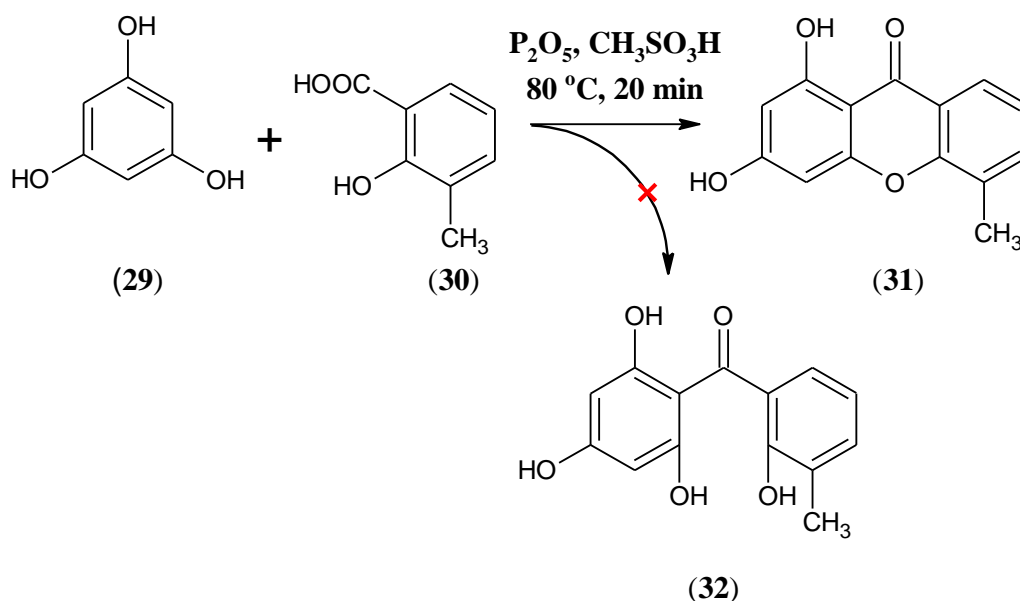
Figure 2.5: Modified Grover, Shah and Shah (GSS) reaction

Table 2.1: Comparison between classical GSS and modified GSS reaction

	Classical GSS reaction	**Modified GSS reaction.**
Reagent used :	Zinc chloride + phosphorus oxychloride	Eaton's reagent
Temperature :	~70 °C	~80 °C
Yield :	Low (13%)	High (90%)
Time :	2 hours	20 minutes

2.2 Synthesis Approaches of Prenylated Xanthone

2.2.1 Direct Prenylation

Molecular modifications via prenylation of xanthones are commonly carried out to improve bio-efficacy of xanthones. This involves nucleophilic substitution reaction of the xanthonic building blocks with prenyl bromide in various alkaline media (Castanheiro and Pinto, 2009) which resulted *O*- and *C*-prenylations.

2.2.1.1 *O*-Prenylation

Study by Castanheiro and Pinto (2009) indicated that direct prenylation with potassium carbonate (K_2CO_3) in an organic medium afforded prenyloxy xanthones (**34, 35**) via *O*-prenylation as shown in the Figure 2.6. Another study by Subba-Rao and Raghawan in 2001 revealed a 80% high yield of *oxy*-prenyl xanthone (**37**) was obtained resulting from reaction of 1,3-dihydroxyxanthone and prenyl bromide in the presence of anhydrous K_2CO_3 in acetone (Figure 2.7). In some cases, diprenylated derivative (**40**) with one prenyl group on the carbon adjacent to the prenyloxy substituent was also obtained (Figure 2.8).
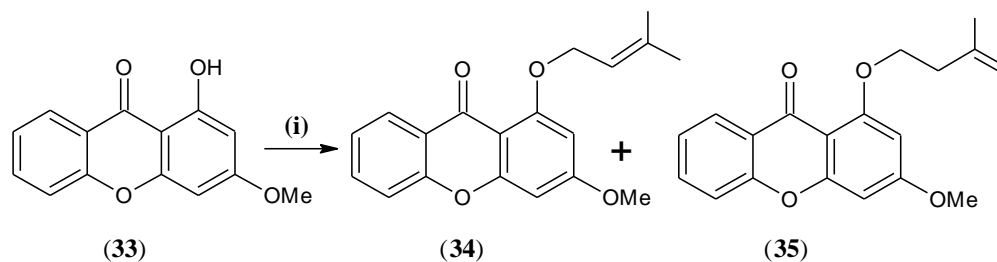
Figure 2.6: *O*-prenylation of xanthone building block. Reagent and conditions: (i) Prenyl bromide, K₂CO₃, DMF, reflux, 48h (34, 60%; 35, 30%)
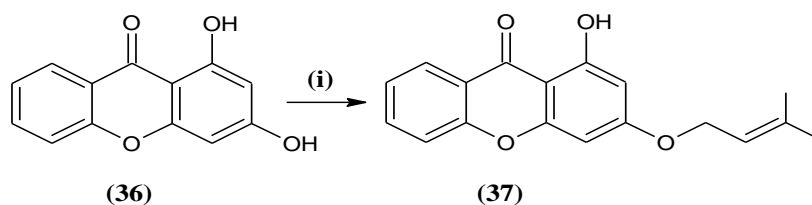
Figure 2.7: *O*-prenylation of xanthone building block. Reagent and conditions: (i) Prenyl bromide, K₂CO₃, acetone, reflux, 6h (37, 80%)
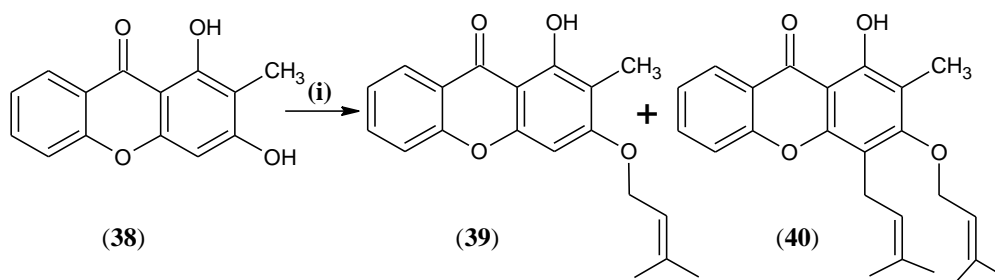
Figure 2.8: *O*-prenylation of xanthone building block. Reagent and conditions: (i) Prenyl bromide, K₂CO₃, acetone, reflux, 8h (39, 46%; 40, 3%)

2.2.1.2 *C*-Prenylation

Reaction of 1,3,5-trihydroxyxanthone with prenyl bromide in the presence of potassium hydroxide solution produced two mono-substituted (**41, 42**) and one di-substituted (**43**) *C*-prenylated xanthones as shown in Figure 2.9 (Helesbeux, et al., 2004).
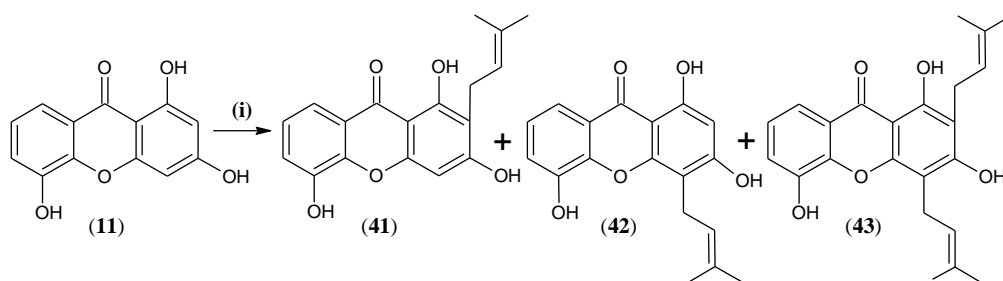
Figure 2.9: *C*-prenylation of xanthone building block. Reagent and conditions: (i) Prenyl bromide, aq. KOH 10%, r.t., overnight (41, 11%; 42, 13%; 43, 10%)

Direct prenylation normally gave a low product yield and long reaction time. As a solution to the problem, Castanheiro and his co-workers (2009) revealed that microwave-assisted organic synthesis (MAOS) was found to accelerate the reaction rate by reducing the reaction time from eight hours to one hour. Moreover, the use of microwave irradiation improved the percentage yield of selected products such as *oxy*-prenylated xanthone (**39**) from 46% to 83%.

2.2.2 Indirect Prenylation

The prenylated xanthone was furnished from a protected aryl (**44**) and benzaldehyde (**45**) by using PPh$_3$/CCl$_4$, which is the key of cyclization. The benzophenone (**47**) was produced from the reaction of compounds **44** and **45**, which then underwent cyclization to form prenylated xanthone (**48**) as shown in Figure 2.10 (Sousa and Pinto, 2005; Castanheiro and Pinto, 2009).
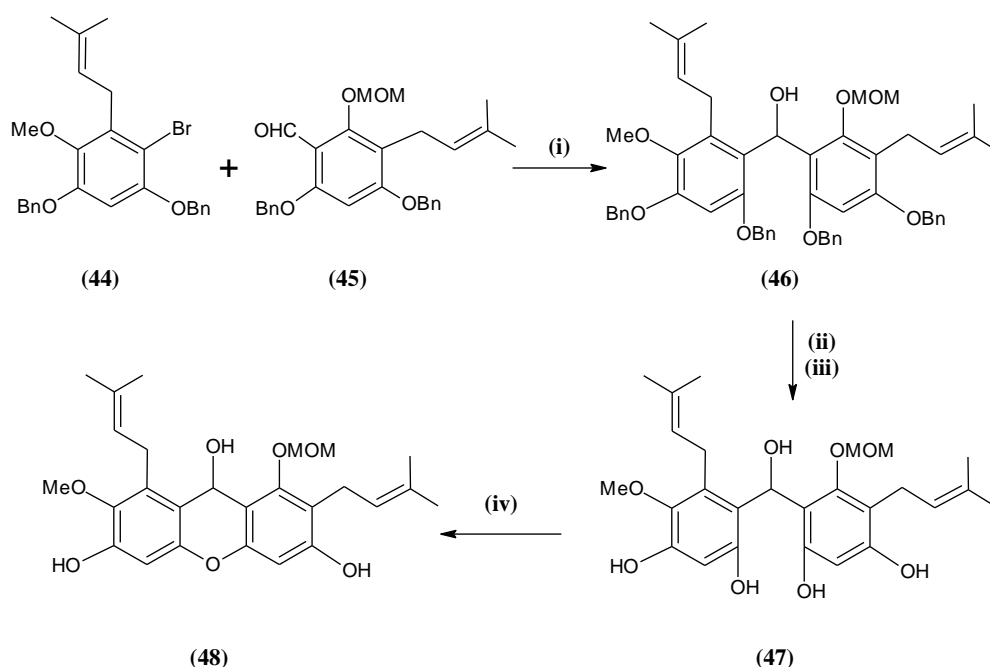
Figure 2.10: Indirect prenylation of building block. Reagent and conditions: (i)sBuLi, THF, -78°C, 49%; (ii) IBX, toluene/DMSO (1/1), r.t., 76%; (iii) 10% Pd/C, HCO$_2$NH$_4$, acetone, r.t., 63%; (iv) PPh$_3$, CCl$_4$, THF, r.t., silica gel, 43%.

2.3 Pharmacological Properties of Xanthones

A lot of researches have been reported in this decade on the isolation and synthesis of xanthone derivatives due to their high therapeutic value. Xanthones exhibit a wide range of pharmacological properties as they serve their important biological role as electron donors (Lee, et al., 2005). The followings are some of the pharmacological properties of xanthones which have drawn attention of many scientists, such as anti-oxidant, anti-inflammatory, anti-malarial, and cytotoxic activities.

2.3.1 Anti-Oxidant Activities

Oxidation is a biological process in human body and living organisms which produces free radicals that are harmful and may be a leading cause of various human diseases (Zarena and Sankar, 2009). During this biochemical process, free radicals known as reactive oxygen species (ROS) are produced in the human tissues. ROS such as superoxide radicals and hydrogen peroxide can lead to severe damage on DNA, protein and lipids if the amount of ROS overwhelmed the capacity of body's defence system to deactivate them. This can lead to cellular and metabolic injury, and accelerating aging, cancer, cardiovascular diseases, and inflammation (Cheng, Huang, Hour and Yang, 2011).

Antioxidant such as xanthone was tested to show stronger antioxidant effect than vitamin C and E. Recent researches also revealed xanthone to play a preventive role against diseases caused by ROS (Lee, et al., 2005). Considerable interest has been paid to plant sources for antioxidants because synthetic antioxidants such as butylated hydroxyanisole (BHA) used in foods preservation is subjected to strict regulation due to the potential health hazards imposed (Zarena and Sankar, 2009).

A review by Lee, et al. (2005), showed that a stronger free radical scavenging activity occurred in xanthones is closely related to the dihydroxyl groups present in the shikimate-derived ring. The isolated xanthones from *G. mangostana* exhibit potent antioxidant effect toward free radical. In the research carried out by Jung and his co-workers (2006), among thirteen isolated xanthones, five xanthones demonstrated a potent antioxidant activity. These five xanthones consist of one or more prenyl side chains attached to the phenolic rings. It is believed that prenylated xanthones with their phenolic nature demonstrate potent antioxidant activities, and hereby antioxidant activity of xanthone is the major concern in this study.

2.3.2 Anti-Inflammatory Activities

Inflammation is defined as the immune system's response to infection and injury which has been implicated in the pathogeneses of arthritis, cancer and

stroke, as well as cardiovascular disease (FitzGerald and Ricciotti, 2011). During the process of removing the offending factors and restoration of tissue structure and physiological function, it causes some cardinal signs such as rubor (redness), calor (heat), tumor (swelling) and dolor (pain). Thus, anti-inflammatory drug development becomes important in the search for new potential leads. Anti-inflammatory drugs are able to prevent the releasing of prostaglandins (PGs), the key role in the regulation of inflammation (Demirkiran, 2007). The well-known anti-inflammatory drugs, α- and β-mangostins isolated from *G.mangostana* were significantly found to reduce production of PGs in a dose-dependent manner (FitzGerald and Ricciotti, 2011).

2.3.3 Anti-Malarial Activities

Malaria is an infection disease that caused by protozoan parasites named *P. falciparum* which has affected over 80 per cent of the cases worldwide (Riscoe, Kelly and Winter, 2005). The malaria parasite digested hemoglobin within the red blood cells (RBCs) where they were shielded from the attack by human immune system. Up to 70 per cent of the haemoglobin were digested by *P. falciparum* whereby each ruptured RBC released about twenty young parasites to attack other normal RBCs (Lew, 2003). Research reported by Dodean, et al. (2008), showed that xanthones prevented invasion of parasites to hemoglobins by forming soluble complexes with heme.

For example, the xanthone 3,6-bis(ω-*N,N*-dienthylaminoamyloxy)-4,5-difluoroxanthone (F2C5) synthesized by Peyto and his co-workers (2008) consisted of a carbonyl bridge, which co-ordinated to the heme iron atom. The aromatic rings of xanthone showed π-π stacking with co-planar aromatic rings of the heme as shown in Figure 2.11. It was found that strong interaction between drug–heme complexes stabilized heme away from parasite digestion.
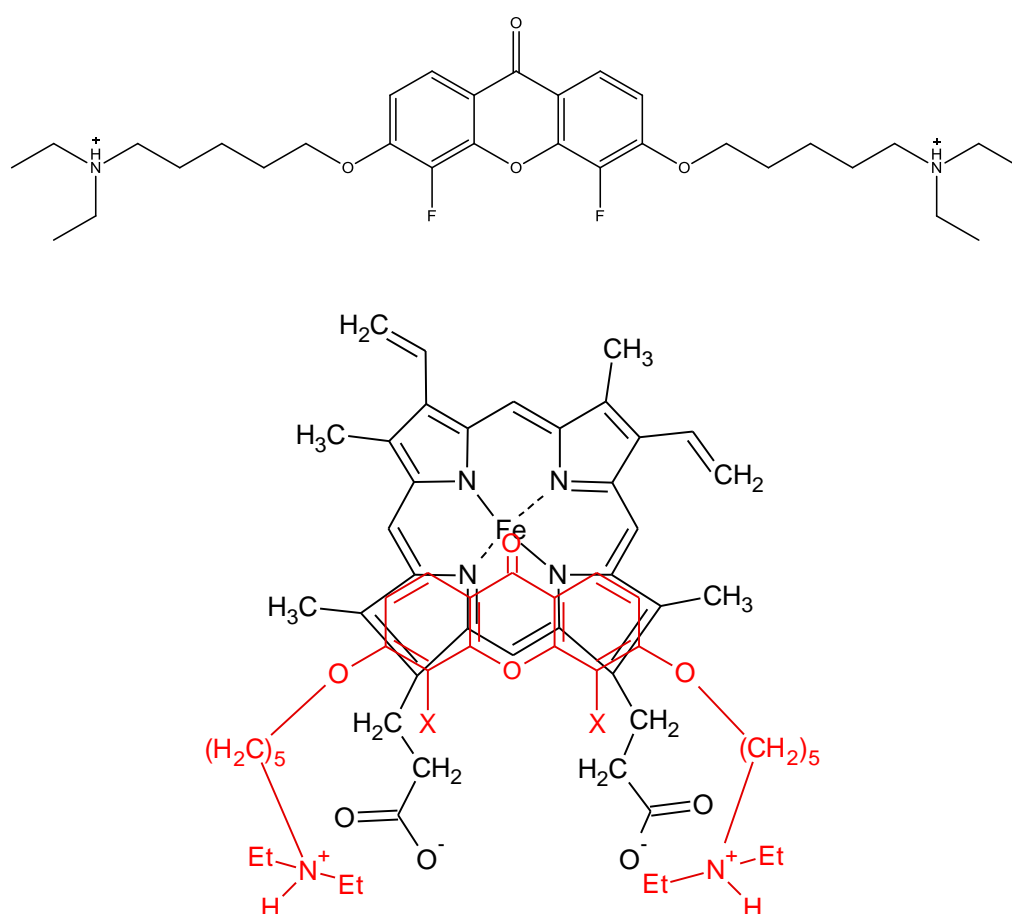
Figure 2.11: Model proposed for the possible docking orientation of F2C5 (shown in red) and heme

2.3.4 Cytotoxic Activities

Study by Ho and his co-workers (2002) revealed garcinone E to possess potent cytotoxic effect against lung carcinoma cancer. They also revealed garcinone E to exhibit a very broad spectrum of cytotoxic effects against a variety cancer cell lines (Ho, Huang and Chen, 2002). Besides, garcinone E was also reported to exhibit potent cytotoxic effect by inhibiting the growth of leukemia cell line (Pinto, Sousa and Nascimento, 2005).

2.4 Antioxidant Assay

2.4.1 DPPH Radical Scavenging Activity

DPPH (1,1-diphenyl-2-picrylhydrazyl) is a *N*-centred stable radical. Due to its simplicity and rapidity, DPPH assay becomes one of the most common antioxidant methods. The DPPH method is found not only to evaluate the electron or hydrogen atom-donating properties of antioxidants, but also the rate of reduction of the stable free radical of DPPH by antioxidants (Khanduja and Bhardwaj, 2003). Due to its odd electron, DPPH gives strong absorption maxima at 517 nm (Khanduja and Bhardwaj, 2003) or 520 nm (Molyneux, 2003) in UV-Visible spectroscopy.

The DPPH radicals are stabilized by accepting the hydrogen donated by the hydroxyl groups present in the antioxidants (Zarena and Sankar, 2009). As the odd electron of the radical becomes paired off and forms a stable end product without further oxidative propagation, the absorption intensity is decreased, and this has resulted decolourization from purple to yellow.

Antioxidant compounds can be classified into water-soluble, or lipid-soluble. Therefore, the most utilised solvents for DPPH method are methanol and ethanol (Batchvarov and Marinova, 2011). Samaga (2012) stated that it is necessary to standardize the amount of DPPH to be taken based on the scavenging activity of the sample. If the activity of sample is relatively weak and high concentration of DPPH is taken, it may lead to a false negative result. However, if the DPPH concentration is too low, this may result in difficulty to obtain IC_{50} value. Hence, it is proposed that the best way of representing the antioxidant activity is by comparison of results with a standard free radical scavenger used in the assay.

Based on the review by Batchvarov and Marinova (2011), it was reported that the concentration of the DPPH working solution ranges in a wide limit which is from 0.05 mM to 1.5 M in which the concentration of 0.10 mM, 0.05 mM, 0.06 mM, and 0.09 mM are generally used in the studies of radical scavenging activity.

The DPPH method was originally introduced by Blois in year 1958 to evaluate the antioxidant activity of the thiol-containing amino acid, cysteine. He proposed the radical scavenging mechanism as shown in Figure 2.12 where DPPH radical and cysteine are represented by Z* and RSH, respectively.

$$Z^* + RSH \rightarrow ZH + RS^*$$

$$RS^* + RS^* \rightarrow RS - SR$$
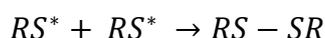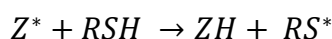
Figure 2.12: DPPH radical scavenging activity by using cysteine

The free radical RS* was proven to react with another radical to form a stable compounds. From the study, it was found that reduction of two molecules of DPPH by two cysteine molecules happened with 1 to 1 ration. However, some molecules have two adjacent sites for hydrogen abstraction such as ascorbic acid may undergo a further hydrogen abstraction after the first abstraction which leads to a 2 to 1 ration (Molyneux, 2004).

There are various types of modification on the original DPPH method. According to the method studied by Kosem and his co-worker (2007), a series of different concentrations of sample and ascorbic acid (positive control) were added to a methanolic 0.4 mM DPPH solution in a 96 well-plate. The mixture was allowed to stand for 30 minutes at 37 $^{\circ}$C representing the temperature of

27

human body. After 30 minutes, the absorbance of the mixture was determined at 517 nm using UV-Vis microplate reader. The principle applied in the DPPH assay is shown in Figure 2.13.

1,1-diphenyl-2-picrylhydrazyl   1,1-diphenyl-2(2,4,6-trinitrophenyl)hydrazine
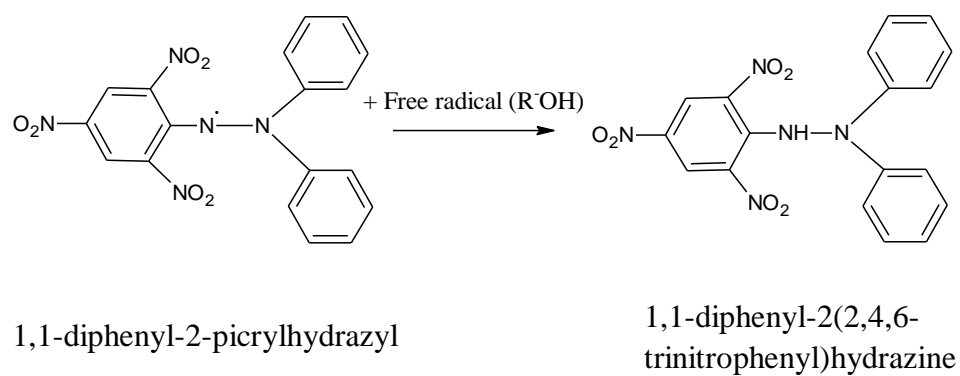
Figure 2.13: Principle applied in antioxidant (DPPH) assay

CHAPTER 3

MATERIALS AND METHODS

3.1 Chemicals

The chemicals used in the synthesis of 1,3,6-trihydroxyxanthone are listed in Table 3.1:

Table 3.1: Chemicals used in the synthesis of 1,3,6-trihydroxyxanthone

Chemical reagents	Molecular formula	Molecular weight, (g.mol^{-1})	Source, Country
2,4-Dihydroxybenzoic acid (97%)	$C_7H_7O_4$	154.12	Acros Organics, Belgium
Phloroglucinol (benzene-1,3,5-triol)	$C_6H_6O_3$	126.11	Sigma–Aldrich, USA
Eaton's reagent	$P_2O_5/MeSO_3H$	-	Acros Organics, Belgium

The chemicals used for prenylation of 1,3,6-trihydroxyxanthone are listed in Table 3.2.

Table 3.2: Chemicals used for prenylation of 1,3,6-trihydroxyxanthone

Chemical reagents	Molecular formula	Molecular weight, (g.mol^{-1})	Source, Country
Acetone	CH_3COCH_3	58.08	QREC, Malaysia
Ethyl acetate	$CH_3COOC_2H_5$	88.11	LAB-SCAN, Ireland
Hydrochloric acid (37%)	HCl	34.46	Fisher Scientific, UK
Potassium carbonate	K_2CO_3	138.21	John Kollin Corporation, USA
t-Butyl alcohol	$(CH_3)_3COH$	74.12	Fisher Scientific, UK
Prenyl bromide (3,3-dimethylallyl bromide)	C_5H_9Br	149.09	Sigma-Aldrich, USA

The solvents and materials used for purification and isolation of synthetic compounds are listed in Table 3.3.

Table 3.3: Solvents and materials used for purification of synthetic compounds

Solvents/Materials	Molecular formula	Density, ρ (g.mL^{-1})	Source, Country
Acetone	CH_3COCH_3	0.791	QREC, Malaysia
Dichloromethane	CH_2Cl_2	1.325	Fisher Scientific, UK
Ethyl acetate	$CH_3COOC_2H_5$	0.902	Lab-Scan, Ireland
n-Hexane	$CH_3(CH_2)_4CH_3$	0.659	Merck, Germany
Methanol	CH_3OH	0.791	Mallinckrodit Chemicals, Phillipsburg
Sodium sulphate anhydrous	Na_2SO_4	-	John Kollin Corporation, USA
Silica gel (60Å)	-	-	a) Silicycle, Canada b) Merck, Germany
Sephadex® LH-20	-	-	New Jersey, United State

The deuterated solvents used in NMR analyses are listed in Table 3.4.

Table 3.4: Deuterated solvents used in NMR analyses

Deuterated solvents/ Materials	Source, Country
Acetone-d_6	Acros Organics, Belgium
Deuterated chloroform ($CDCl_3$)	Acros Organics, Belgium
Methanol-d_4	Acros Organics, Belgium

The LCMS grade solvents and materials used in LC-MS and material used in chemical analysis are listed in Table 3.5.

Table 3.5: Solvents and materials used in LC-MS analysis

Solvents/Materials	Molecular formula	Density, ρ ($g.mL^{-1}$)	Source, Country
Acetonitrile	C_2H_3N	41.05	Fisher Scientific, UK
Methanol	CH_3OH	32.04	Fisher Scientific, UK
Nylon syringe filter	-	-	Membrane-Solution, USA

Chemical reagents and materials used in antioxidant assay are listed in Table 3.6.

Table 3.6: List of materials and reagents used in antioxidant assay

Reagents/Materials	Source, Country
96-well plate	Techno Plastic Products AG, Switzerland
Ascorbic acid	Sigma- Aldrich, USA
Kaempferol	Sigma- Aldrich, USA
DPPH (**1,1-diphenyl-2-picrylhydrazyl**)	Sigma- Aldrich, USA

3.2 Methodology

3.2.1 Synthesis of Xanthonic Block, 1,3,6-Trihydroxyxanthone

50 mmol (7.7 g) of salicylic acid (**12**) and 50 mmol (6.31 g) of phloroglucinol (**13**) were mixed well in a 250 mL flat-bottomed flask. 100 mL of Eaton's reagent was then added slowly into the mixture. The mixture was heated in a water bath at $80 \pm 3\ ^{\circ}C$ for 30 minutes with constant stirring. After that, the mixture was cooled down to room temperature by immersing into cold water bath. The cooled mixture was then poured into crushed ice and stirred for 15 minutes. The precipitate was filtered out by using Buchner filtration, and dried in an oven at $50\ ^{\circ}C$ for overnight. The crude product obtained was subsequently purified by using column chromatography to give 1,3,6-trihydroxyxanthone (**15**).

dihydroxybenzoic acid   phloroglucinol   1,3,6-trihydroxyxanthone

(2-hydroxybenzoic acid)   (benzene-1,3,5-triol)

(**12**)   (**13**)   (**15**)
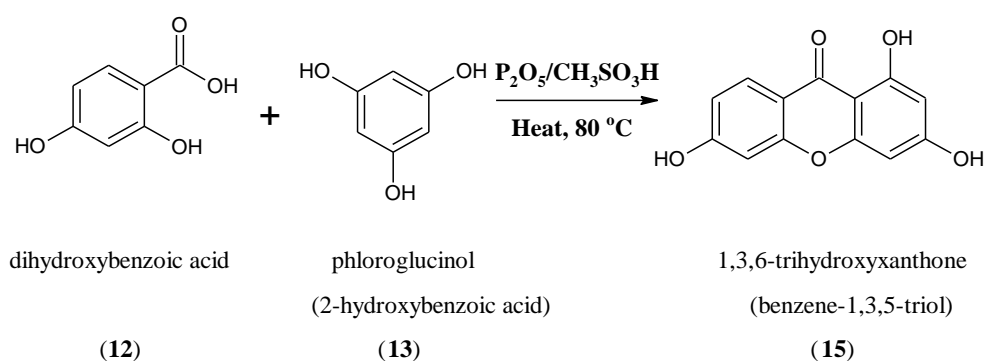
Figure 3.1: Synthesis of 1,3,6-trihydroxyxanthone

3.2.2 Prenylation of 1,3,6-Trihydroxyxanthone via Potassium Carbonate in *t*-Butyl Alcohol

A mixture of 13.98 g (100 mmol) of potassium carbonate in 50 mL of *t*-butyl alcohol was prepared in a 250 mL flat-bottomed flask. Then, 0.5 g (20 mmol) of 1,3,6-trihydroxyxanthone was added into the flask and stirred for 15 minutes. After that, 1.79 g (12 mmol) of prenyl bromide in 2 mL acetone was injected via syringe into the reaction mixture. The mixture was then stirred for 24 hours at room temperature. Subsequently, the mixture was acidified with 100 mL of 10% HCl followed by extraction with dichloromethane. The organic layer collected was removed for its solvent by using rotary evaporator. The crude product was then subjected to column chromatography with gradient elution to give 1-hydroxy-2-(3-methylbut-2-en1-yl)-3,6-bis((3-methylbut-2-en-1-yl)oxy)-9*H*-xanthen-9-one (**50**) and 2,2,4,4-tetrakis(3-methylbut-2-en-1-yl)-6-((3-methylbut-2-en-1-yl)oxy)-1*H*-xanthene-1,3,9(2*H,4H)*-trione (**51**).
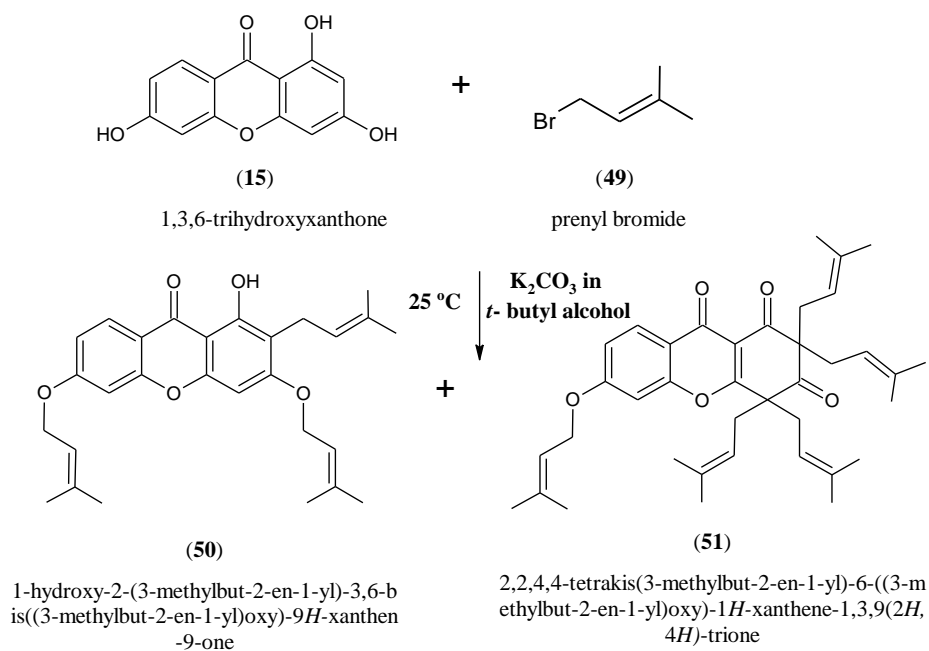
Figure 3.2: Synthetic route for prenylated xanthones

3.2.3 Column Chromatography

Silicycle or Merck silica gel (40 - 63 μm) was mixed with hexane to form slurry and then it was poured into a vertical glass chromatography column. The slurry was allowed to settle down to form a compact packing in the column. The sample was prepared via dry packing method. Firstly, the sample was dissolved in a little amount of solvent and was then mixed dropwisely with dry silica gel. The mixture was left to dry at ambient temperature overnight and it was then introduced into the packed column. In the separation of compounds, gradient elution with hexane/ dichloromethane/ ethyl acetate / acetone / methanol was conducted in increasing polarity of the mobile phase. The fractions collected were then analysed using Thin Layer Chromatography (TLC).

Figure 3.3: Column chromatographic apparatus

3.2.4 Thin Layer Chromatography (TLC)

In this study, 4 cm x 6 cm of aluminium plate coated with Merck brand silica gel 60 F254 was used to monitor the content of fractions collected from column chromatography. A thin capillary tube was dipped into the sample solution and spotted onto the baseline drawn on the plate. Meanwhile, a chamber with known composition of solvents was prepared and it was left until the developing chamber saturated with the vapour of mobile phase. The TLC plate was then placed into the chamber until the solvent reached the solvent front line. Then, the plate was visualized under ultra-violet lamp with both short (254 nm) and long (365 nm) wavelengths. The retention factor, R_f of each spot was obtained according to the equation below:

$$R_f = \frac{distance\ traveled\ by\ the\ compound\ (cm)}{distance\ of\ the\ solvent\ front\ (cm)}$$
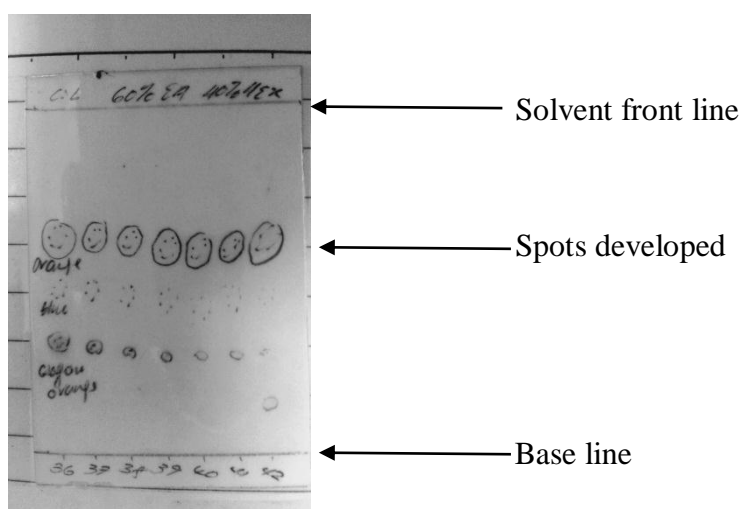
Figure 3.4: TLC plate set up

3.3 Instruments

3.3.1 Nuclear Magnetic Resonance (NMR)

Nuclear Magnetic Resonance (NMR) spectroscopy is a useful technique for determination of structure of organic compounds. In this study, JEOL JNM-ECX 400 MHz spectrometer was used for sample analyses. Both ^{1}H-NMR and ^{13}C-NMR were used to elucidate the chemical structure of xanthone and its derivative. The 2D-NMR, HMQC (Heteronuclear Multiple Quantum Correlation) and HMBC (Heteronuclear Multiple Bond Correlation) were used for determination of carbon to hydrogen connectivity. Both analyses were 2-dimensional inverse H,C correlation techniques in which HMQC was used to detect direct C-H coupling (^1J coupling) and HMBC shows long range coupling between proton and carbon (^2J and ^3J couplings).

NMR samples were prepared by dissolving each sample in a small amount of deuterated-solvents (acetone-d_6 or deuterated-chloroform, $CDCl_3$). The solvent used was dependant on the extent of dissolution of the sample in the solvent, whereas tetramethylsilane (TMS) was used as an internal standard.

3.3.2 Ultraviolet-Visible (UV-Vis) Spectroscopy

Ultraviolet-visible spectroscopy was used to study the samples with conjugated structure. Compounds with conjugated system are found to absorb lights in UV-Visible region. Perkin-Elmer Lambda (25/35/45) UV-Vis spectrophotometer was used for sample analysis in this study. The absorption spectra of the synthetic xanthones were measured in a diluted solution in comparison with a solvent blank prepared in 98% absolute ethanol since most of the compounds are soluble in it (Harborne, 1998). The absorption maxima of the yellowish isolated compounds were measured in the range of 200 nm to 400 nm.

3.3.3 Infrared (IR) Spectroscopy

Infrared (IR) spectroscopy is commonly used to identify the chemical functional groups present in the sample and also to provide unique characteristic identification of the sample. In this study, Perkin Elmer 2000-FTIR spectrometer was used for sample analysis in the range of 4000 cm^{-1} to 400 cm^{-1}. A relatively small amount of solid sample was mixed with potassium bromide in a ratio of 1:10 and the mixture was then compressed under high pressure to form KBr sample pellet.

3.3.4 Liquid Chromatography–Mass Spectrometry

LC-MS is a coupled technique in which compounds are separated via HPLC before they are run into mass spectrometer for structural analysis. In this study, G6520B Q-TOF LC/MS spectrometer was used to obtain structural information about the sample. Electrospray ionization (ESI) method was applied which was a soft ionization technique used to determine the accurate molecular weight of the test compound without much fragmentation. Ionized sample solution was sprayed out into small droplets and further desolvation produces free ions to be analysed by the detector. The samples were prepared by dissolving it either in HPLC grade methanol or acetonitrile depending on the dissolution of the samples. The samples were then prepared at the concentration below 100 ppm and then it was filtered by using nylon syringe filter (pore size = 0.22 μm) to remove any undissolved solid before it was injected in to the LC-MS.

3.3.5 Melting Point Apparatus

Melting point of a compound is the temperature at which the solid sample changes into liquid. Pure crystalline or powder form sample has a clear and sharp defined melting point, whereas impurities may give interference on the melting point measurement by enlarging the melting range of a substance. In this study, Barnstead Electrothermal 9100 melting point apparatus was used to

determine the melting point of samples. The solid sample was introduced into a haematocrit capillary and heated until it melted completely. The temperature range in which the solid start and completely melted was recorded.

3.4 Antioxidant Assay

All samples and standard compounds (Vitamin C and Kaempferol) were dissolved in methanol for preparation of master stocks at a concentration of 1 mg/mL. The master stocks were sonicated for 5 minutes to ensure all the solids were fully dissolved. At the meantime, 4 mg/mL of DPPH (1,1-diphenyl-2-picrylhydrazyl) in methanol was prepared. The solution was then sonicated and stored in dark condition.

A series of concentration at 240, 120, 60, 30, 15, 7.5, and 5 μg/mL of standard compounds and test compounds were prepared by dilution of master stocks with methanol in a 96-well plate followed by addition of 5 μL of DPPH solution. All test compounds were run in triplicate and the readings were averaged. The DPPH methanolic solution without treatment was taken as the negative control.

The plate was wrapped with aluminium foil immediately after the addition of DPPH solution to avoid evaporation and exposure to light. The plate was then stored in dark at room temperature for 30 minutes. After 30 minutes, the absorbance of the mixture in each well was measured at 520 nm using a microplate reader (Model 680, Bio-Rad Laboratories, Hercules, CA, USA) and results were interpreted by the Microplate Manager®, Version 5.2.1 software.

3.5 Calculation

3.5.1 Percentage Yield of Xanthones

The percentage yield of each synthetic xanthone was calculated by using the equation below:

Percentage yield of xanthone

$$\text{Percentage yield (\%)} = \frac{\text{Experimental yield of xanthone}}{\text{Thoretical yield of xanthone}} \times 100\%$$

3.5.2 Inhibition Rate

Inhibition rates of the test compounds were calculated by using the formula below:

$$\text{Inhibition Rate (\%)} = \frac{A_o - A_1}{A_o} \times 100\%$$

where

A_o = Absorbance of the negative control (blank)

A_1 = Absorbance of the test compound

The inhibition rate was plotted against the sample concentration to obtain IC_{50}, defined as the concentration of sample necessary to cause 50% inhibition to the DPPH radical scavenging activity.

CHAPTER 4

RESULTS AND DISCUSSION

4.1 Synthesis of 1,3,6-Trihydroxyxanthone

The synthesis of xanthone block via condensation of 50 mmol of salicylic acid and 50 mmol of phloroglucinol in the presence of Eaton's reagent (Figure 4.1) has resulted 1,3,6-trihydroxyxanthone (**15**) with a relatively low percentage yield of 29.0%. Compound **15** was deduced to have a molecular formula of $C_{13}H_8O_5$ by High Resolution Electrospray Ionization Mass Spectrometry (HRESIMS) analysis based on the accurate molecular mass obtained as 244.0376 g.mol^{-1}. Xanthonic block, **15** appeared as yellowish solid with a melting point range of 320 to 322 $^{\circ}$C. It gave a single spot with R$_f$ value of 0.53 on a TLC plate with hexane: ethyl acetate in 3:2 ratios served as a mobile phase. The summary of physical data of 1,3,6-trihydroxyxanthone is tabulated in Table 4.1.
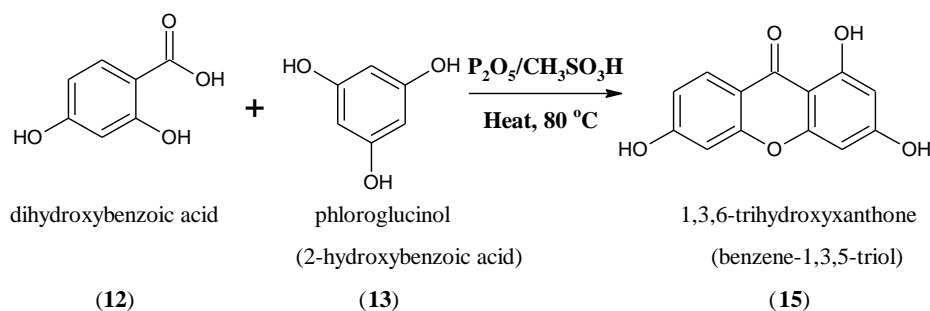
Figure 4.1: Synthesis of 1,3,6-trihydroxyxanthone

Table 4.1: Summary of physical data of 1,3,6-trihydroxyxanthone

Molecular formula :	$C_{13}H_8O_5$
Molecular weight, g.mol^{-1} :	244.0376
	Library value: 244.0372
Physical appearance :	Yellowish solid
Mass obtained, g :	3.5554
Melting point, ^{o}C :	320 – 322
Percentage yield, % :	29.0
R$_f$ value :	0.53
	(TLC solvent system of Hex: EA = 3:2)
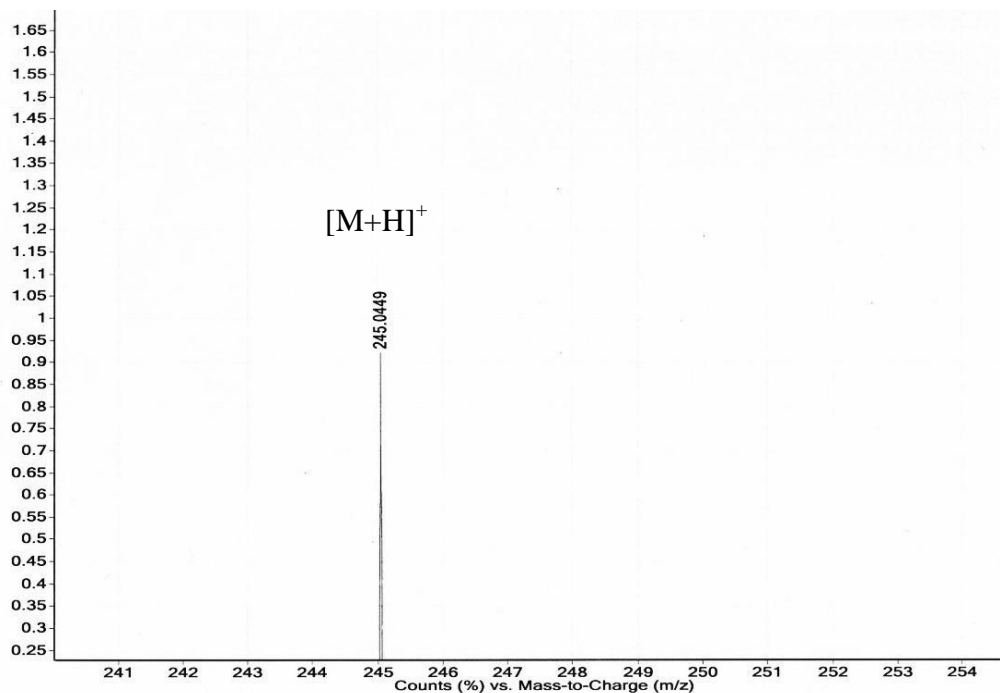
Figure 4.2: HRESIMS spectrum of 1,3,6-trihydroxyxanthone

4.1.1 Proposed Mechanism for Synthesis of 1,3,6-Trihydroxyxanthone

$$2 \ P_2O_5 \ + \ 6 \ H_2O \longrightarrow 4 \ H_3PO_4$$
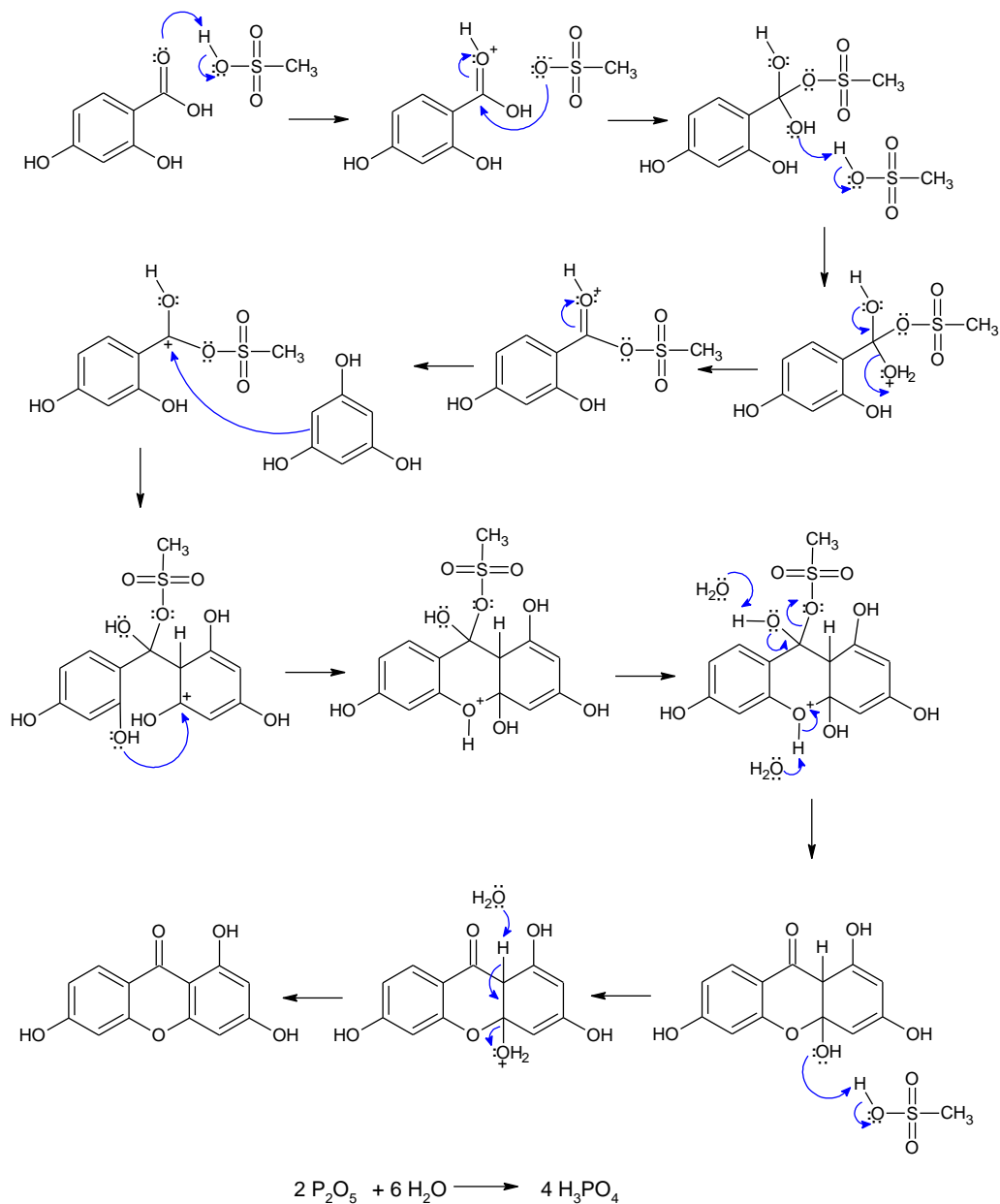
Figure 4.3: Proposed mechanism for synthesis of 1,3,6-trihydroxyxanthone

(15)

4.1.2 Structural Elucidation of 1,3,6-Trihydroxyxanthone
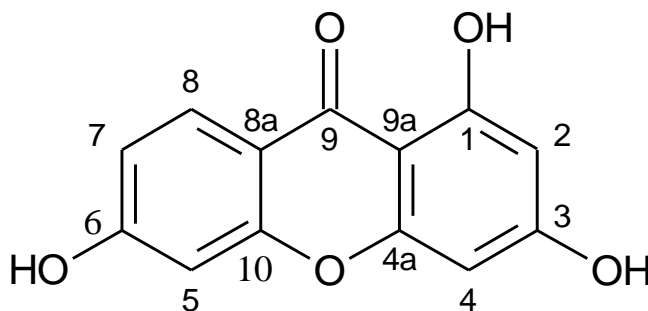
Figure 4.4 Structure of 1,3,6-trihydroxyxanthone (15)

Detailed elucidation of compound **15** was performed by using Nuclear Magnetic Resonance (NMR). The ^{1}H NMR spectrum (Figure 4.5) showed five proton signals in the aromatic region δ_H 6.20 (1H, d, J = 2.4 Hz), 6.40 (1H, d, J = 2.4 Hz), 6.85 (1H, d, J = 2.4 Hz), 6.93 (1H, dd, J = 9.2, 2.4 Hz) and 8.03 (1H, d, J = 9.2 Hz) which were assigned to five aromatic protons in the xanthonic nucleus, and a downfield singlet at δ 13.09 revealed the presence of a chelated phenolic hydroxyl group. The presence of a doublet of doublets at δ 6.90 was assigned to proton H-7 which is *meta*-coupled (J = 2.4 Hz) with proton H-5 and *ortho*-coupled (J = 9.2 Hz) with proton H-8.

The *peri*-position proton, H-8 showed relatively a higher chemical shift than the other aromatic protons due to the anisotropic effect induced by the adjacent carbonyl group. Furthermore, the hydroxyl proton, 1-OH formed a strong intra-molecular hydrogen bonding with the carbonyl group, resulted a highly

deshielded signal at δ 13.09 in the ^{1}H-NMR spectrum. Silva and Pinto (2005) reported the remaining two hydroxyl protons, 3-OH and 6-OH should give signals between δ 10.80 - 11.00. However, signals for 3-OH and 6-OH were not observed in the ^{1}H-NMR spectrum due to the rapid proton exchanges. The rate at which hydroxyl protons exchanged with one another or with acid residues in solvent was faster than the rate of NMR spectrometer could respond to the exchanges (Lampman, Pavia, Kriz and Vyvyan, 2010).

The ^{13}C NMR spectrum (Figure 4.6) showed a total 12 signals. Among these signals, five carbon signals at δ 127.5, 113.8, 102.3, 98.1 and 93.9 were assigned to the five protonated carbons C-8, C-7, C-5, C-2 and C-4, respectively which were supported by Heteronuclear Multiple Quantum Correlation (HMQC) assignment as shown in Figure 4.7. In the Heteronuclear Multiple-Bond Correlation (HMBC) spectrum (Figure 4.8), correlation of hydroxyl proton, 1-OH to carbons C-2 and C-9a further confirmed that the chelated hydroxyl group was bonded to carbon C-1. HMBC correlations between proton H-4 to carbons C-2, C-3, C-9a, and C-4a revealed that the second hydroxyl group was located at C-3 (δ 165.1) and hence based on the above correlations, xanthone ring A was established to be 1,3-dihydroxylated. On the other hand, the remaining hydroxyl group was assigned to C-6 (δ 164.1) according to HMBC correlations shown between proton H-5 to carbons C-6, C-7 and C-10a. Hence, the structure of compound **15** was unambiguously assigned as 1,3,6-trihydroxyxanthone and the NMR spectral data are summarized in Table 4.2.

Ultraviolet-visible and infrared spectroscopies were used as elemental analysis of xanthone derivatives. The IR spectrum (Figure 4.9) showed a broad absorption peak at 3435 cm^{-1} for hydroxyl group whereas a sharp peak at 1612 cm^{-1} indicated the presence of carbonyl group. Another two absorbance bands located at 1289 and 1183 cm^{-1} revealed the presence of C-O group in which asymmetric stretching gave higher energy than the symmetric stretching. Harborne (1998) stated that xanthones have absorption maxima in the ranges of 230 - 245, 250 - 265, 305 - 330, and 340 - 440 nm which are typical for xanthone chromophores (Botha, 2005; Ghazali, Gwendoline and Ghani, 2010). Absorption maxima of 1,3,6-trihydroxyxanthone at 202.03, 229.79, 309.42 nm in the UV range are shown in Figure 4.10. The auxochrome attached to the xanthone nucleus might result in characteristic bathochromic or hypsochromic shift in the UV spectrum. Furthermore, the absorption bands in the range between 340 - 440 nm were not detectable due to low molar absorptivity.

Table 4.2: Summary of NMR data of 1,3,6-trihydroxyxanthone

Position	δH (ppm)	δC (ppm)	HMBC ^2J	^3J
1	-	163.9	-	-
2	6.20 (1H, d, $J = 2.4$ Hz)	98.1	-	C4, C9a
3	-	165.1	-	-
4	6.40 (1H, d, $J = 2.4$ Hz)	93.9	C3, C4a	C2, C9a
4a	-	158.0	-	-
5	6.85 (1H, d, $J = 2.4$ Hz)	102.3	C6, C10a	C7
6	-	164.1	-	-
7	6.93 (1H, dd, $J = 9.2, 2.4$ Hz)	113.8	-	C5, C8a
8	8.03 (1H, d, $J = 9.2$ Hz)	127.5	-	C6, C9, C10a
8a	-	113.4	-	-
9	-	179.8	-	-
9a	-	102.5	-	-
10a	-	158.0	-	-
1-OH	13.09 (OH, s)	-	C1	C2, C9a
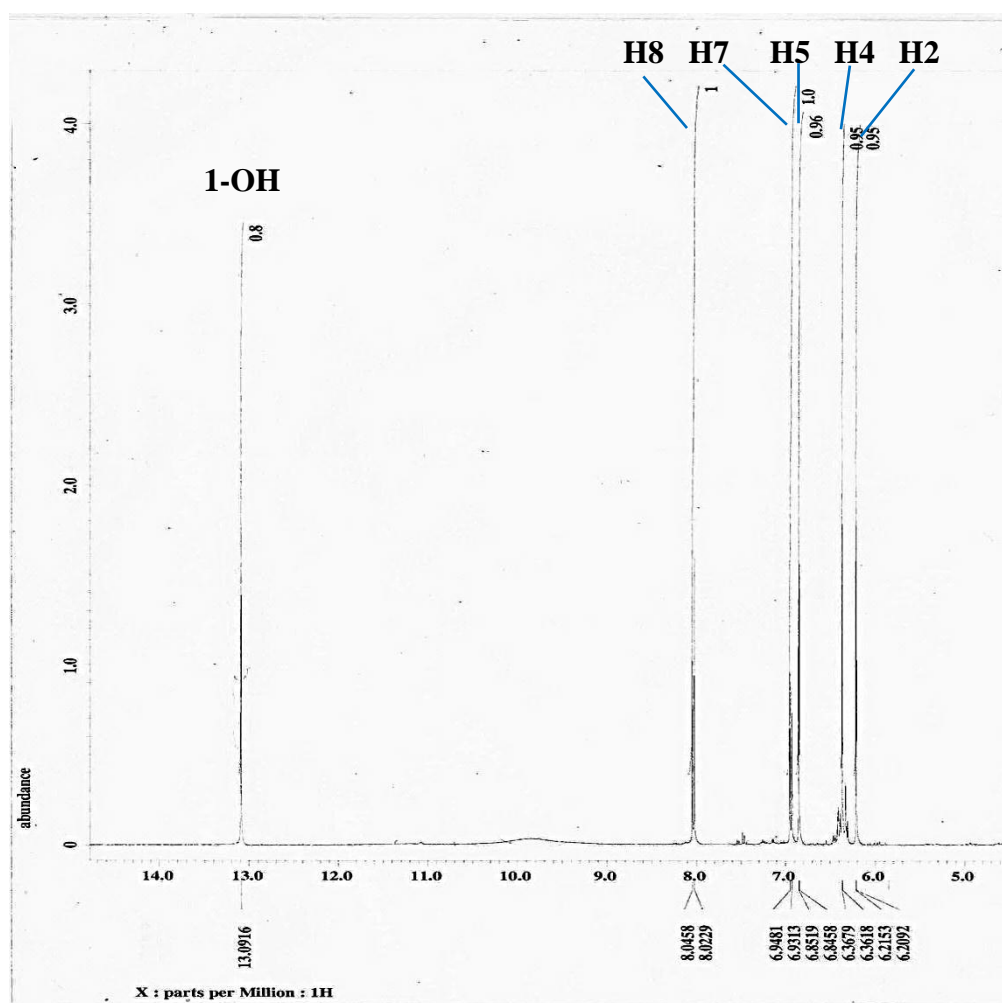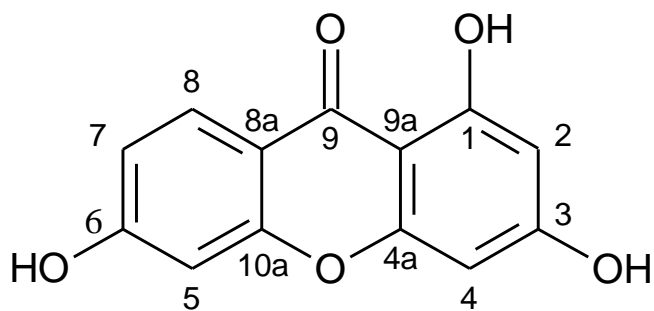
Figure 4.5: ¹H-NMR spectrum of 1,3,6-trihydroxyxanthone

(400 MHz, acetone-d₆)
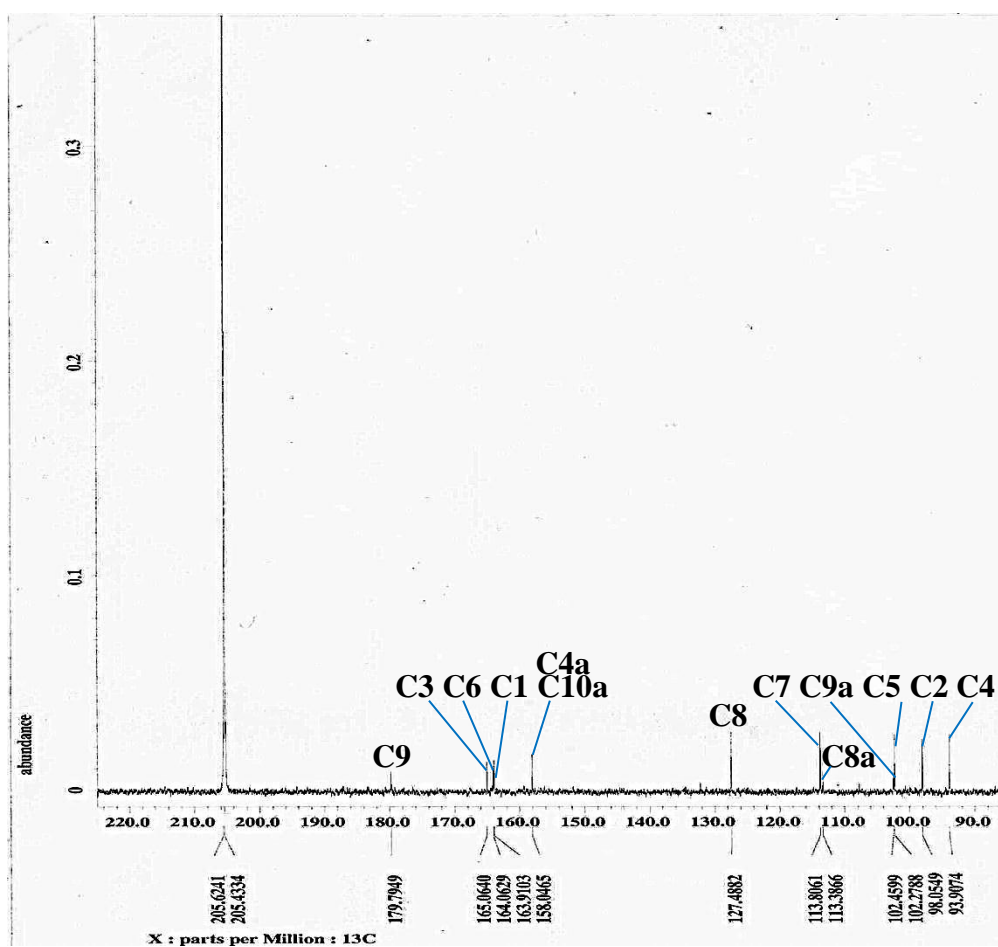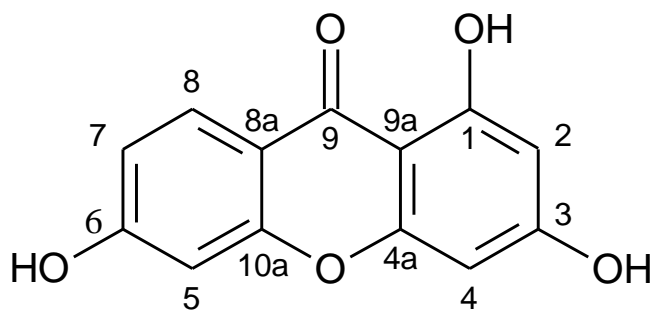
Figure 4.6: ^{13}C-NMR spectrum of 1,3,6-trihydroxyxanthone

(100 MHz, acetone-d$_6$)
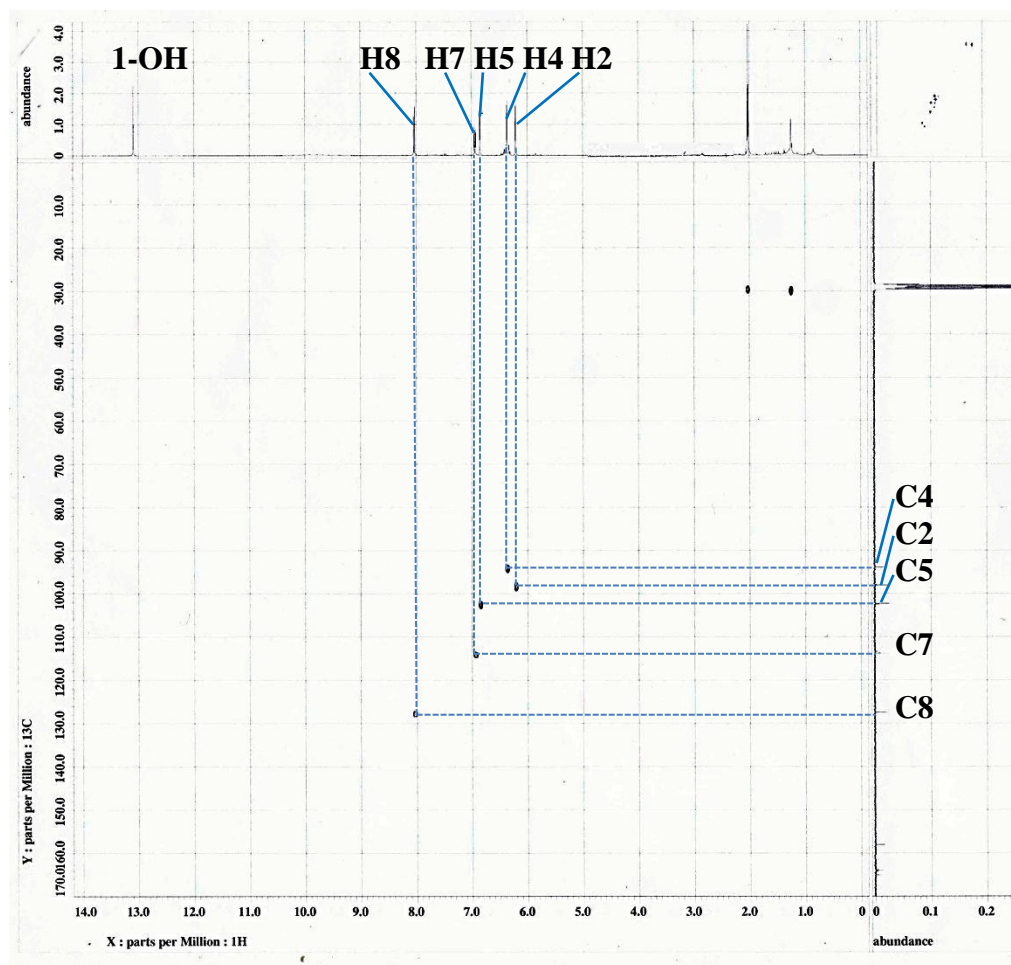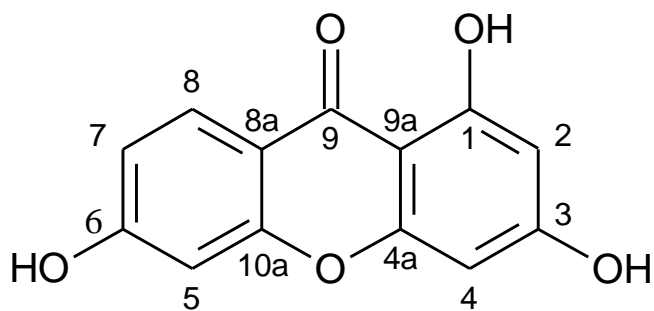
Figure 4.7: HMQC spectrum of 1,3,6-trihydroxyxanthone
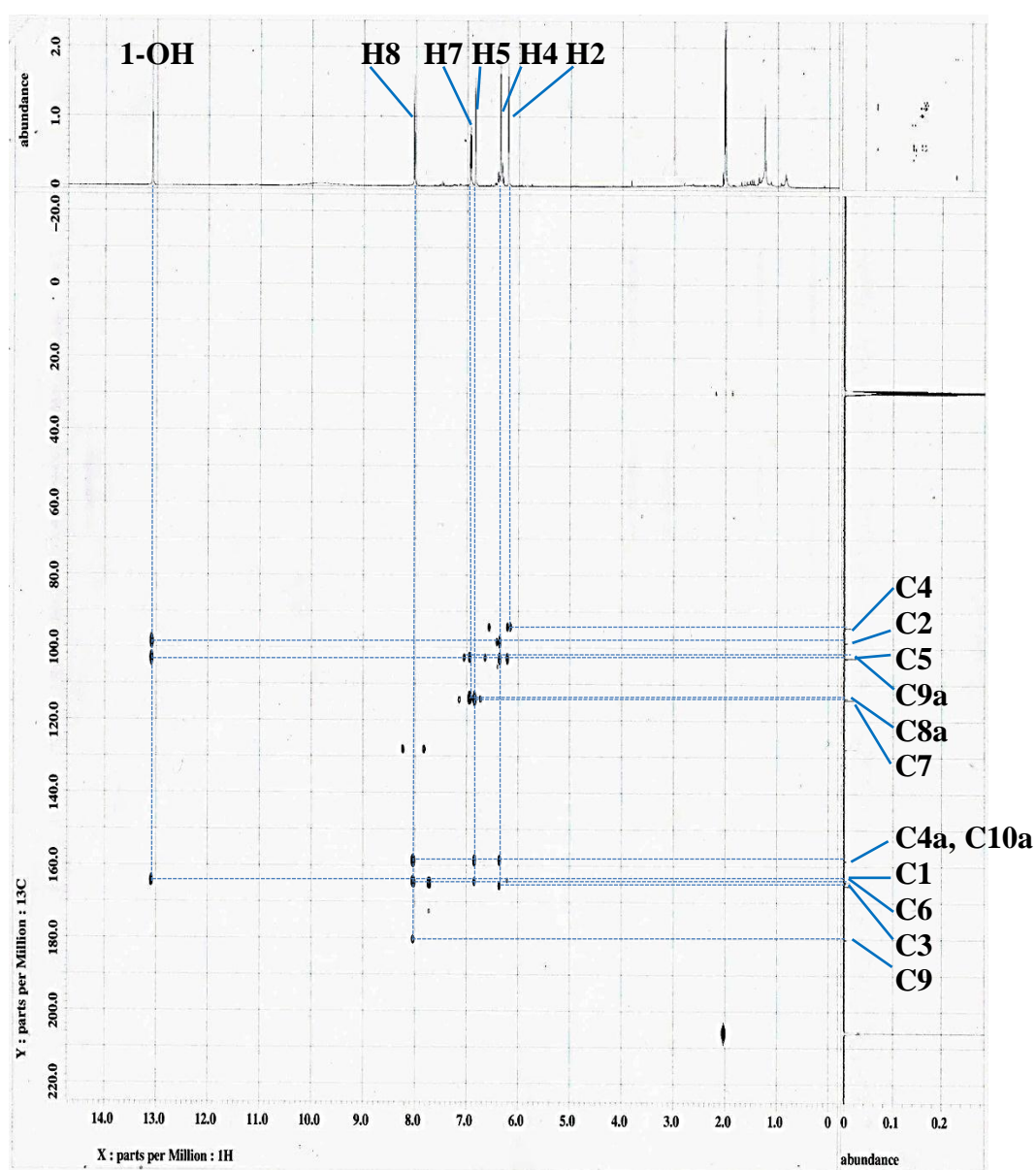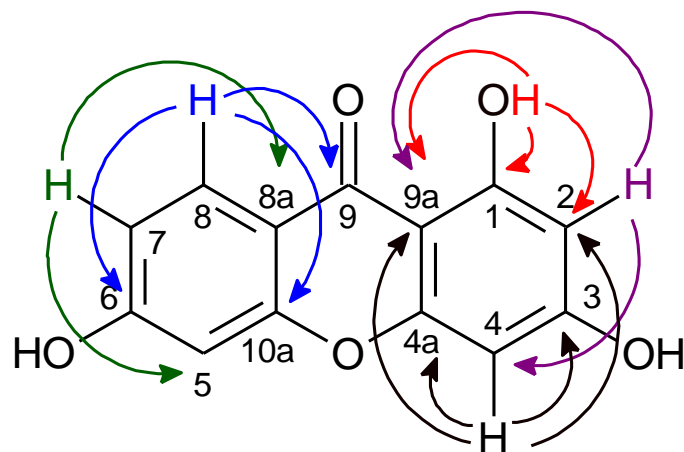
Figure 4.8: HMBC spectrum of 1,3,6-trihydroxyxanthone
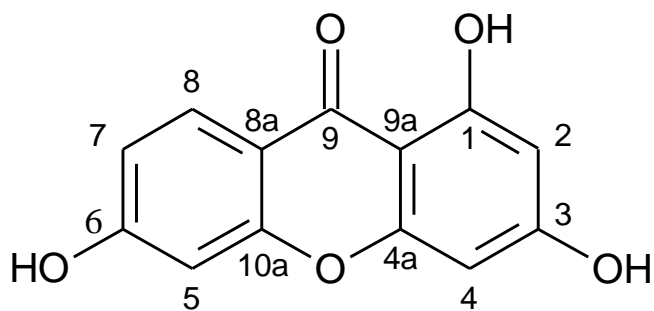
1,3,6-Trihydroxyxanthone (**15**)

Molecular formula: $C_{13}H_8O_5$

Molecular weight: 244.0376 g mol^{-1}
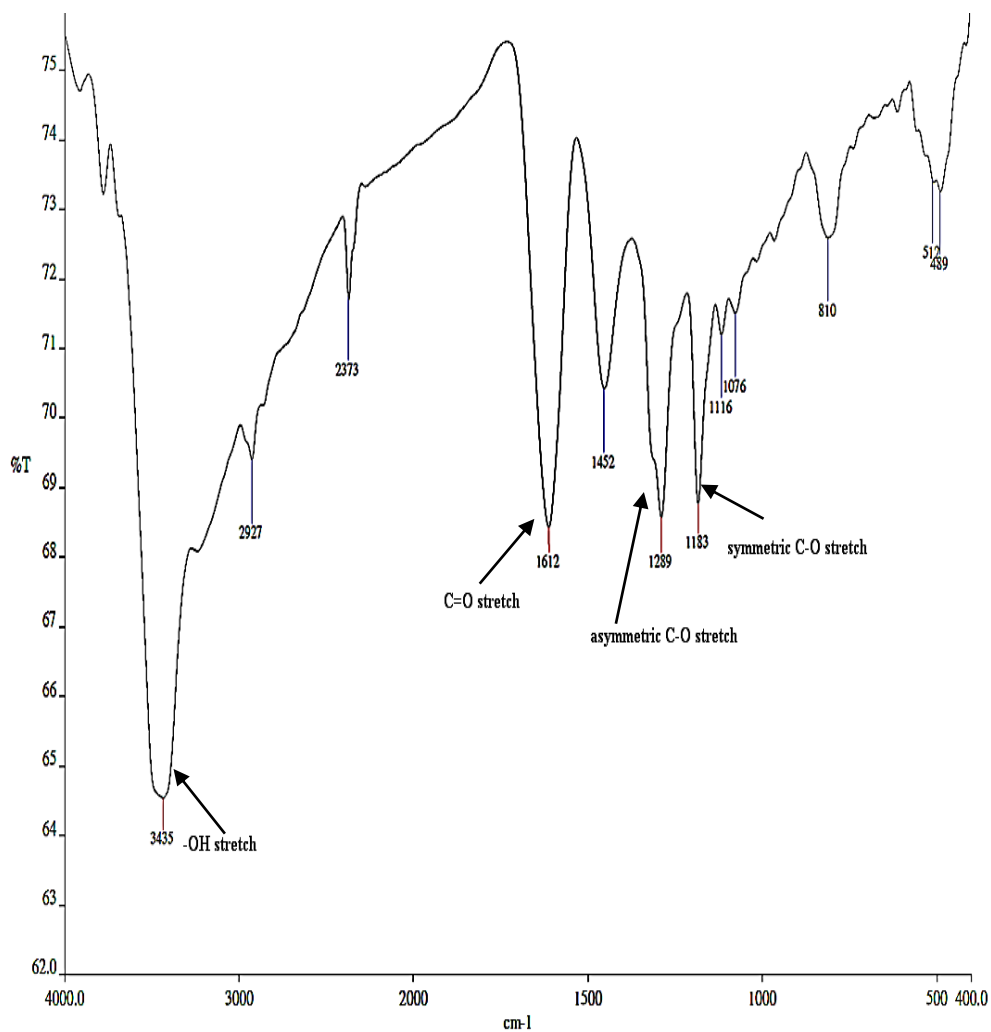
Figure 4.9: IR spectrum of 1,3,6-trihydroxyxanthone
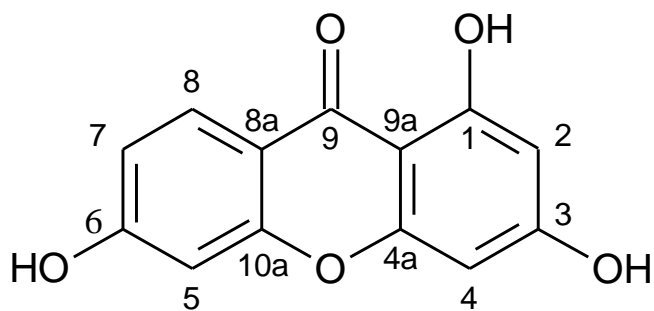
1,3,6-Trihydroxyxanthone (**15**)

Molecular formula: $C_{13}H_8O_5$

Molecular weight: 244.0376 g mol^{-1}
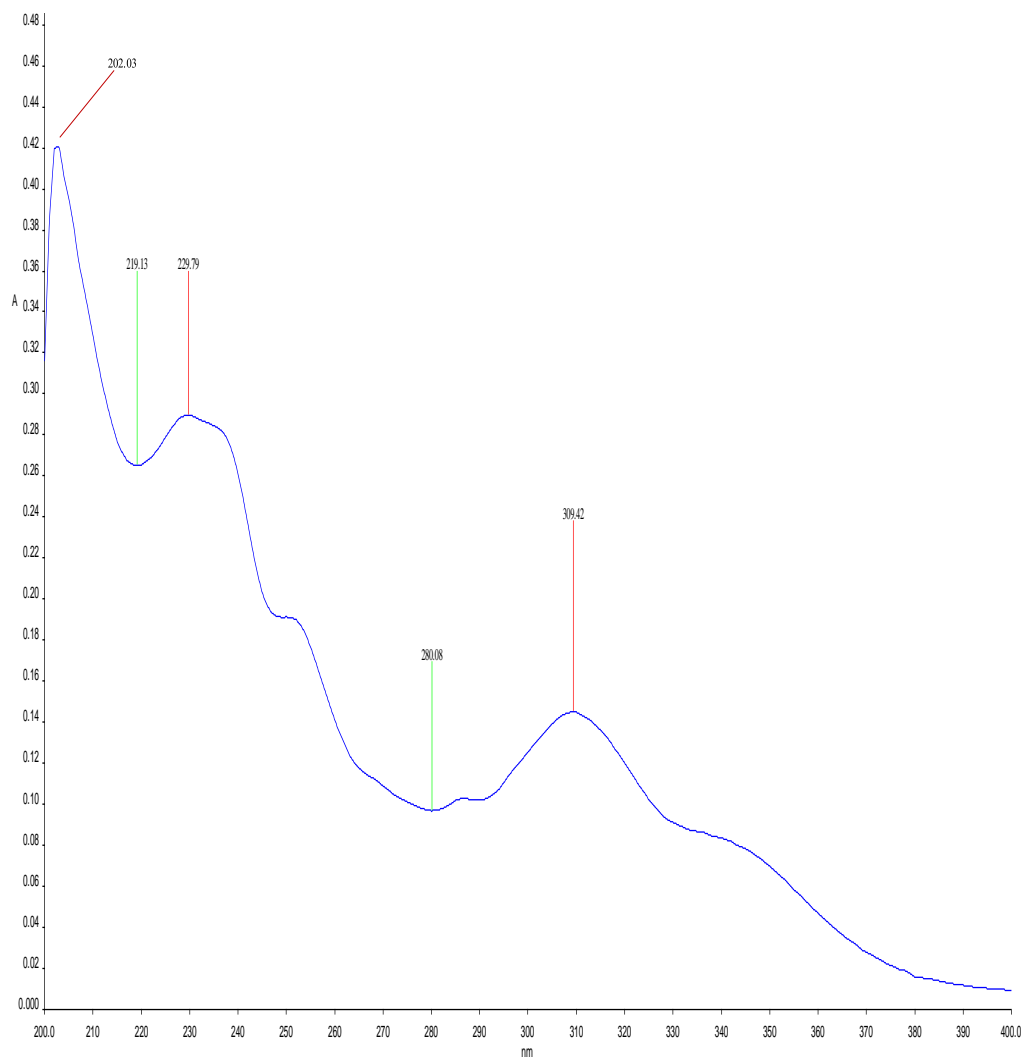
Figure 4.10: UV-Vis spectrum of 1,3,6-trihydroxyxanthone

4.2 Prenylation of 1,3,6-Trihydroxyxanthone

The synthetic method employed for the prenylated compounds is depicted in Figure 4.11 whereby prenylation was conducted by using potassium carbonate and prenyl bromide in an organic medium which was *t*-butyl alcohol. As a result, a novel prenylated xanthone **51** was obtained as major product, having the percentage yield of 18.4% whereas a new prenylated xanthone **50** was obtained as minor product, having the percentage yield of 1.2%.

Compound **50** was isolated as yellowish crystals, having a melting range of 113 - 116 ^{o}C. The accurate molecular mass of 448.2257 g.mol^{-1} obtained from HRESIMS (Figure 4.12) was consistent with the molecular formula of $C_{28}H_{32}O_5$. It showed a R_f value of 0.42 on a TLC plate eluted with 40% dichloromethane: 60% hexane. On the other hand, compound **51** with a molecular formula of $C_{38}H_{48}O_5$ was obtained as white crystals with a melting range of 121 - 124 ^{o}C and this compound was analysed to show an accurate molecular mass of 584.3503 g.mol^{-1} as shown in Figure 4.13. It gave a R_f value of 0.36 when developed on a TLC plate eluted with a solvent mixture of 20% ethyl acetate: 80% hexane. The physical data of these two prenylated xanthones are summarized in Table 4.3.

(15)
1,3,6-trihydroxyxanthone

(49)
prenyl bromide

25 °C | K₂CO₃ in t-butyl alcohol

(50)
1-hydroxy-2-(3-methylbut-2-en-1-yl)-3,6-bis((3-methylbut-2-en-1-yl)oxy)-9H-xanthen-9-one

(51)
2,2,4,4-tetrakis(3-methylbut-2-en-1-yl)-6-((3-methylbut-2-en-1-yl)oxy)-1H-xanthene-1,3,9(2H, 4H)-trione
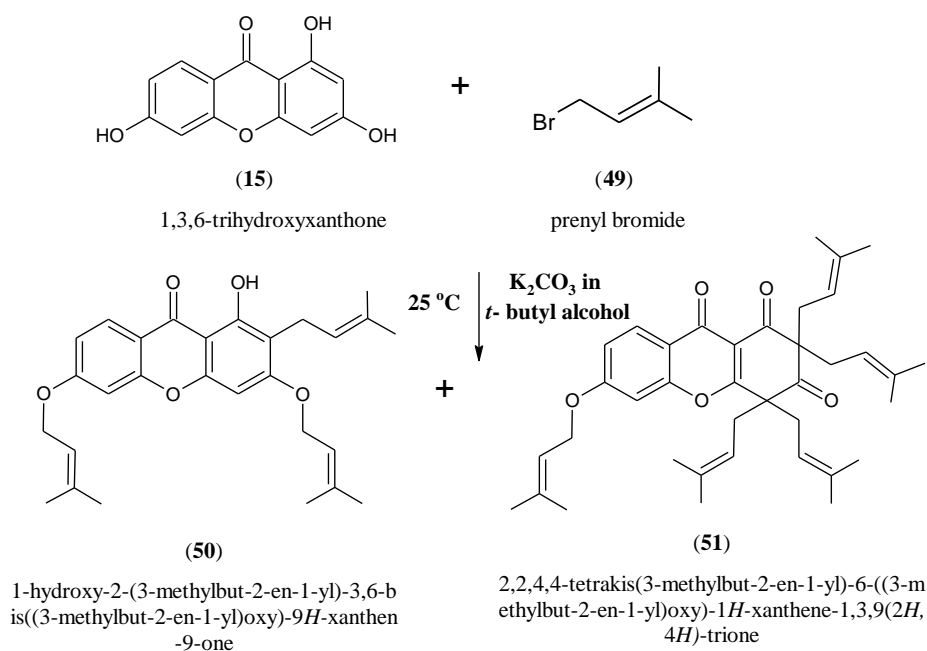
Figure 4.11: Synthesis route for prenylated xanthones

Table 4.3: Summary of physical properties of prenylated xanthones

Compound	50	51
Molecular formula :	$C_{28}H_{32}O_5$	$C_{38}H_{48}O_5$
Molecular weight, g.mol^{-1} :	448.2257	584.3503
	Library value: 448.2250	Library value: 584.3502
Physical appearance :	Yellowish crystals	White crystals
Mass obtained, g :	0.0124	0.2203
Melting point, °C :	113 - 116	121 - 124
Percentage yield, % :	1.2	18.4
R$_f$ value :	0.42	0.36
	(TLC solvent system of Hex: DCM = 3:2)	(TLC solvent system of Hex: EA = 8:2)
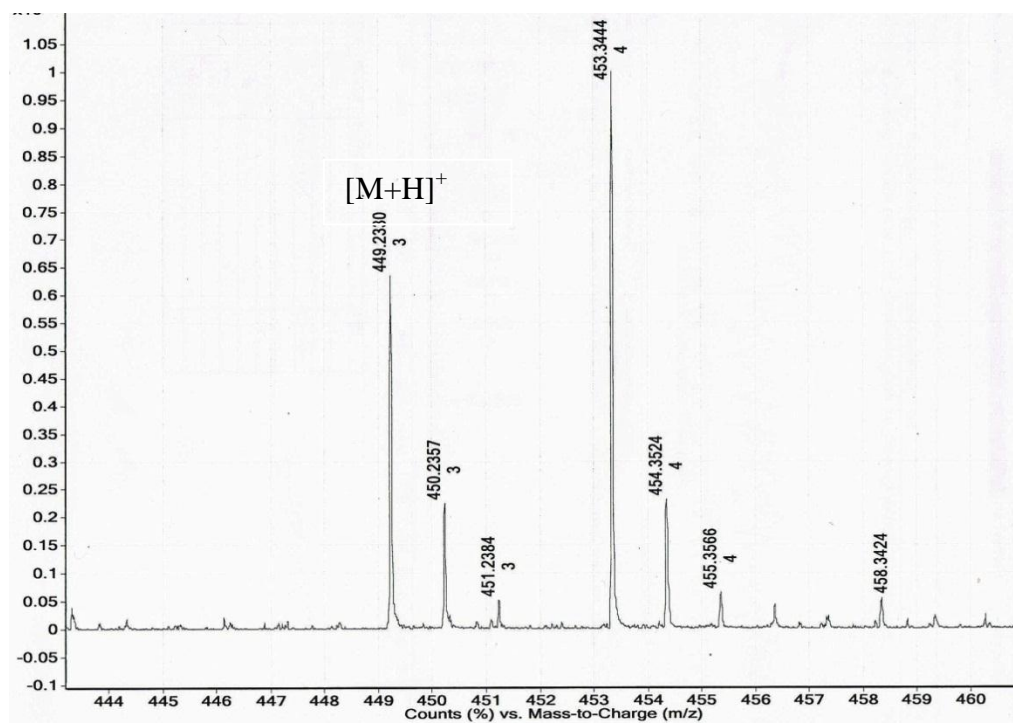
Figure 4.12: HRESIMS spectrum of 1-hydroxy-2-(3-methylbut-2-en-1-yl)-

3,6-bis((3-methylbut-2-en-1-yl)oxy)-9*H*-xanthen-9-one (50)
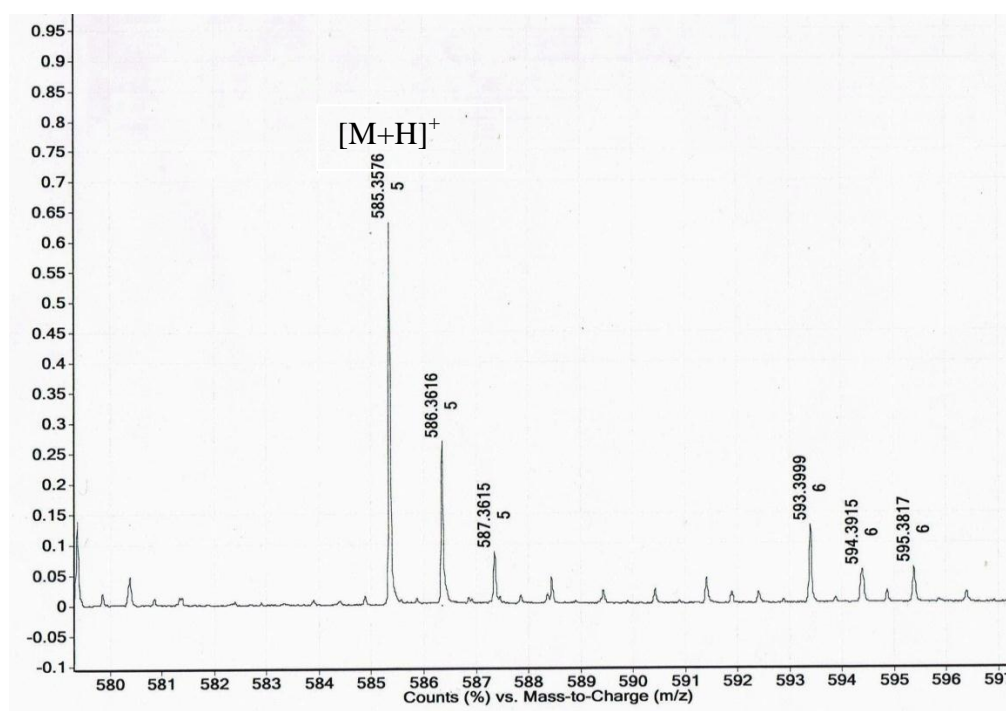
Figure 4.13: HRESIMS spectrum of 2,2,4,4-tetrakis(3-methylbut-2-en-1-

yl)-6-((3-methylbut-2-en-1-yl)oxy)-1*H*-xanthene-

1,3,9(2*H*,4*H*)-trione (51)

4.2.1 Proposed Mechanism for Synthesis of 1-Hydroxy-2-(3-methylbut-2-en-1-yl)-3,6-bis((3-methylbut-2-en-1-yl)oxy)-9*H*-xanthen-9-one
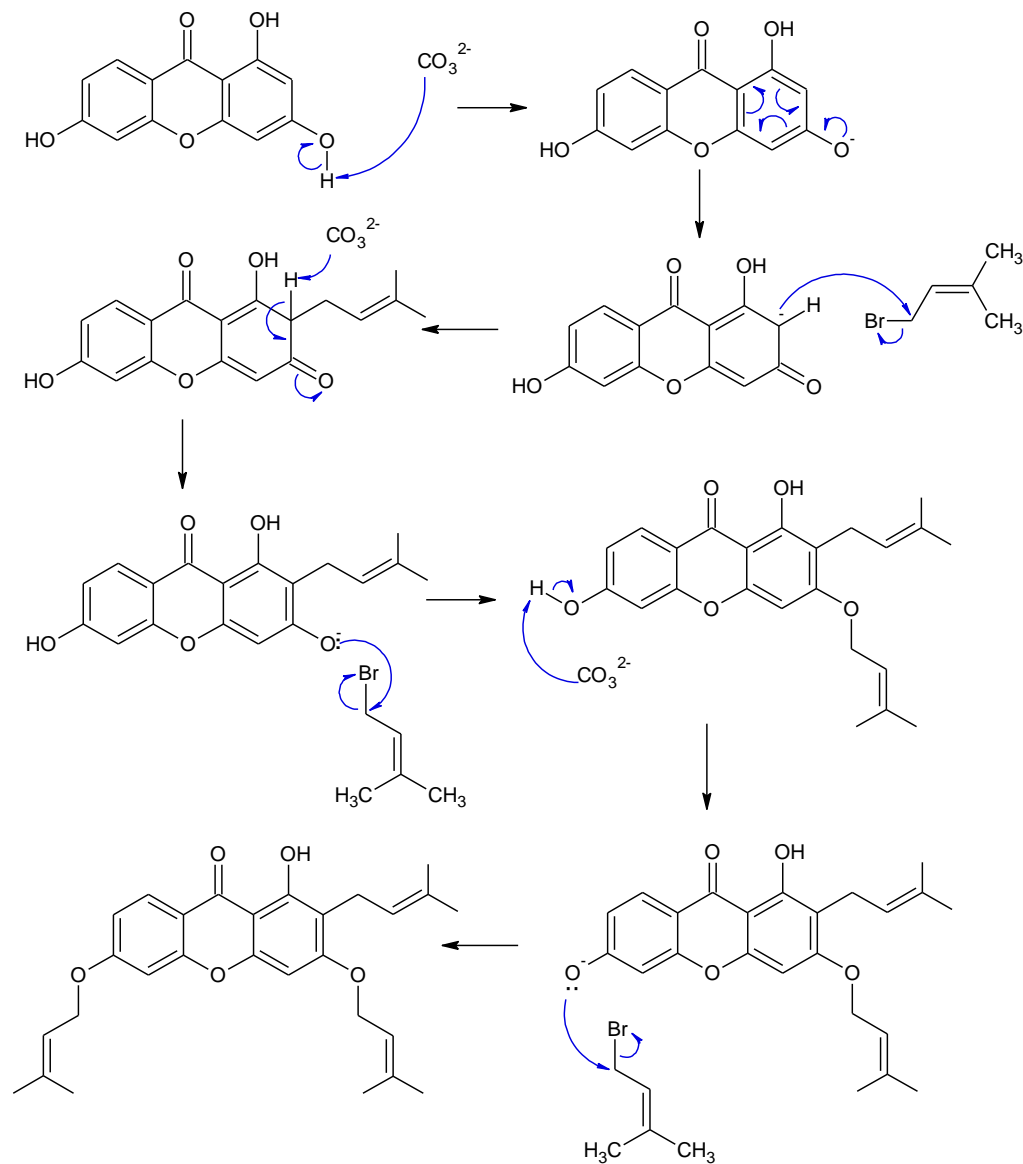
Figure 4.14: Proposed mechanism for synthesis of 1-hydroxy-2-(3-methylbut-2-en-1-yl)-3,6-bis((3-methylbut-2-en-1-yl)oxy)-9*H*-xanthen-9-one (50)

4.2.2 Structural Elucidation of 1-Hydroxy-2-(3-methylbut-2-en-1-yl)-3,6-bis((3-methylbut-2-en-1-yl)oxy)-9*H*-xanthen-9-one
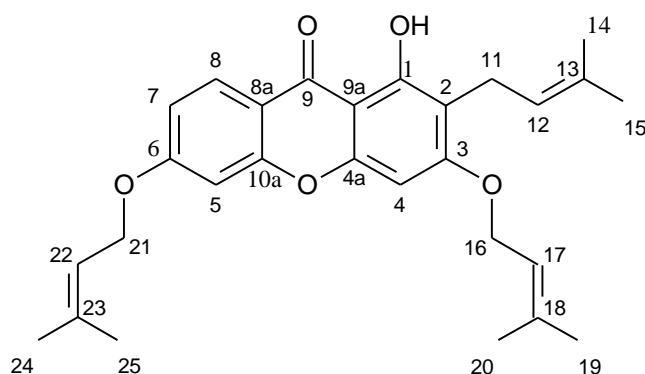
Figure 4.15: Structure of 1-hydroxy-2-(3-methylbut-2-en-1-yl)-3,6-bis((3-methylbut-2-en-1-yl)oxy)-9*H*-xanthen-9-one (50)

The ^{1}H NMR spectrum (Figure 4.16) showed signal of chelated hydroxyl at δ 13.03 (1-OH, s), four aromatic protons at δ 6.40 (1H, s), 6.80 (1H, d, J = 2.4 Hz), 6.90 (1H, dd, J = 9.2, 2.4 Hz) and 8.10 (1H, d, J = 9.2 Hz) which were assigned to protons H-4, H-5, H-7 and H-8, respectively. The absence of the proton signal around δ 6.21 in comparison with ^{1}H-NMR spectrum (Figure 4.5) of xanthonic block indicated *C*-prenylation at the carbon position C-2. Furthermore, the appearance of a doublet signal at δ 4.61 (2H, d, J = 6.7 Hz) integrated for 4 protons revealed the existence of two *O*-prenyl units in the compound **50**.

From the ^{13}C-NMR spectrum (Figure 4.17), a chelated carbonyl group was revealed at δ 180.2, and five quaternary aromatic carbons were assigned at δ 112.0 (C-2), 156.2 (C-4a), 157.9 (C-10a), 114.5 (C-8a) and 103.5 (C-9a). The

presence of four carbons signal at δ 90.6, 100.8, 113.5 and 127.4 were assigned to the protonated aromatic carbons C-4, C-5, C-7 and C-8, respectively and three downfield carbon signals at δ 159.7, 163.3 and 164.4 were assigned to the oxygenated carbons C-1, C-3 and C-6, respectively.

The attachment position of the prenyl unit on the xanthone nucleus was further confirmed on the basis of HMQC and HMBC spectra as shown in Figures 4.18 and 4.19, respectively. From the HMQC analysis, the four protonated aromatic carbon signals at δ 90.6, 100.8, 113.5 and 127.4 were correlated to the proton signals at δ 6.40, 6.80, 6.90 and 8.10, respectively. The cross-peak of proton at δ 4.61 (4H, d, J = 6.7 Hz) with two carbon signals at δ 65.5 and 65.6 revealed the presence of two separate methylene groups in two different prenyl moieties. Besides, correlation of proton signal at δ 3.30 (2H, d, J = 7.3 Hz) to carbon signal at δ 21.5 indicated the presence of third prenyl group attached to the xanthone nucleus. Furthermore, two upfield carbons signals at δ 25.8 and 25.9 showed correlation to two methyl proton signals at δ 1.78 (3H, s) and 1.76 (3H, s), and a methyl proton signal at δ 1.68 (3H, s), respectively. Apart from that, an overlapped proton signal integrated for six protons at δ 1.78 was correlated to the two carbon signals at δ 17.9 and 25.8 signifying the presence of two methyl groups based on the given correlation.

The attachment position of a prenyl moiety to the xanthonic block was further concluded to be at carbon position C-2 based on the HMBC correlations of proton signal H-11 to carbon signals C-2, C-12, and C-13. The proton signals

at δ 1.68 and 1.78 both formed long range heteronuclear connectivity with carbon signals C-12 and C-13. Therefore, carbon signals at δ 17.9 and 25.9 were assigned to be C-14 and C-15, respectively. The remaining two *O*-prenyl groups gave sets of HMBC correlations involved proton signals δ 1.82 (3H, s), and 1.78 (3H, s) to carbons C-17 and C-18; proton signals δ 1.76 (3H, s) and 1.80 (3H, s) to carbons C-22 and C-23.

The IR spectrum in Figure 4.20 exhibited the absorption bands at 3435 (O-H stretch), 2871, 2924, and 2965 (C-H stretch), 1610 (C=O stretch), 1570 and 1448 (aromatic C=C stretch), 1199 cm^{-1} (C-O stretch). The UV-Vis spectrum (Figure 4.21) of compound **50** indicated UV absorption maxima at 203.10, 242.60, 314.37 nm which were typical for xanthone chromophores (Harborne, 1998).

Table 4.4: Summary of NMR data of 1-hydroxy-2-(3-methylbut-2-en-1-yl)-3,6-bis((3-methylbut-2-en-1-yl)oxy)-9H-xanthen-9-one (50)

Position	δH (ppm)	δC (ppm)	HMBC ^2J	HMBC ^3J
1	-	159.7	-	-
2	-	112.0	-	-
3	-	163.3	-	-
4	6.40 (1H, s)	90.6	C3, C4a	C2, C9a
4a	-	156.2	-	-
5	6.80 (1H, d, $J = 2.4$ Hz)	100.8	C6, C10a	C7
6	-	164.4	-	-
7	6.90 (1H, dd, $J = 9.2, 2.4$ Hz)	113.5	-	C5, C8a
8	8.10 (1H, d, $J = 9.2$ Hz)	127.4	-	C6, C9, C10a
8a	-	114.5	-	-
9	-	180.2	-	-
9a	-	103.5	-	-
10a	-	157.9	-	-
11	3.30 (2H, d, $J = 7.3$ Hz)	21.5	C2, C12	C1, C3, C13
12	5.20 (1H, t, $J = 7.3$ Hz)	122.3	-	-
13	-	131.0	-	-
14	1.78 (3H, s)	17.9	C13	C12
15	1.68 (3H, s)	25.9	C13	C12
16	4.61 (2H, d, $J = 6.7$ Hz)	65.5	C17	C18
17	5.50 (1H, m)	119.2	-	-
18	-	139.5	-	-
19	1.82 (3H, s)	17.9	C18	C17
20	1.78 (3H, s)	25.8	C18	C19
21	4.61 (2H, d, $J = 6.7$ Hz)	65.6	C22	C23
22	5.50 (1H, m)	118.6	-	-
23	-	138.5	-	-
24	1.80 (3H, s)	18.4	C23	-
25	1.76 (3H, s)	25.8	C23	C22
1-OH	13.03 (OH, s)	-	C1	C2, C9a
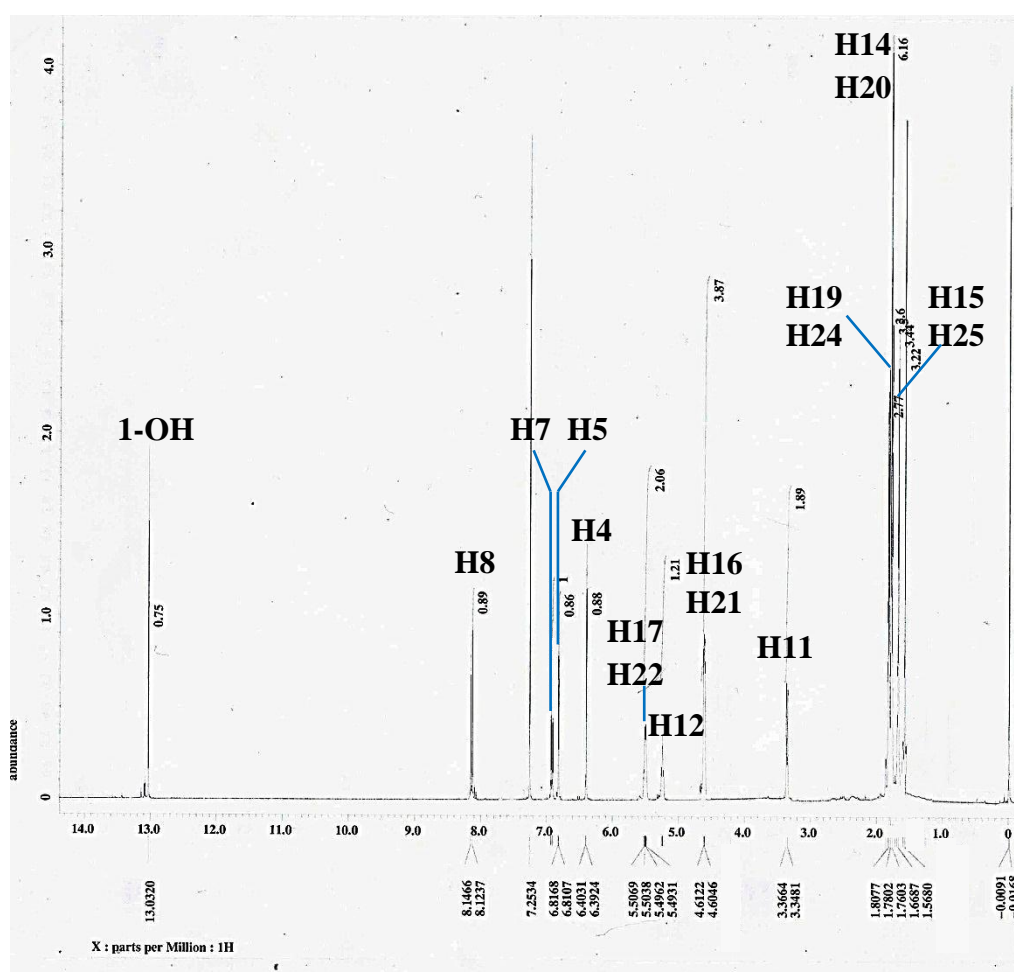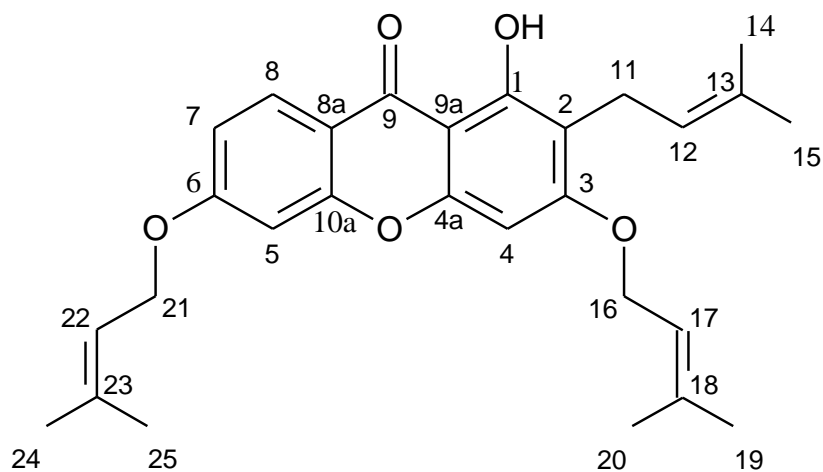
Figure 4.16: ^{1}H-NMR spectrum of 1-hydroxy-2-(3-methylbut-2-en-1-yl)-

3,6-bis((3-methylbut-2-en-1-yl)oxy)-9*H*-xanthen-9-one (50)

(400 MHz, CDCl$_3$)
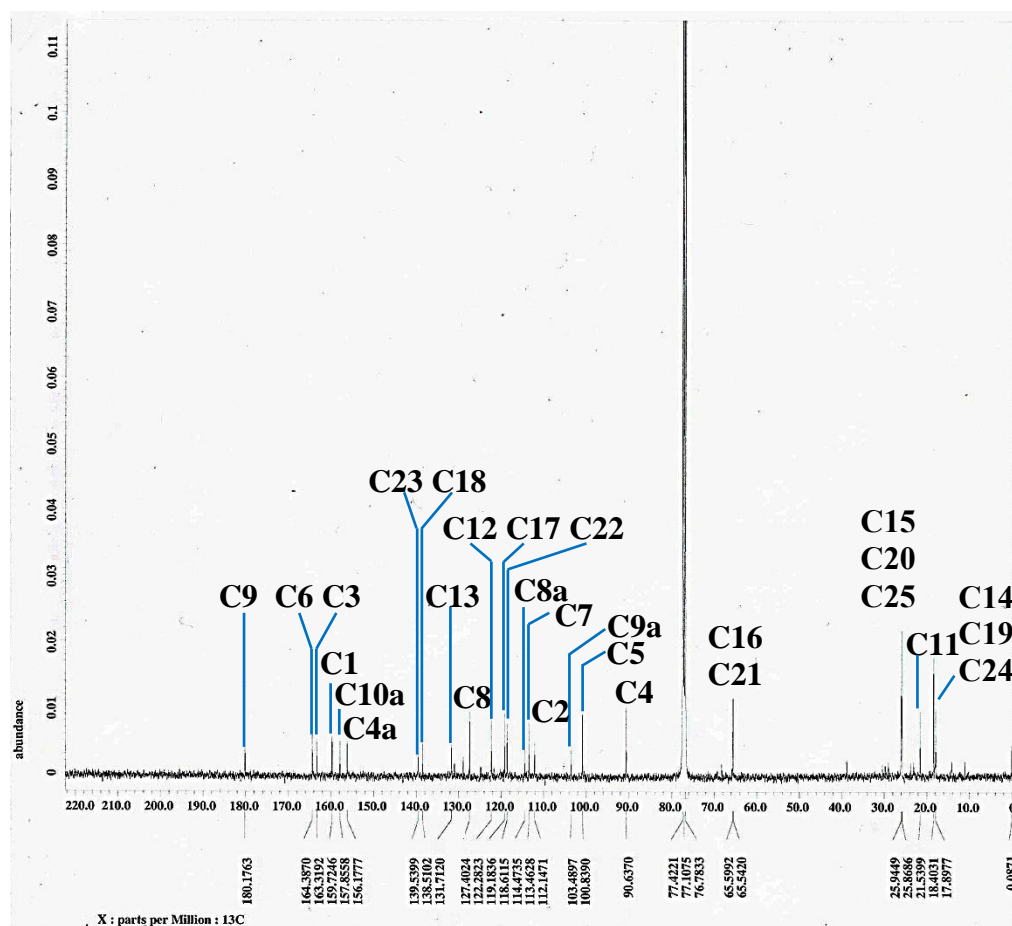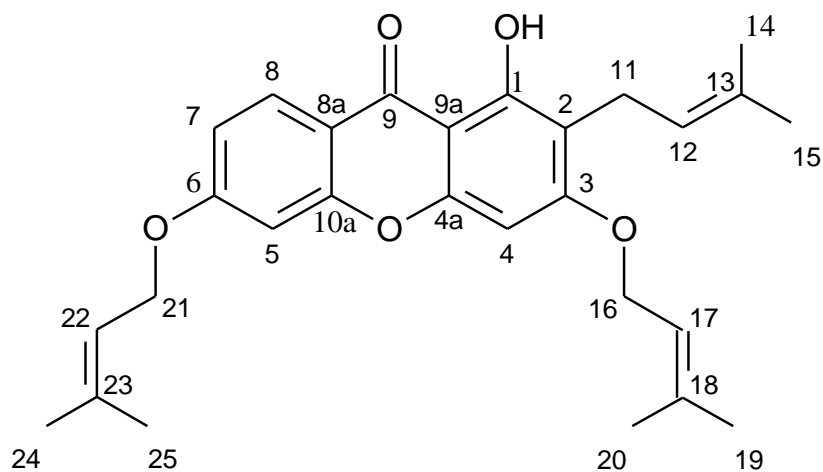
Figure 4.17: ^{13}C-NMR spectrum of 1-hydroxy-2-(3-methylbut-2-en-1-yl)-

3,6-bis((3-methylbut-2-en-1-yl)oxy)-9*H*-xanthen-9-one (50)

(100 MHz, CDCl$_3$)
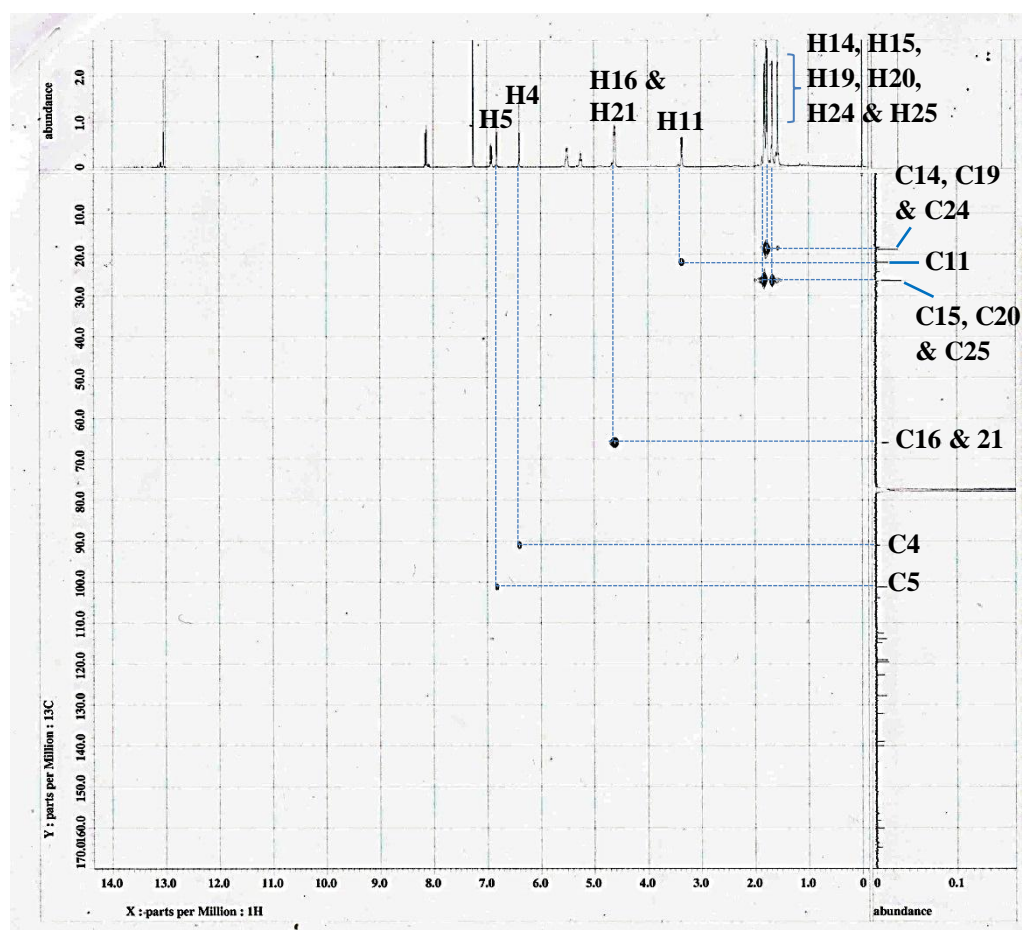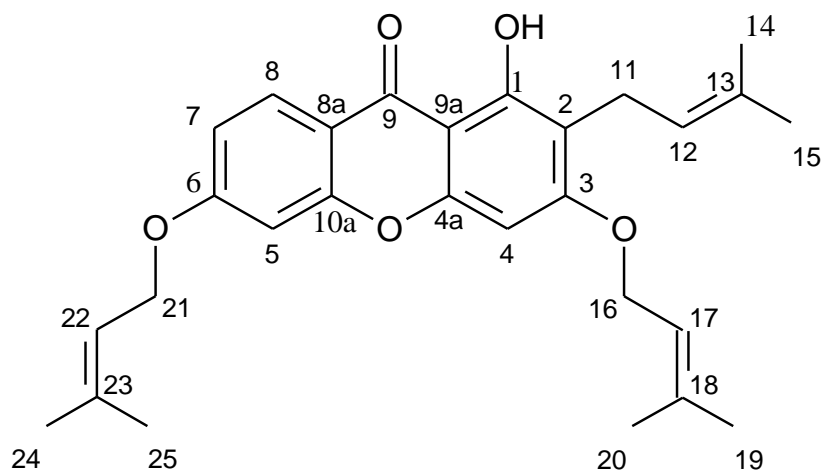
Figure 4.18: HMQC spectrum of 1-hydroxy-2-(3-methylbut-2-en-1-yl)-

3,6-bis((3-methylbut-2-en-1-yl)oxy)-9*H*-xanthen-9-one (50)
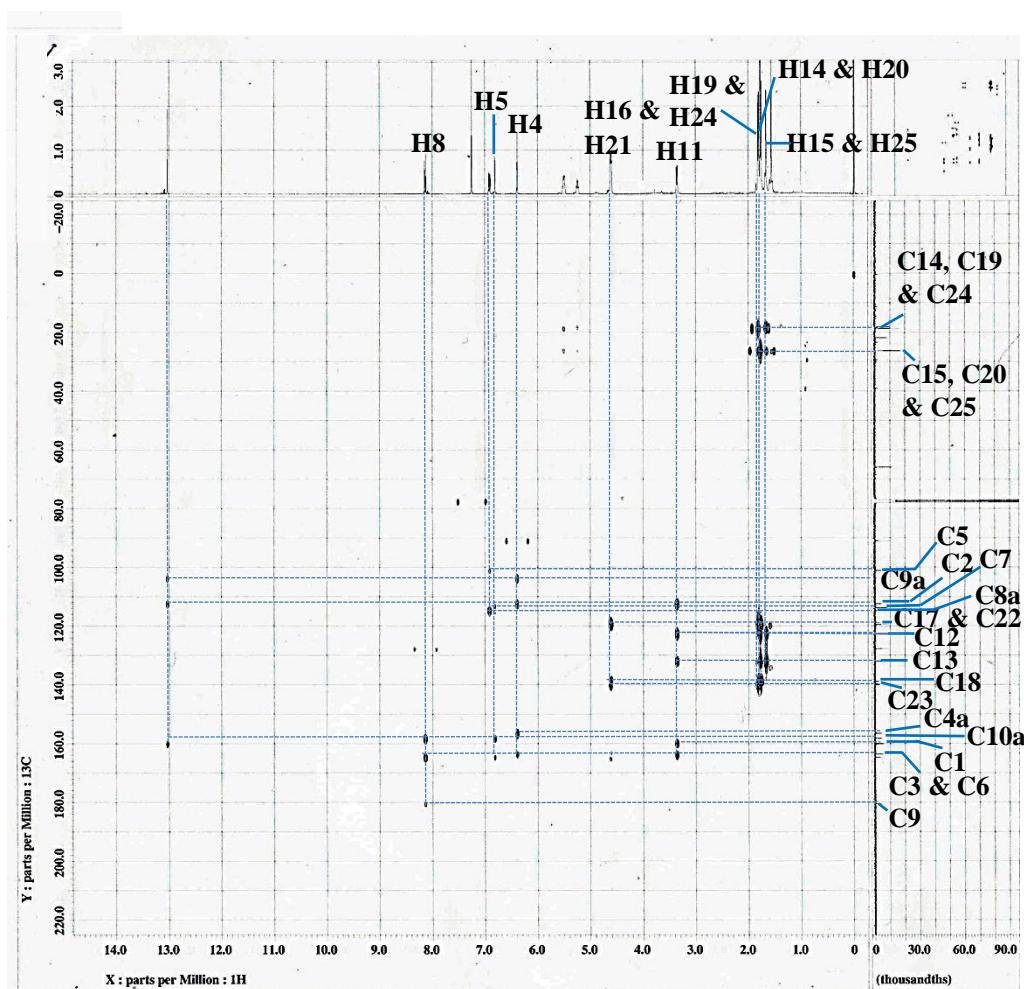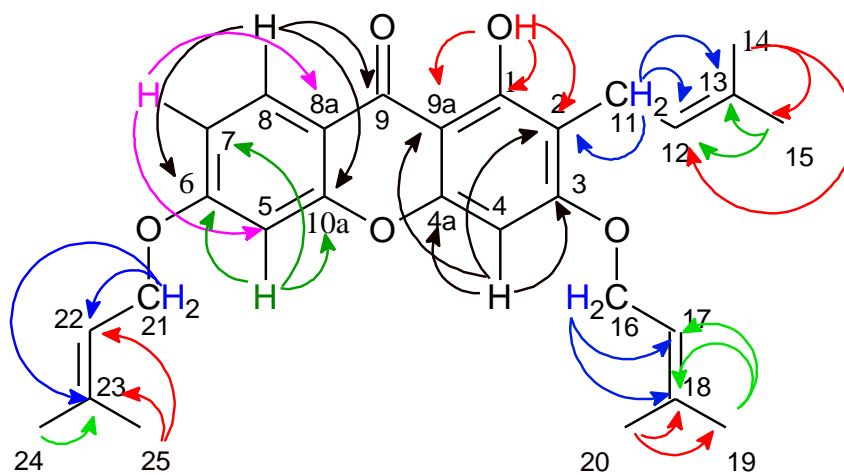
Figure 4.19: HMBC spectrum of 1-hydroxy-2-(3-methylbut-2-en-1-yl)-
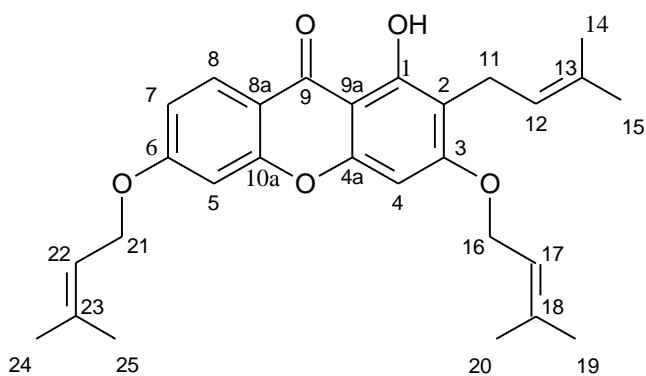
3,6-bis((3-methylbut-2-en-1-yl)oxy)-9H-xanthen-9-one (50)

1-Hydroxy-2-(3-methylbut-2-en-1-yl)-3,6-bis((3-methylbut-2-en-1-yl)oxy)-

9*H*-xanthen-9-one (**50**)

Molecular formula: $C_{28}H_{32}O_5$

Molecular weight: 448.2257 g.mol^{-1}
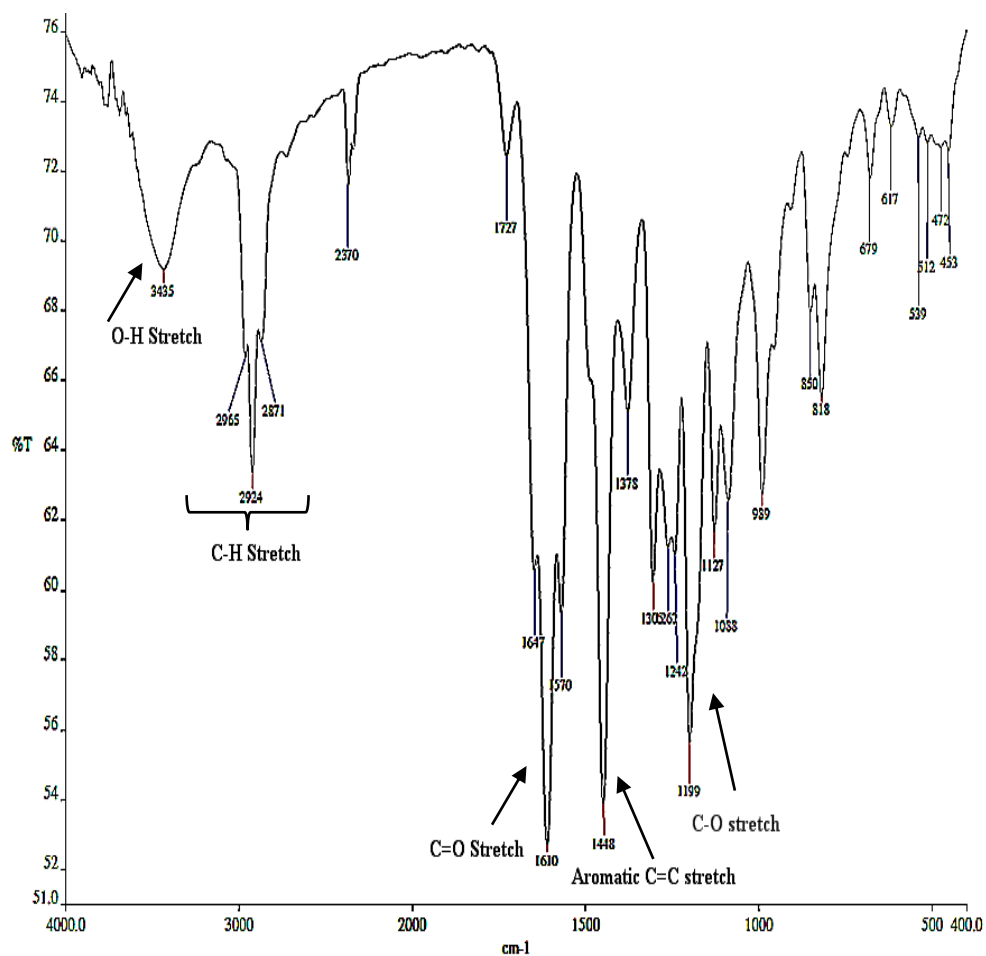
Figure 4.20: IR spectrum of 1-hydroxy-2-(3-methylbut-2-en-1-yl)-3,6-
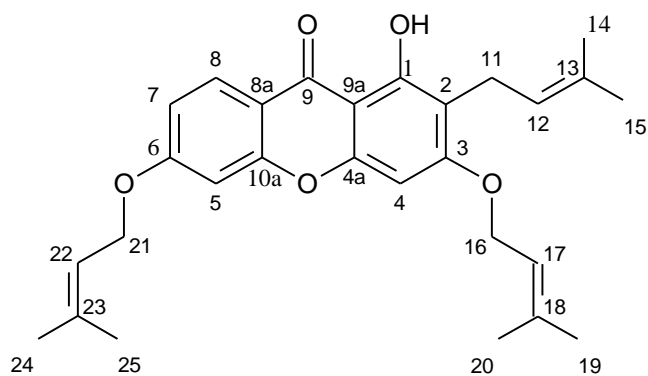
bis((3-methylbut-2-en-1-yl)oxy)-9*H*-xanthen-9-one (50)

1-Hydroxy-2-(3-methylbut-2-en-1-yl)-3,6-bis((3-methylbut-2-en-1-yl)oxy)-

9*H*-xanthen-9-one (**50**)

Molecular formula: $C_{28}H_{32}O_5$

Molecular weight: 448.2257 g.mol^{-1}
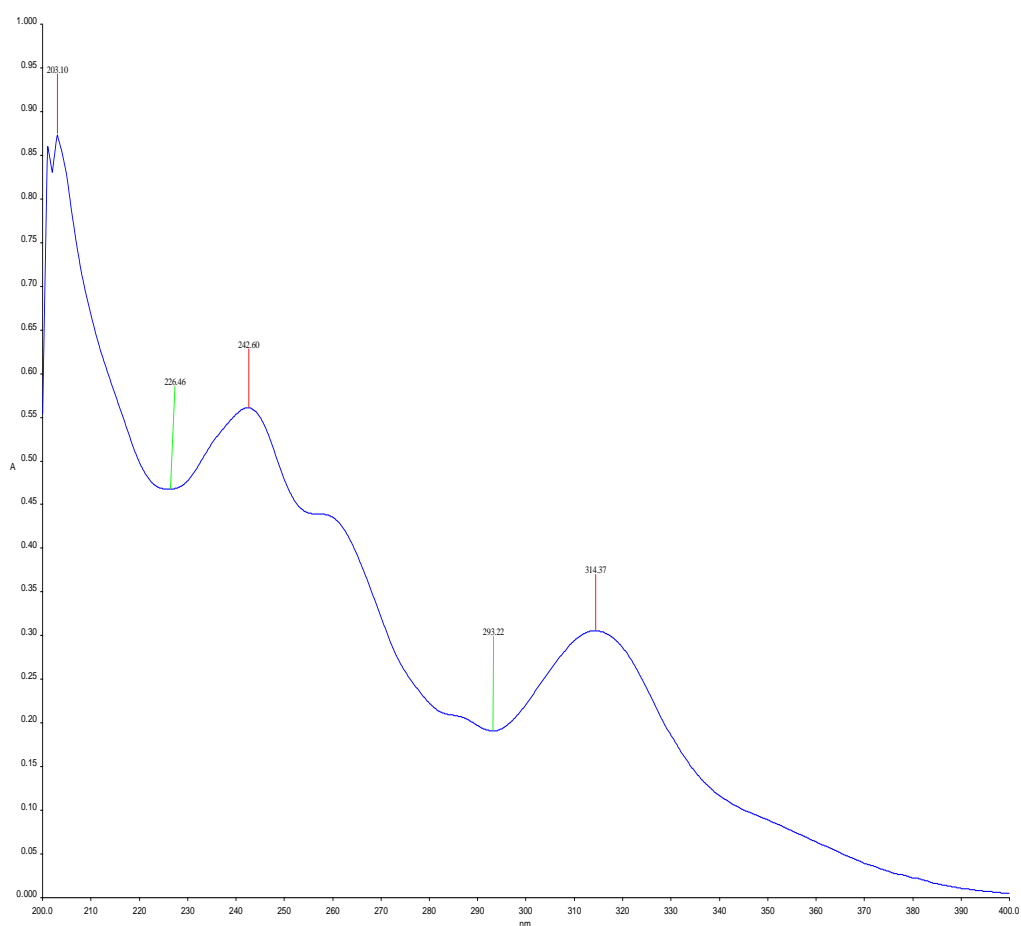
Figure 4.21: UV-Vis spectrum of 1-hydroxy-2-(3-methylbut-2-en-1-yl)-3,6-

bis((3-methylbut-2-en-1-yl)oxy)-9*H*-xanthen-9-one (50)

4.2.3 Proposed Mechanism for Synthesis of 2,2,4,4-Tetrakis(3-methylbut-

2-en-1-yl)-6-((3-methylbut-2-en-1-yl)oxy)-1*H*-xanthene-1,3,9
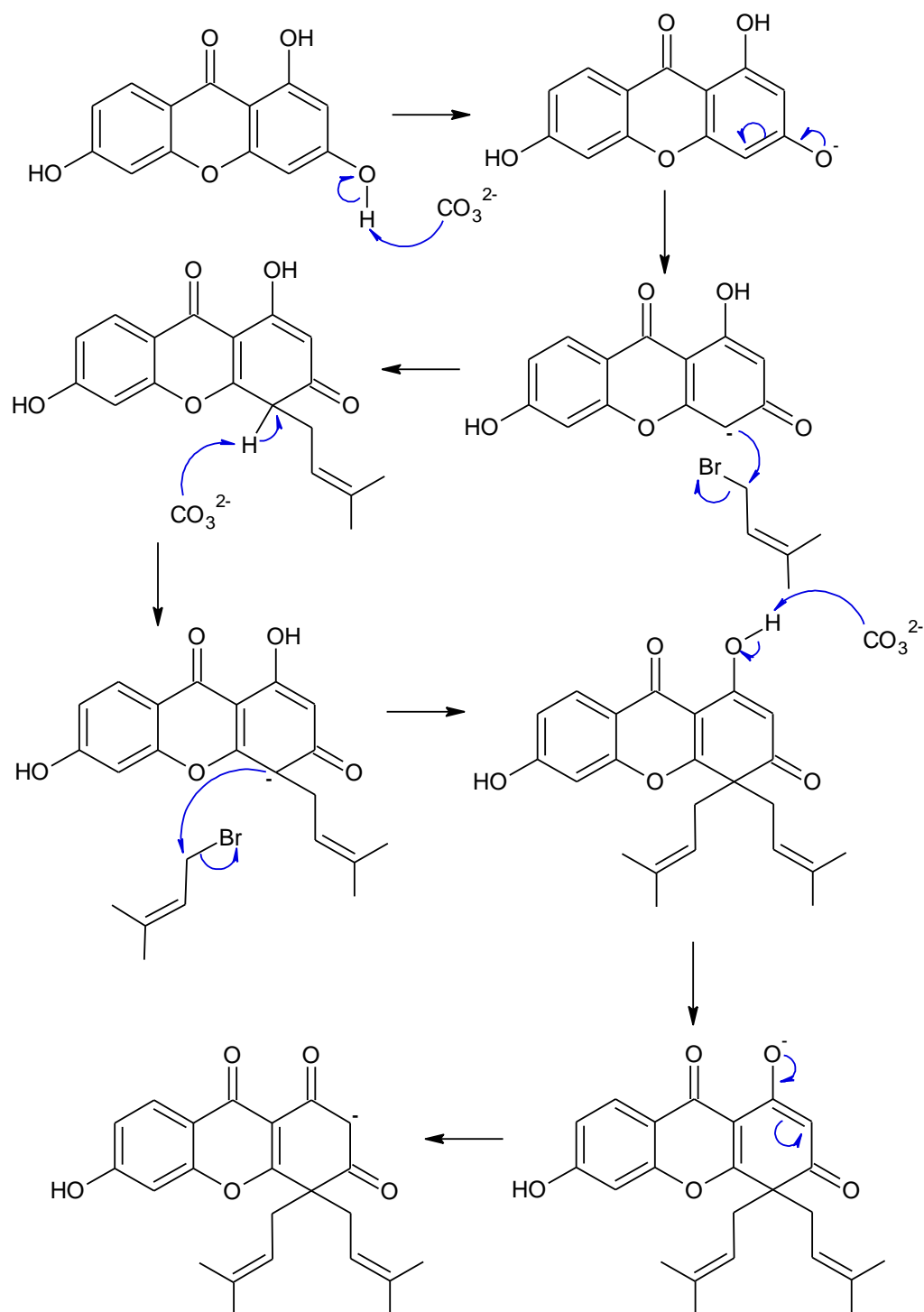
(2*H*,4*H*)-trione

4.2.3 Proposed Mechanism for Synthesis of 2,2,4,4-Tetrakis(3-methylbut-2-en-1-yl)-6-((3-methylbut-2-en-1-yl)oxy)-1*H*-xanthene-1,3,9 (2*H*,4*H*)-trione (continued)
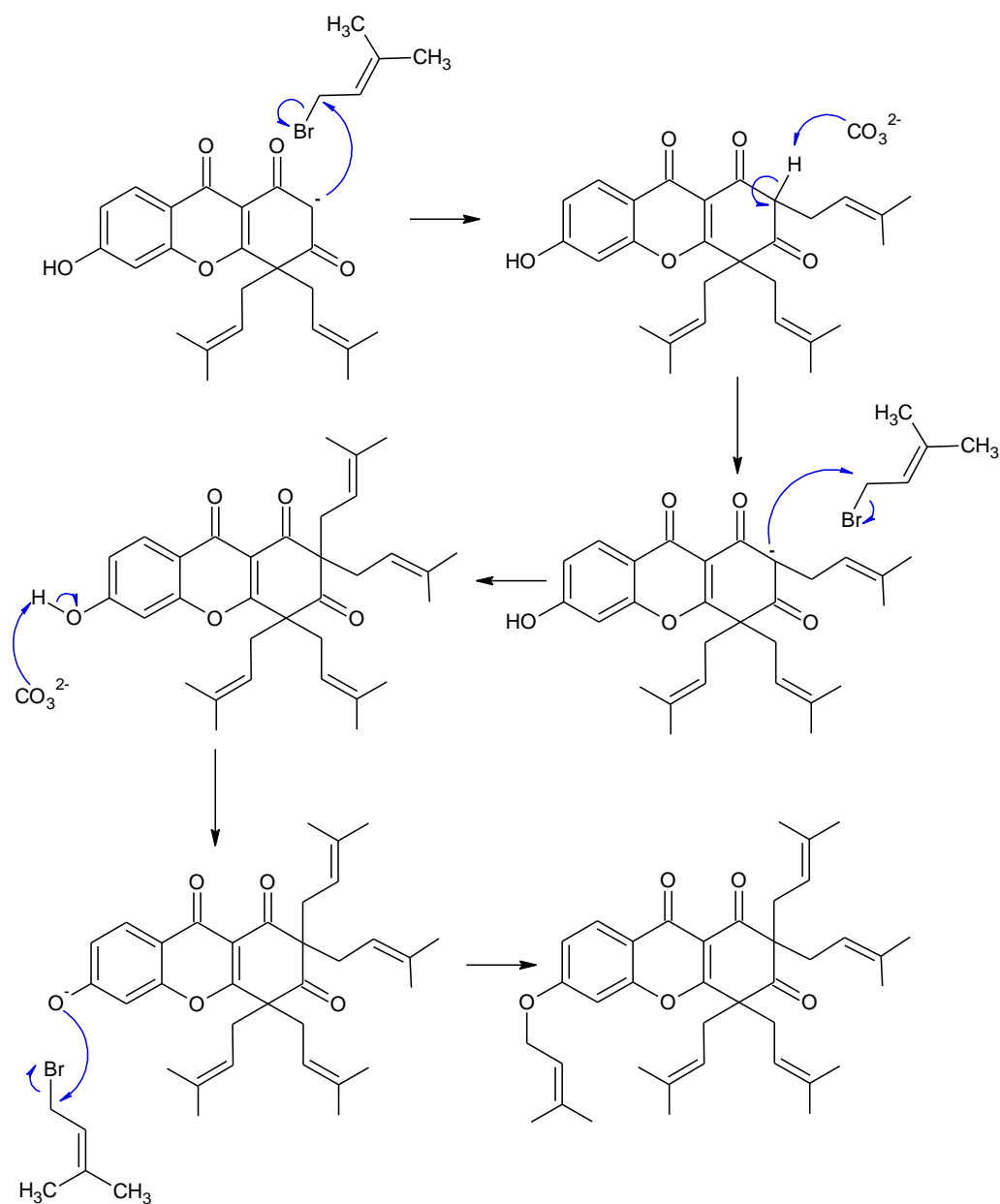
Figure 4.22: Proposed mechanism for 2,2,4,4-tetrakis(3-methylbut-2-en-1-yl)-6-((3-methylbut-2-en-1-yl)oxy)-1*H*-xanthene-1,3,9(2*H*,4*H*)-trione (51)

4.2.4 Structural Elucidation of 2,2,4,4-Tetrakis(3-methylbut-2-en-1-yl)-6-((3-methylbut-2-en-1-yl)oxy)-1*H*-xanthene-1,3,9(2*H*,4*H*)-trione
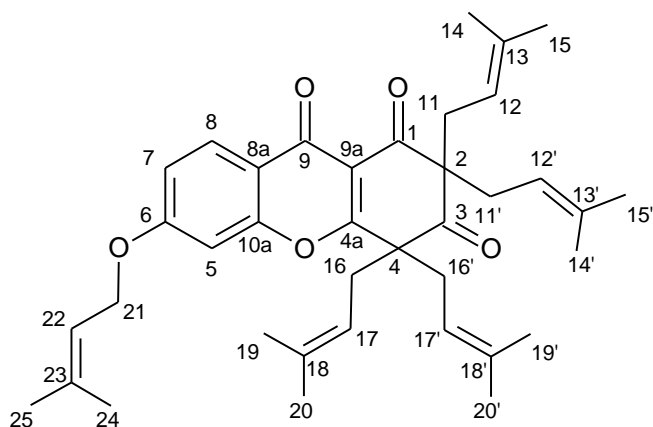
Figure 4.23: Structure of 2,2,4,4-tetrakis(3-methylbut-2-en-1-yl)-6-((3-methylbut-2-en-1-yl)oxy)-1*H*-xanthene-1,3,9(2*H*,4*H*)-trione **(51)**

According to the ^{1}H-NMR in Figure 4.24, the absence of a chelated hydroxyl proton in the downfield region of δ 11.00 to 13.00 confirmed that compound **51** does not carry any hydroxyl group at carbon position C-1. The resonances at δ 6.80 (1H, d, J = 2.1 Hz), 7.00 (1H, dd, J = 8.6, 2.1 Hz), and 8.20 (1H, d, J = 8.6 Hz) were assigned to the protons H-5, H-7 and H-8, respectively in the xanthonic ring B based on the *ortho*-coupling of proton signals H-7 to H-8 (J = 8.6 Hz) and *meta*-coupling of H-7 to H-5 (J = 2.1 Hz). Besides, substitution of protons H-2 and H-4 with the prenyl groups in compound **51** was evidenced by no peak appeared in the range of δ 6.50 - 6.00. The presence of prenyl groups were further confirmed by the presence of characteristic proton signals in the region of δ 2.00 – 6.00.

The ^{13}C-NMR spectrum (Figure 4.25) showed resonances for 28 carbons including three highly deshielded carbonyl signals at δ 201.9 (C-1), 193.2 (C-3), and 173.0 (C-9). The xanthone skeleton was found to be distorted in which carbons C-2 and C-4 were sp^3 hybridized with attachment of two prenyl groups to each of the carbons C-2 and C-4 in the ring, which was found to be different from typical xanthone nucleus with sp^2 hybridized carbons C-2 and C-4. The resonances at δ 101.7, 118.8 and 118.6 were assigned to carbons C-5, C-7 and C-8, respectively. The sp^3 hybridized carbons, C-2 and C-4 were observed at δ 66.9 and 58.9, respectively.

From the HMQC spectrum (Figure 4.26), a cross-peak was observed between proton signal δ 4.60 (2H, d, J = 7.4 Hz) and carbon signal δ 66.2 revealing the presence of *oxy*-methylene group assigned to carbon position C-21. Other correlations observed were δ 1.81 (3H, s) to C-24, δ 1.78 (3H, s) to C-25, δ 1.61 (6H, s) to C-14 & 14', δ 1.57 (6H, s) to C-15 & 15', δ 5.50 (1H, t, J = 7.4 Hz) to C-22, δ 1.52 (6H, s) to C-19 & 19', and δ 1.49 (6H, s) to C-20 & 20'.

In the HMBC spectrum (Figure 4.27), proton signals δ 2.40 (2H, dd, J = 14.0, 6.1 Hz), and 2.50 (2H, dd, J = 14.0, 8.0 Hz) were correlated to the carbons at C-2 and C-12 & C-12' by ^2J coupling and C-1, C-3, C-13 and C-13' by ^3J coupling revealing the presence of geminal diprenyl groups at carbon C-2. The other set of correlations of proton signals δ 2.60 (1H, dd, J = 13.4, 7.3 Hz) and 2.80 (1H, dd, J = 13.4, 8.0 Hz) to carbon signals C-4, C-17, C-17', C-18 and C-18' indicated another pair of geminal diprenyl groups attached to carbon C-4.

The *O*-prenyl group was assigned to carbon C-6 because carbons C-1 and C-3 were oxidized to become carbonyl carbons in the ring which disengaged them from *O*-prenylation.

The IR spectrum in Figure 4.28 indicated absorption bands for compound **51** at 2865, 2924, and 2965 (C-H stretch), 1688 (unconjugated C=O stretch), 1621 (conjugated C=O stretch), 1395 (aromatic C=C stretch), and 1243 cm^{-1} (C-O stretch). Absence of broad peak in the range of 2400 to 3400 cm^{-1} deduced that hydroxyl group was no longer present in this compound (**51**) in comparison with its block (**15**). The UV-Vis spectrum (Figure 4.29) displayed absorption bands at 203.59, 250.22, and 297.03 nm which were typical for xanthone.

Table 4.5: Summary of NMR data of 2,2,4,4-tetrakis(3-methylbut-2-en-1-yl)-6-((3-methylbut-2-en-1-yl)oxy)-1*H*-xanthene-1,3,9(2*H*,4*H*)-trione (51)

| Position	δH (ppm)	δC (ppm)	HMBC ^2J	HMBC ^3J
1	-	207.9	-	-
2	-	66.9	-	-
3	-	193.2	-	-
4	-	58.9	-	-
4a	-	174.1	-	-
5	6.80 (1H, d, J = 2.1 Hz)	101.7	C6, C10a	C7, C8a
6	-	164.3	-	-
7	7.00 (1H, dd, J = 8.6, 2.1 Hz)	118.8	C8	C5
8	8.20 (1H, d, J = 8.6 Hz)	118.6	-	C6, C9, C10a
8a	-	115.0	-	-
9	-	173.0	-	-
9a	-	128.9	-	-
10a	-	157.0	-	-
11	2.40 (1H, dd, J = 14.0, 6.1 Hz)	33.6	C2, C12	C1, C3, C13
	2.50 (1H, dd, J = 14.0, 8.0 Hz)			
12	4.80 (1H, t, J = 8.0 Hz)	119.0	-	C14, C15
13	-	135.7	-	-
14	1.61 (3H, s)	18.5	C13	C15
15	1.57 (3H, s)	26.6	-	C12, C14
16	2.60 (1H, dd, J = 13.4, 7.3 Hz)	38.1	C4, C17	C4a, C18
	2.80 (1H, dd, J = 13.4, 8.0 Hz)			
17	4.90 (1H, t, J = 8.0 Hz)	118.3	-	C19, C20
18	-	137.5	-	-
19	1.52 (3H, s)	18.4	C18	C17, C20
20	1.49 (3H, s)	26.3	C18	C17, C19
21	4.60 (2H, d, J = 7.4 Hz)	66.2	C22	C23
22	5.50 (1H, t, J = 7.4 Hz)	118.9	-	-

Table 4.5: Summary of NMR data 2,2,4,4-Tetrakis(3-methylbut-2-en-1-yl)-

6-((3-methylbut-2-en-1-yl)oxy)-1*H*-xanthene-1,3,9 (2*H,4H)*-

trione (51) (continued)

Position	δH (ppm)	δC (ppm)	HMBC ^2J	HMBC ^3J
23	-	140.3	-	-
24	1.81 (3H, s)	18.9	-	C25
25	1.78 (3H, s)	26.4	C23	C22, C24
11'	2.40 (1H, dd, *J* = 14.0, 6.1 Hz)	33.6	C2, C12'	C1, C3,
	2.50 (1H, dd, *J* = 14.0, 8.0 Hz)			C13'
12'	4.80 (1H, t, *J* = 8.0 Hz)	119.0	-	C14', C15'
13'	-	135.7	-	-
14'	1.61 (3H, s)	18.5	C13'	C15'
15'	1.57 (3H, s)	26.6	-	C14'
16'	2.60 (1H, dd, *J* = 13.4, 7.3 Hz)	38.1	C4, C17'	C18'
	2.80 (1H, dd, *J* = 13.4, 8.0 Hz)			
17'	4.90 (1H, t, *J* = 8.0 Hz)	118.3	-	C19', C20'
18'	-	137.5	-	-
19'	1.52 (3H, s)	18.4	C18'	C17', C20'
20'	1.49 (3H, s)	26.3	C18'	C17', C19'

Figure 4.24: ^{1}H-NMR spectrum of 2,2,4,4-tetrakis(3-methylbut-2-en-1-yl)-

6-((3-methylbut-2-en-1-yl)oxy)-1*H*-xanthene-1,3,9(2*H*,4*H*)-

trione (51) (400 MHz, CDCl$_3$)
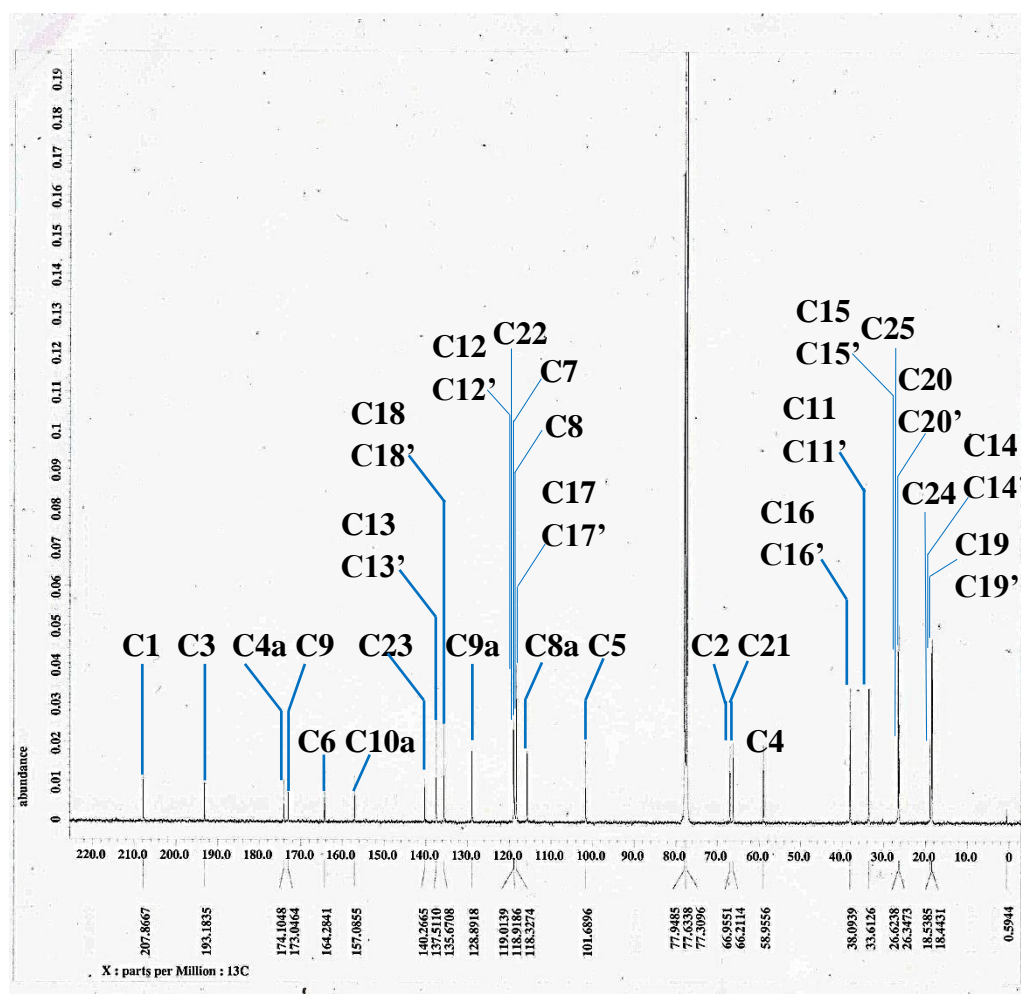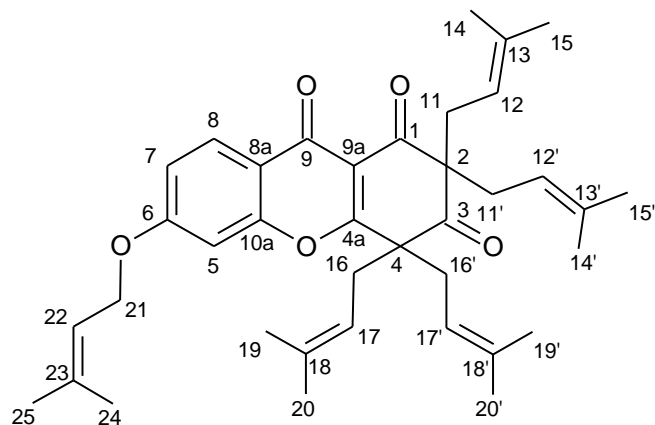
Figure 4.25: ¹³C-NMR spectrum of 2,2,4,4-tetrakis(3-methylbut-2-en-1-yl)-

6-((3-methylbut-2-en-1-yl)oxy)-1*H*-xanthene-1,3,9(2*H*,4*H*)-

trione (51) (100 MHz, CDCl₃)
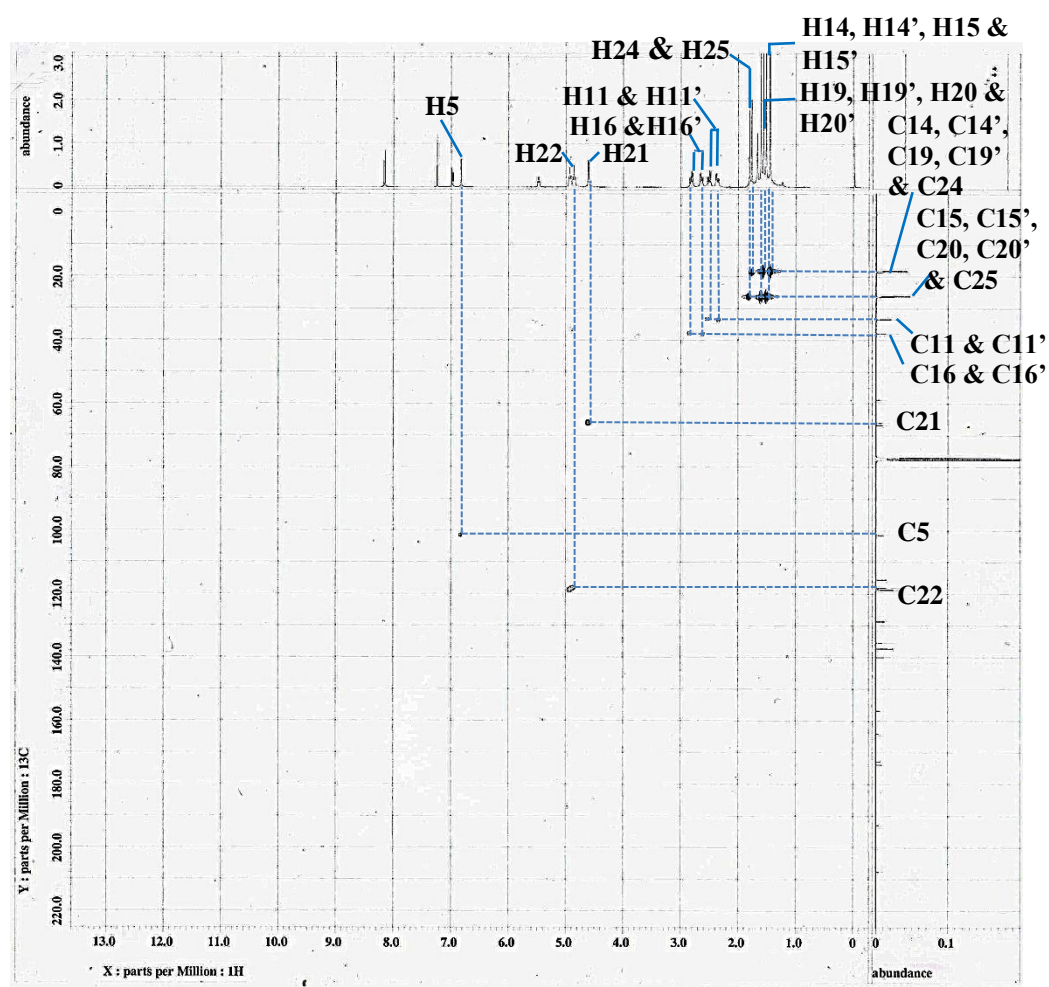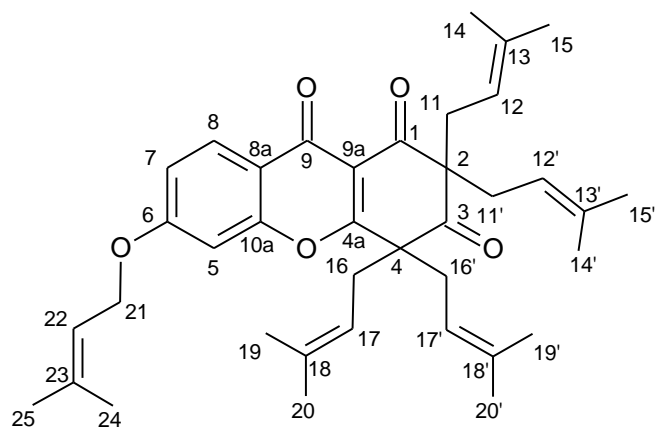
Figure 4.26: HMQC spectrum 2,2,4,4-tetrakis(3-methylbut-2-en-1-yl)-6-((3-methylbut-2-en-1-yl)oxy)-1*H*-xanthene-1,3,9(2*H*,4*H*)-trione (51)
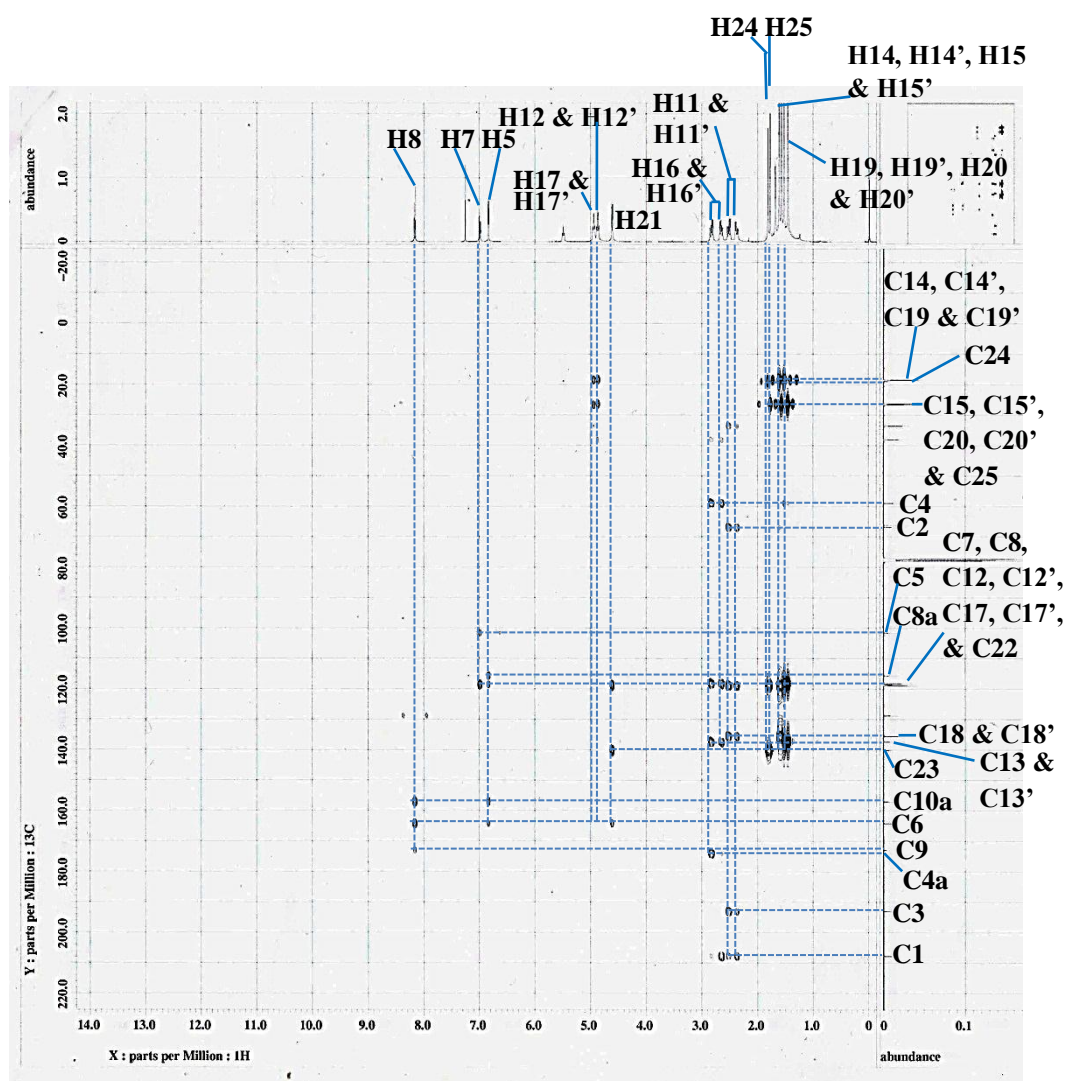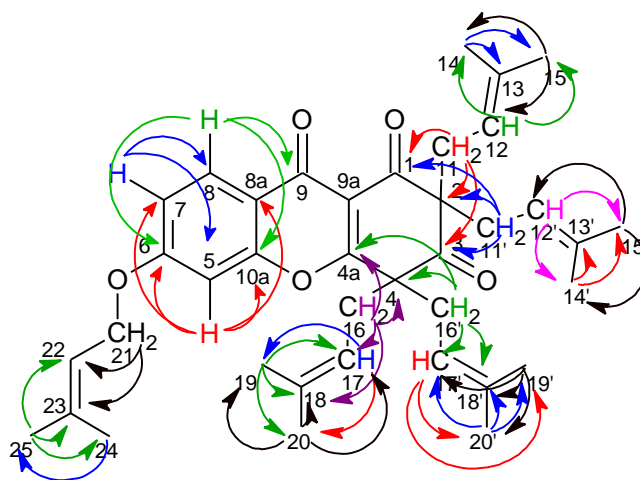
Figure 4.27: HMBC spectrum 2,2,4,4-tetrakis(3-methylbut-2-en-1-yl)-6-((3-methylbut-2-en-1-yl)oxy)-1H-xanthene-1,3,9(2H,4H)-trione (51)
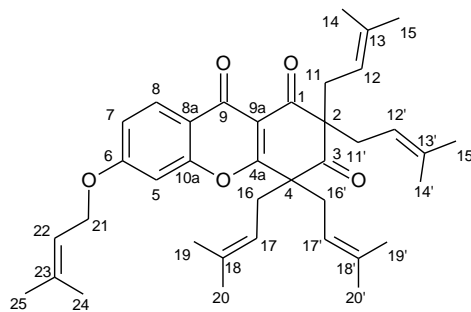
2,2,4,4-Tetrakis(3-methylbut-2-en-1-yl)-6-((3-methylbut-2-en-1-yl)oxy)-1*H*-

xanthene-1,3,9 (2*H*,4*H*)-trione (**51**)

Molecular formula: $C_{38}H_{48}O_5$

Molecular weight: 584.3503 g.mol^{-1}
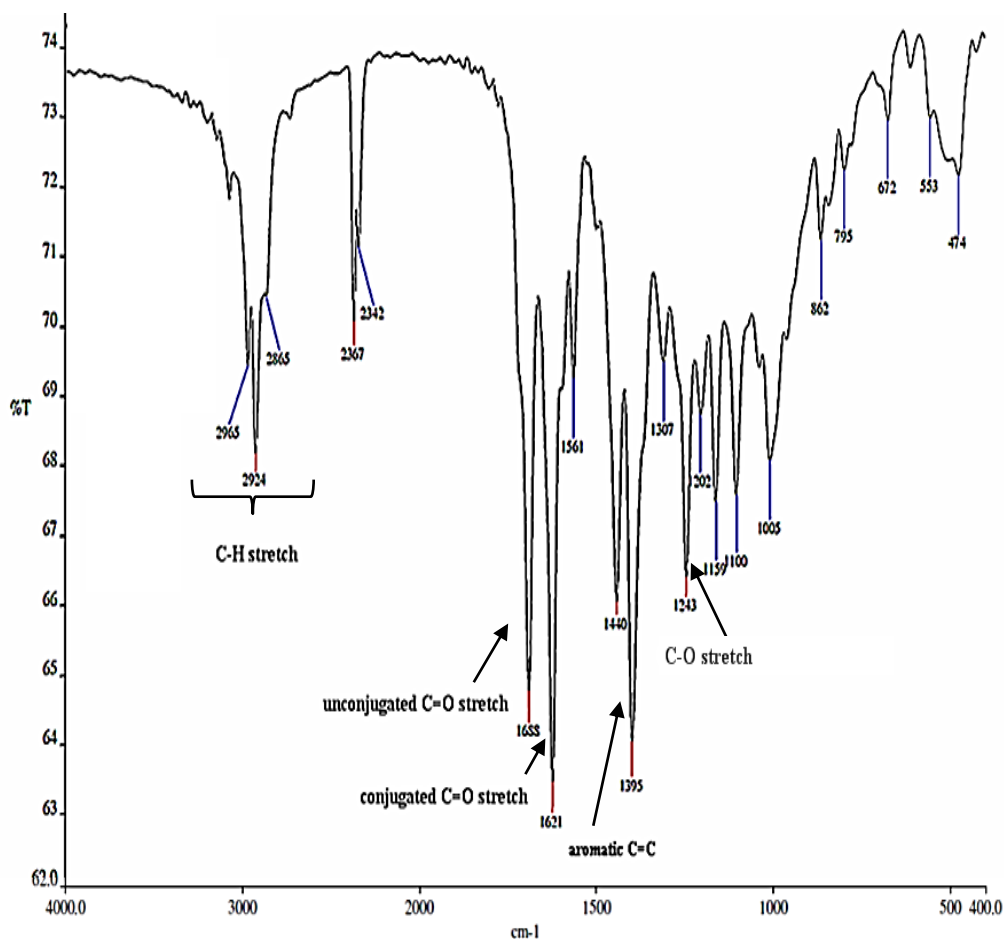
Figure 4.28: IR spectrum of 2,2,4,4-tetrakis(3-methylbut-2-en-1-yl)-6-((3-methylbut-2-en-1-yl)oxy)-1*H*-xanthene-1,3,9(2*H*,4*H*)-trione (51)
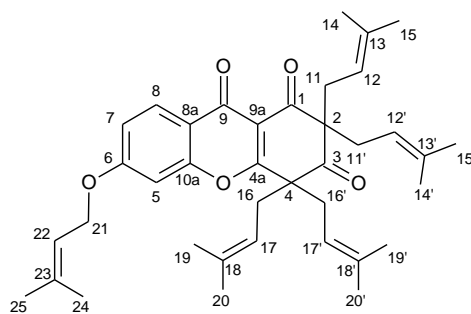
2,2,4,4-Tetrakis(3-methylbut-2-en-1-yl)-6-((3-methylbut-2-en-1-yl)oxy)-1*H*-

xanthene-1,3,9 (2*H*,4*H)*-trione (**51**)

Molecular formula: $C_{38}H_{48}O_5$

Molecular weight: 584.3503 g.mol^{-1}
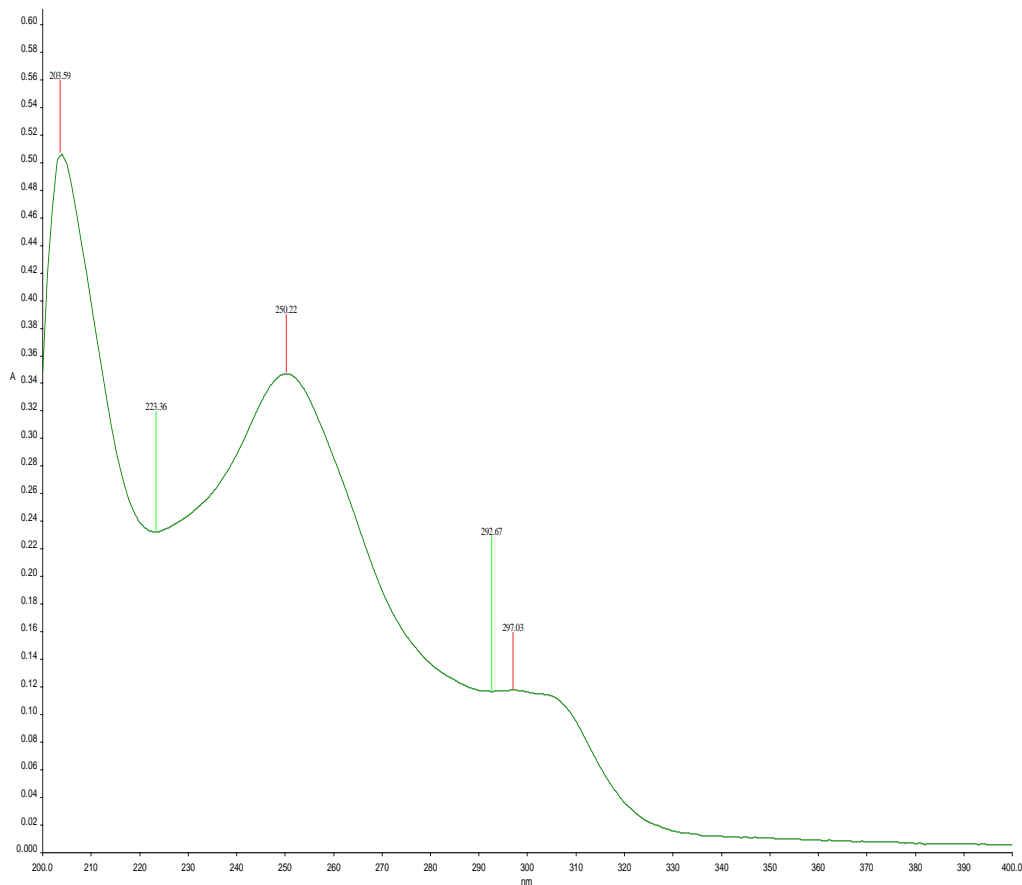
Figure 4.29: UV-Vis spectrum of 2,2,4,4-tetrakis(3-methylbut-2-en-1-yl)-6-

((3-methylbut-2-en-1-yl)oxy)-1*H*-xanthene-1,3,9(2*H*,4*H)-

trione (51)

4.3 Antioxidant Activities

DPPH (1,1-diphenyl-2-dipicrylhydrazyl) assay is a rapid, simple and inexpensive method commonly used to study the antioxidant activities of the test compounds. The antioxidant activity of the test compounds were expressed in inhibition rate (%) with reference to the two reference standards which were ascorbic acid and kaempferol.

Polyphenolic compounds are classified as antioxidant based on the electron donating (labile H atoms) ability to the radicals. Radical scavenging activity depends not only on the rate of labile H atom abstraction from the phenol molecules by DPPH radicals but also on the stability of the phenolic radical formed (Dizhbite, Telysheva, Jurkjane and Viesturs, 2004). Phenolic compounds are usually correlated to antioxidant properties due to its stable aromatic ring. After the scavenging by DPPH radicals, phenolic compound (A-OH) becomes radical (A-O•) but delocalization of π electron makes it become relatively stable. Predominant termination reaction involves further loss of another H atom from the radical, yielding a quinone (A=O). The mechanism is shown as below:

$$\text{A-OH} + \text{DPPH•} \rightarrow \text{A-O•} + \text{DPPH-H}$$

$$\text{AO• (semi-quinone)} \xrightarrow{-\text{H}^+} \text{A=O (quinone)}$$
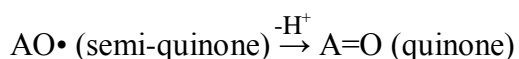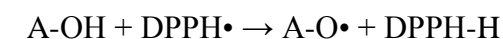
DPPH is a stable free radical giving purple colour and displays a maximum absorption wavelength at 520 nm, which is decolourized to yellow upon reduction to the corresponding hydrazine DPPH-H. The resulted decolourization is stoichiometric with respect to the number of electron captured which in turn shows a decrease absorbance at λ_{max} indicating the scavenging activity of phenolic compounds on the DPPH radicals.

The IC_{50} values defined as effective concentration leading to a 50% loss of DPPH radical activity were obtained by linear regression analysis of the dose response curves, which were plots of percentage of inhibition rate versus concentration as depicted in Figures 4.30, 4.31, 4.32, 4.33 and 4.34. The trihydroxyl groups at C-1, C-3, and C-6 of compound (**15**) gave weak antioxidant activity with IC_{50} value of 167 μg/mL and its DPPH radical scavenging ability was much weaker than that of the standard compounds, ascorbic acid (IC_{50} = 15 μg/mL) and kaempferol (IC_{50} = 8 μg/mL). Meanwhile compounds **50** and **51** showed no significant antioxidant activities although compound **50** possessed a hydroxyl group at C-1. The aromatic ring structure of compound **51** was distorted with the presence of two carbonyl groups positioned at carbons C-1 and C-3 and inhibited from the abstraction of labile H atom by DPPH. As reported by Dizhbite and his co-workers (2004), radical scavenging activity was dependent on the labile hydrogen atom abstraction from the phenolic xanthone compounds.

Table 4.6:   Free radical scavenging activities of the test compounds and the standards used

| Compounds	IC$_{50}$ (µg/mL)
Ascorbic acid (Vitamin C)	15
Kaempferol	8
1,3,6-Trihydroxyxanthone (15)	167
1-Hydroxy-2-(3-methylbut-2-en-1-yl)-3,6-bis((3-methylbut-2-en-1-yl)oxy)-9*H*-xanthen-9-one (50)	>200
2,2,4,4-Tetrakis(3-methylbut-2-en-1-yl)-6-((3-methylbut-2-en-1-yl)oxy)-1*H*-xanthene-1,3,9 (2*H*,4*H*)-trione (51)	>200
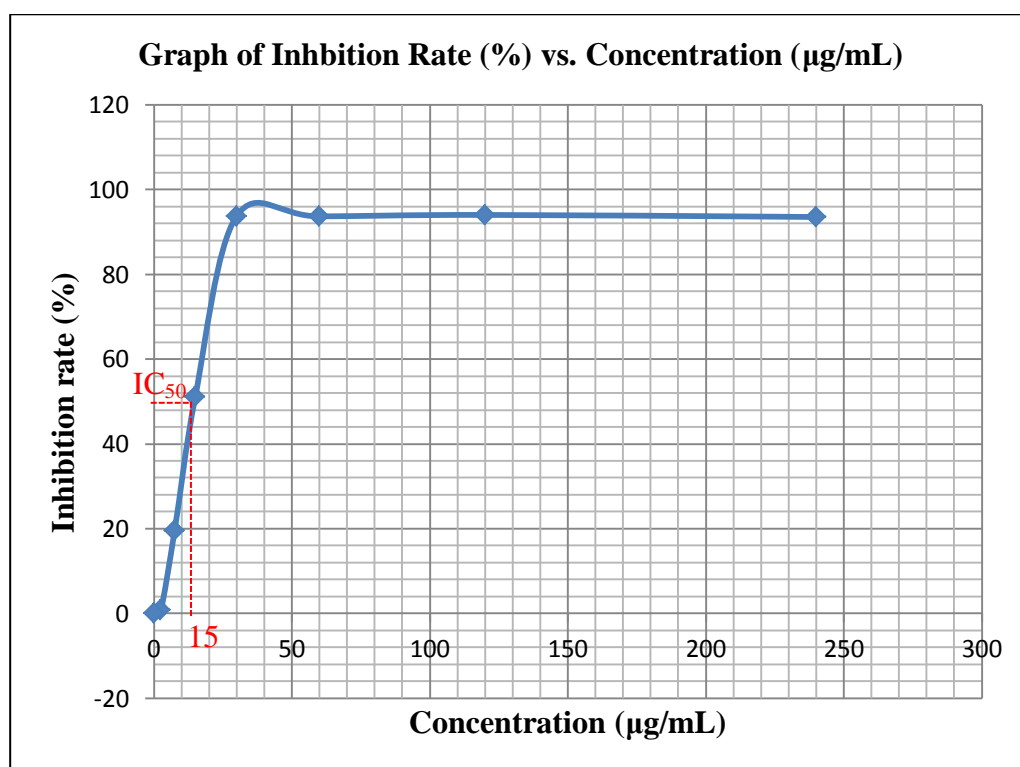
Figure 4.30: Graph of inhibition rate (%) vs. concentration (µg/mL) of ascorbic acid
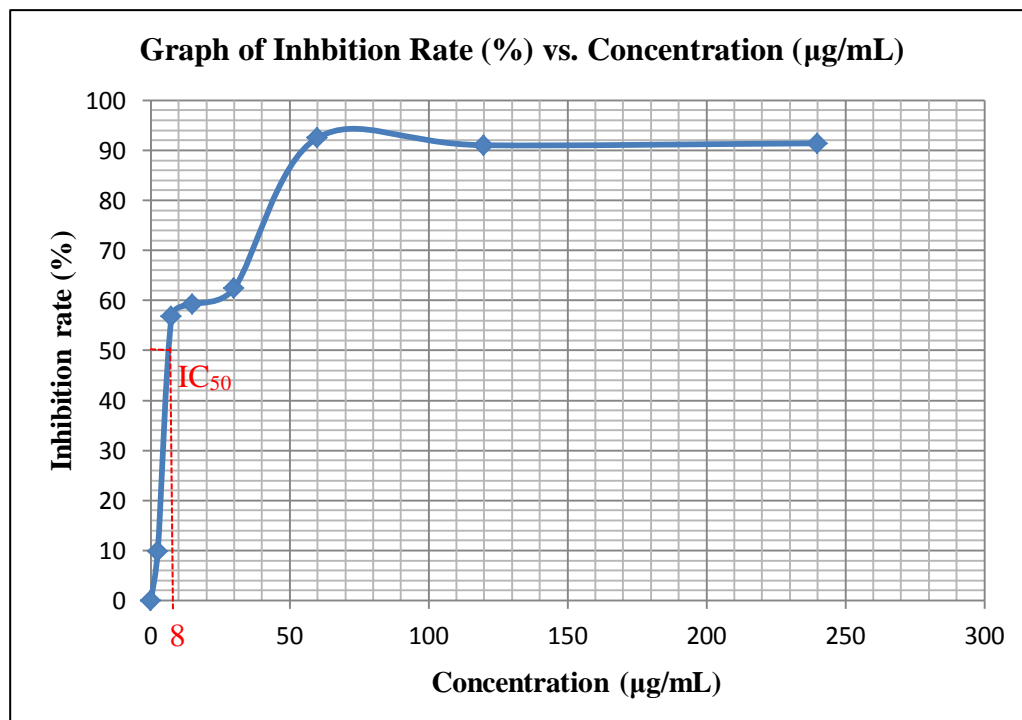
Figure 4.31: Graph of inhibition rate (%) vs. concentration (μg/mL) of

kaempferol
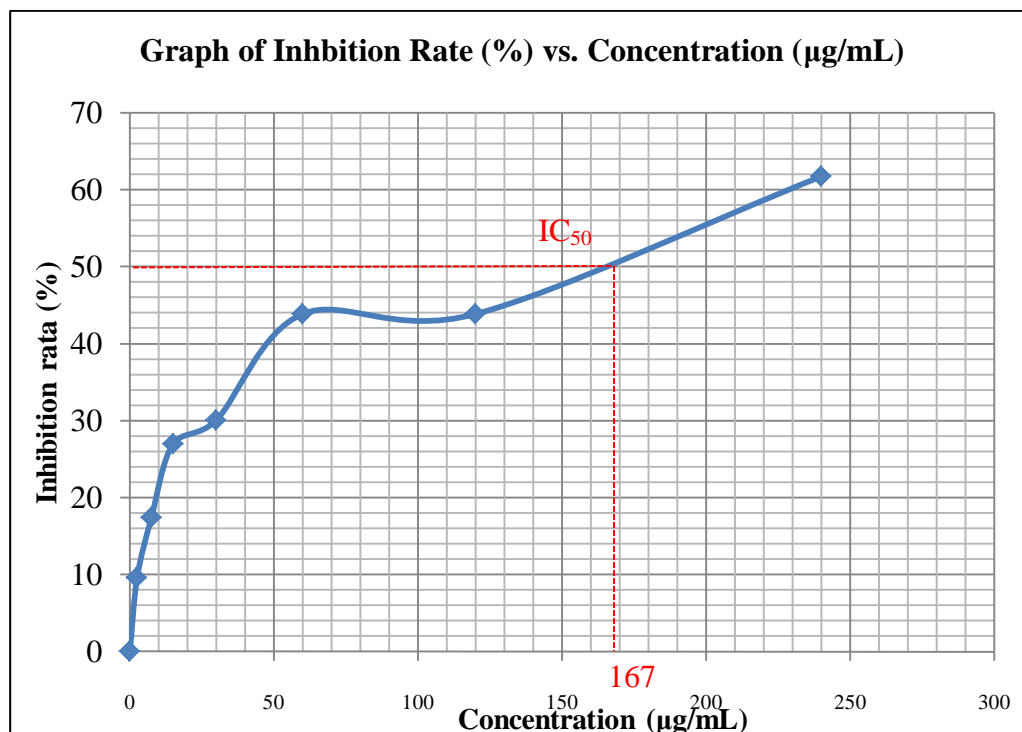
Figure 4.32: Graph of inhibition rate (%) vs. concentration (μg/mL) of

1,3,6-trihydroxyxanthone (15)
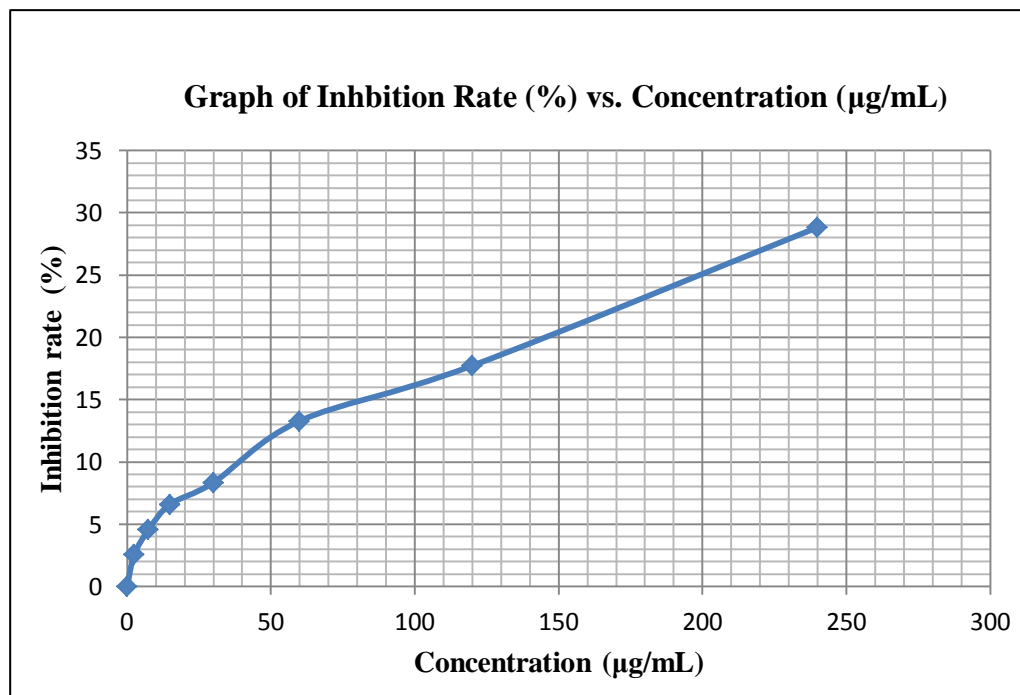
Figure 4.33: Graph of inhibition rate (%) vs. concentration (μg/mL) of 1-hydroxy-2-(3-methylbut-2-en-1-yl)-3,6-bis((3-methylbut-2-en-1-yl)oxy)-9*H*-xanthen-9-one (50)
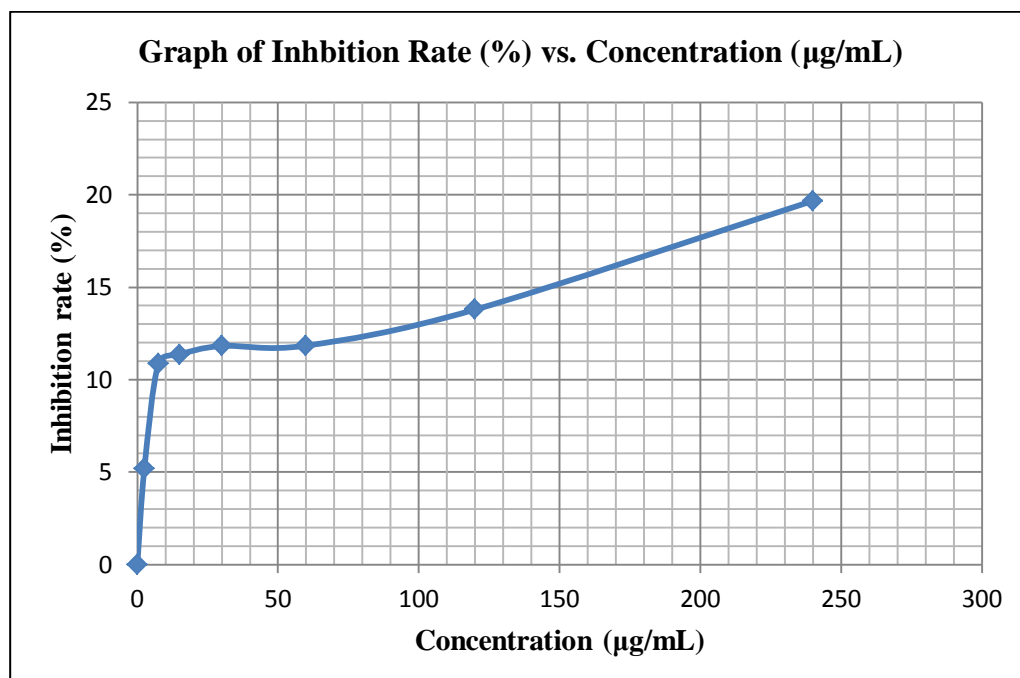
Figure 4.34: Graph of inhibition rate (%) vs. concentration (μg/mL) of 2,2,4,4-tetrakis(3-methylbut-2-en-1-yl)-6-((3-methylbut-2-en-1-yl)oxy)-1*H*-xanthene-1,3,9(2*H*,4*H*)-trione (51)

CHAPTER 5

CONCLUSIONS

5.1 Conclusions

In this study, a xanthonic block 1,3,6-trihydroxyxanthone (**15**) and two new prenylated xanthone derivatives, namely 1-hydroxy-2-(3-methylbut-2-en-1-yl)-3,6-bis((3-methylbut-2-en-1-yl)oxy)-9*H*-xanthen-9-one (**50**), and 2,2,4,4-tetrakis(3-methylbut-2-en-1-yl)-6-((3-methylbut-2-en-1-yl)oxy)-1*H*-xanthene-1,3,9(2*H,4H*)-trione (**51**) were successfully synthesized. The structures of these pure compounds were elucidated through UV-Vis, IR, ^{1}H-NMR, ^{13}C-NMR analyses, and were further confirmed on the basis of 2D-NMR including HMQC and HMBC analyses, and based on the accurate molecular mass data provided by HRESIMS analysis.

The DPPH radical scavenging assay was carried out to study the antioxidant activities of the test compounds, and the results indicated compound **15** showed a much weaker antioxidant activity with an IC$_{50}$ value of 167 μg/mL as compared to the reference compounds, ascorbic acid and kaempferol with their IC$_{50}$ values of 15 μg/mL and 8 μg/mL, respectively. Meanwhile, compounds **50**

and **51** gave insignificant antioxidant activities with their IC_{50} values exceeding 200 µg/mL.

5.2 Future Studies

Microwave-assisted organic synthesis (MAOS) is suggested to be applied in prenylation of xanthone in order to increase the percentage yield of the product and reduce the time of reaction. This technique has proven to increase the yield of *oxy*-prenylated xanthone with a two folds increase in the yields (Castanheiro and Pinto, 2009). Moreover, a chemical synthesis by coupling microwave irradiation with the use of Montmorillonite K10 clay could be carried out in milder conditions, with or without the use of solvent which is found to be more eco-friendly. Study done by Castanheiro and Pinto in year 2009 showed that Claisen rearrangement of prenyl moiety into a fused transformation ring was improved in term of product yield via the technique above.

Secondly, the synthesized compounds in this study should be extended for their biological study on other pharmacological activities such as anti-microbial, cytotoxic, anti-malarial and anti-inflammatory. Moreover, more advanced chromatographic method such as high performance liquid chromatography is suggested to be used to improve separation of the crude products and reduce the time of purification.

REFERENCES

Akrawi, O., Mohammed, H., Patonay, T., Villinger, A. and Langer, 2012. Synthesis of arylated xanthones by site-selective Suzuki Miyaura reactions. *Tetrahedron.*

Banerjee, S. and Mazumdar, S., 2012. Electrospray ionization mass spectrometry: A technique to access the information beyond the molecular weight of the analyte. *International Journal of Analytical Chemistry*, [online] Available at: <http://www.hindawi.com/journals/ijac/2012/282574/>. [Accessed 21 March 2013].

Batchvarov, V. and Marinova, G., 2011. Evaluation of the methods for determination of the free radical scavenging activity by DPPH. *Bulgarian Journal of Agricultural Science,* 17, pp. 11-24.

Blois, M. S., 1958. Antioxidant determinations by the use of a stable free radical. *Nature,* 181(4617), pp. 1199-1200.

Botha, M., 2005. *Use of near infrared spectroscopy (NRIS) and spectrophotometric methods in quality control of Green Rooibos (Aspalathus Linearis) and Honeybush (Cyclopia Genistoides).* Master Thesis, Stellenbosch University, South Africa.

Castanheiro, R. and Pinto, M. M. M., 2009. Improved methodologies for synthesis of prenylated xanthones by microwave. *Tetrahedron,* 1(65), pp. 3848-3857.

Chen, L. G., Yang, L. L. and Wang, C. C., 2008. Anti-inflammatory activity of mangostins from Garcinia mangostana. *Food Chemical Toxicology*, l(46), pp. 688-693.

Cheng, J. H., Huang, A. M., Hour, T. C. and Yang, S. C., 2011. Antioxidant xanthone derivatives induce cell cycle arredt and apoptosis and enhancec cell death induced by cisplation in NTUB1 cells associated with ROS. *European Journal of Medicinal Chemistry,* 46(1), pp. 1222-1231.

Chun-Hui, Y., Li, M., Zhen-ping, W., Feng, H. and Jing, G., 2012. Advances in isolation and synthesis of xanthone derivatives. *Chinese Herbal Medicines,* 4(2), pp. 87-102.

Demirkiran, O., 2007. Xanthone in hypericum: synthesis and biological activities. *Toprical Heterocyclic Chemistry,* 9, pp. 139-178.

Dizhbite, T., Telysheva, G., Jurkjane, V. and Viesturs, U., 2004. Characterization of the radical scavenging activity of lignins-natural antioxidant. *Bioresource Technology,* 95, pp. 309-317.

Dodean, et al., 2008. Synthesis and heme-binding correlation with antimalarial activity of 3,6-bis-(omega-N,N-diethylaminoamyloxy)-4,5-difluoroxanthone. *Bioorganic & Medicinal Chemistry,* 16(3), pp. 1174-1183.

Eaton, P. E., Carlson, G. R. and Lee, J. T., 1973. Phosphorus pentoxide-methanesulfonic acid. Convenient alternative to polyphosphoric acid. *Journal Organic Chemistry,* 38(23), pp. 4071–4073.

El-seedi, et al., 2009. Naturally occuring xanthones; Latest investigations: isolation, strucutre, elucidation and chemosystematic significance. *Current Medicinal Chemistry,* 16, pp. 2581-2626.

Esteves, C. I., Santos, C. M. M., Brito, M. C., Silva, A. M. S. and Caveleiro, J. A. S., 2011. Synthesis of novel 1-aryl-9*H*-xanthene-9-ones. *SYNLETT,* 10, pp. 1403-1406.

Farrell, D., 2006. *Xanthones - the super antioxidant.* [Online]. Available at: http://newconnexion.net/articles/index.cfm/2006/03/xanthones.html [Acceseed 28 December 2012].

FitzGerald, G. A. and Ricciotti, E., 2011. Prostaglandins and Inflammation. *Journal of Arteriosclerosis Thrombosis and Vascualr Biology,* 31(5), pp. 986–1000.

Franklin, G. A., Conceição, L. F., and Komrink, E. and Dias, A. C., 2009. Xanthone biosynthesis in hypericum perforatum cells provides antioxidant and antimicrobial protection upon biotic stress. *Phytochemistry,* 70, pp. 60-68.

Gales, L. and Damas, A. M., 2005. Xanthones- a structural perspective. *Current Medicinal Chemistry,* 12, pp. 2499-2515.

Ghazali, A. I. S. M., Gwendoline, E. C. L. and Ghani, D. A., 2010. Chemical constituent from roots of Garcinia Mangostana (Linn.). *International Journal of Chemistry,* 2(1), pp. 134-142.

Grover, P. I., Shah, G. D. and Shah, R. C., 1955. Xanthones. Part IV. A new synthesis of hydroxyxanthones and hydroxybenzophenones. *National Chemical Laboratory of India*, pp. 3982-3985.

Harborne, J. B., eds 1998. *Phytochemical methods a guide to modern techniques of plant analysis*. New York: Chapman & Hall

Helesbeux, et al., 2004. Synthesis of 2-hydroxy-3-methylbut-3-enyl substituted coumarins and xanthones as natural products. Application of the Schenck ene reaction of singlet oxygen with *ortho*-prenylphenol precursors. *Tetrahedron,* 60, pp. 2293–2300.

Hepworth, H., 1924. *Chemical Synthesis : Studies in the investigation of Natural Organic Products*. London: Blackie and Son Limited.

Ho, C. K., Huang, Y. L. and Chen, C. C., 2002. Garcinone E, a xanthone deriavative, has potent cytotoxic effect against hepatocellular carcinoma cell lines.*Planta Medica,* 68(1), pp. 975-979.

Ignatushcheko, M. V., Winter, R. W. and Riscoe, M., 2000. Xanthones as antimalarial agents: stage specificity. *The American Society of Tropical Medicine and Hygiene,* 62(1), pp. 77–81.

Jiang, D. J., Dai, Z. and Li, Y. J., 2004. Pharmacological effects of xanthones. *Cardiovascular Drug Reviews,* 22(2), pp. 91–102.

Jung, H. A., Su, B. N., Keller, W. J., Mehta, R. G. and Kinghorn, D., 2006. Antioxidant xanthones from pericarp of Garcinia magostana (mangosteen). *Journal of Agricultural and Food Chemistry,* 54(1), pp. 2077-2082.

Khanduja, L. and Bhardwaj, A., 2003. Stable free radical scavenging and antiperoxidative properties of resceratrol compared in vitro with some other bioflavanoids. *Indian Journal of Biochemistry Biophysics,* 40(1), pp. 416-422.

Kosem, N., Han, Y. H. and Moongkarndi, P., 2007. Antioxidant and cytoprotective activities of methanolic extract from Garcinia mangostana hulls. *Science Asia*, 33(1), pp. 283-292.

Kraus, G. A. and Liu, F., 2012. Synthesis of polyhydroxylated xanthones via acyl radical cyclizations. *Tetrahedron Letters,* 53, pp. 111-114.

Kumar, S., 2006. *Spectroscopy of Organic Compounds*.[Online]. Available at: http://nsdl.niscair.res.in/bitstream/123456789/793/1/spectroscopy+of+organic+compounds.pdf [Accessed 16 March 2013].

Lampman, G. M., Pavia, D. P., Kriz, G. S. and Vyvyan, J. R., eds 2010. S*pectroscopy*. USA: Brooks/Cole.

Lee, et al., 2005. Antioxidant and cytotoxic activities of xanthones. *Bioorganic & Medicinal Chemistry Letters,* 15, pp. 5548–5552.

Lesch, B. and Bräse, S., 2004. A short, atom-economical entry to tetrahydroxanthenones. *Angewandte Chemie International Edition,* 43(1), pp. 115-118.

Lew, V., 2003. *Haemoglobin consumption: Eating to stop bursting*. [Online]. Available at: http://malaria.wellcome.ac.uk/doc_WTD023863.html [Accessed 14 March 2013].

Masters, K. S. and Bräse, S., 2012. Xanthones from fungi, lichens, and bacteria: the natural products. *Chemical Reviews,* 112, pp. 3717−3776.

Mengwasser, J. H., 2011. *Lead compounds from nature: synthesis of natural xanthones and chroman aldehydes that inhibit HIV-1*. Graduate Theses and Dissertations, Iowa State University, United States.

Merza, et al., 2004. Prenylated xanthones and tocotrienols from Garcinia virgata. *Phytochemistry,* 65, pp. 2915–2920.

Molyneux, P., 2003. The use of the stable free radical diphenylpicrylhydrazyl(DPPH) for estimating antioxidant activity, *ThaiScience*, 26(2), pp. 211-219.

Molyneux, P., 2004. The use of the stable free radical diphenylpicrylhydrazyl (DPPH) for estimating antioxidant activity. *The Songklanakarin Journal of Science and Technology,* 26(2), pp. 211-219.

Muggia, L., Schmitt, I. and Grube, M., 2009. Lichens as treasure chests of natural products, *Society for Industrial Microbiology and Biotechnology*, May/June, pp. 85-97.

Naidon, J. M., 2009. *Novel methodology for the synthesis of xanthones*. Master Thesis, University of the Witwatersrand, Johannesburg.

Odrowaz-Sypbiewski, R. M., Tsoungas, G. P., Varvounis, G. and Cordopatis, P., 2009. Xanthone in synthesis: a reactivity profile via direct lithiation of its dimethyl ketal. *Tetrahendrom Letters*, pp. 5981-5983.

Petersen, O. H., Spät, A. and Verkhratsky, A., 2005. Introduction: reactive oxygen species in health and disease. *Philosophical Transactions of the Royal Society B,* 360(1464), pp. 2197-2199.

Pedro, M., Cerqueira, F., Sousa, M. E., Nascimento, S. J. and Pinto, M., 2002. Xanthones as inhibitors of growth of human cancer cell. *Bioorganic & Medicinal Chemistry*, 10, pp. 3725–3730.

Peyto, D., Kellyb, K. X. and Dodeana, R. A., 2008. Synthesis and heme-binding correlation with antimalarial activity of 3,6-bis-(ω-N,N-diethylaminoamyloxy)-4,5-difluoroxanthone. *Bioorganic & Medicinal Chemistry,* 16(3), pp. 1174–1183.

Pinto, M. M. M., Sousa, M. E. and Nascimento, M. S. J., 2005. Xanthones derivatives: new insight in biological activities. *Current Medicinal Chemistry,* 12, pp. 2517-2538.

Rai, M. and Chikindas, M. L., 2011. Biologically active chemical constitutents of Garcinia plants. *Natural Antimicrobials in Food Safety and Quality*, United State: CABI.

Riscoe, M., Kelly, J. X. and Winter, R., 2005. Xanthone as antimalarial agent: discovery, mode of action, and optimization. *Current Medicinal Chemistry,* 12, pp. 2539-2549.

Samaga, P. V., 2012. *Using DPPH Radical scavenging assay to measure antioxidants in vegetable oil.* [Online]. Available at: http://www.researchgate.net/post/Using_DPPH_Radical_scavenging_ assay_to_measure_antioxidants_in_vegetable_oil10 [Accessed 21 March 2013].

Shifko, R., 2010. *What are the benefits of xanthones ?* [Online]. Available at: http://www.livestrong.com/article/323087-what-are-the-benefits-of-xanthones/ [Accessed 1 January 2013].

Silva, A. M. S. and Pinto, D. C. G. A., 2005. Structure elucidation of xanthone deriavatives: studies of nuclear magnetic resonance spectroscopy. *Current Medicinal Chemistry,* 12, pp. 2481-2497.

Sousa, M. E. and Pinto, M. M. M., 2005. Synthesis of xanthones: an overview. *Current Medicinal Chemistry,* 12, pp. 2447-2479.

Subba-Rao, G. S. R. and Raghavan, S., 2001. Synthetic studies on morellin. Part 4: synthesis of 2,2-dimethyl-2-[3-methylbut-2-enyl]-2H,6H-pyrano[3,2-b]xanthen-6-one. *Journal of the Indian Insitutet of Science,* 81, pp. 393-401.

Tanaka, N., Kashiwada, Y., Kim, S. Y., Sekiya, M. and Ikeshiro, Y., 2009. Xanthones from hypericum chinense and their cytotoxicity evaluation. *Phytochemistry,* 70, pp. 1456-1461.

Yang, et al., 2012. Preparation of tetrahydroisoquinoline-3-ones via cyclization of phenyl acetamides using Eaton's reagent', *Organic Syntheses,* 89, pp. 44-54.

Yu, et al., 2007. Phenolics from hull of Garcinia mangostana fruit and their antioxidant activities. *Food Chemistry,* 104, pp. 178-181.

Zarena, A.S. and Sankar, K.U., 2009. Supercritical carbon dioxide extraction of xanthones with antioxidant activity. *Journal of Supercritical Fluids,* 4, pp. 330–337.

Zhang, Y., Song, Z., Hao, J., Qiu, S. and Xu, Z., 2010. Two new prenylated xanthones and a new prenylated tetrahydroxanthone. *Fitoterapia,* 81, pp. 595–599.

APPENDICES

APPENDIX A

The following table summarizes the results of inhibition rates at different concentrations for ascorbic acid from the DPPH assay.

Concentration	Absorbance				Inhibition rate (%)
	1st	2nd	3rd	Mean[1]	
240.0	0.0882	0.0734	0.0671	0.0762 ± 0.0108	93.52
120.0	0.0685	0.0705	0.0726	0.0705 ± 0.0021	94.01
60.0	0.0750	0.0761	0.0729	0.0747 ± 0.0016	93.66
30.0	0.0752	0.0688	0.0768	0.0736 ± 0.0042	93.75
15.0	0.6535	0.8640	0.2077	0.5751 ± 0.3351	51.15
7.5	0.9907	0.7656	1.0867	0.9477 ± 0.1648	19.50
2.5	1.3920	1.0256	1.0871	1.1682 ± 0.1962	0.76
0.0	1.2891	1.0706	1.1718	1.1772 ± 0.1093	0.00

[1] Each value was obtained by calculating the average of three experiments ± standard deviation.

APPENDIX B

The following table summarizes the results of inhibition rates at different concentrations for kaempferol from the DPPH assay.

Concentration	Absorbance				Inhibition
	1st	2nd	3rd	Mean[1]	rate (%)
240.0	0.0724	0.0844	0.0743	0.0770 ± 0.0065	91.40
120.0	0.0688	0.0680	0.1046	0.0805 ± 0.0209	91.02
60.0	0.0632	0.0647	0.0739	0.0673 ± 0.0058	92.49
30.0	0.3209	0.3576	0.3303	0.3363 ± 0.0191	62.46
15.0	0.3865	0.3896	0.3200	0.3654 ± 0.0393	59.21
7.5	0.3753	0.3484	0.4370	0.3869 ± 0.0454	56.81
2.5	0.8210	0.8409	0.7593	0.8071 ± 0.0425	9.90
0.0	0.9590	0.9642	0.7640	0.8957 ± 0.1141	0.00

[1] Each value was obtained by calculating the average of three experiments $\pm$ standard deviation.

APPENDIX C

The following table summarizes the results of inhibition rates at different concentrations for 1,3,6-trihydroxyxanthone (**15**) from the DPPH assay.

Concentration	Absorbance						Inhibition
	1st	2nd	3rd	Mean[1]			rate (%)
240.0	0.6401	0.6054	0.5706	0.6054	±	0.0348	61.71
120.0	0.8806	0.8732	0.9098	0.8879	±	0.0194	43.84
60.0	0.7411	0.8486	1.0734	0.8877	±	0.1696	43.85
30.0	1.2484	0.9322	1.1363	1.1056	±	0.1603	30.06
15.0	0.9020	1.1931	1.3678	1.1543	±	0.0356	26.98
7.5	1.2696	1.3052	1.3407	1.3052	±	0.0921	17.44
2.5	1.5216	1.3375	1.4296	1.4296	±	0.2353	9.57
0.0	1.6933	1.5789	1.4705	1.5809	±	0.1114	0.00

[1] Each value was obtained by calculating the average of three experiments ± standard deviation.

APPENDIX D

The following table summarizes the results of inhibition rates at different concentrations for 1-hydroxy-2-(3-methylbut-2-en-1-yl)-3,6-bis((3-methylbut-2-en-1-yl)oxy)-9*H*-xanthen-9-one (**50**) from the DPPH assay.

Concentration	Absorbance						Inhibition rate (%)
	1st	2nd	3rd	Mean[1]			
240.0	0.9482	0.8765	1.1279	0.9842	±	0.1295	28.83
120.0	1.1038	1.1714	1.1377	1.1376	±	0.0338	17.73
60.0	1.2445	1.0792	1.2734	1.1990	±	0.1048	13.29
30.0	1.2703	1.1964	1.3359	1.2675	±	0.0698	8.34
15.0	1.2574	1.3027	1.3141	1.2914	±	0.0300	6.61
7.5	1.3377	1.2555	1.3657	1.3196	±	0.0573	4.57
2.5	1.2875	1.2204	1.5343	1.3474	±	0.1653	2.56
0.0	1.3520	1.4021	1.3945	1.3829	±	0.0270	0.00

[1] Each value was obtained by calculating the average of three experiments ± standard deviation.

APPENDIX E

The following table summarizes the results of inhibition rates at different concentrations for 2,2,4,4-tetrakis(3-methylbut-2-en-1-yl)-6-((3-methylbut-2-en-1-yl)oxy)-1*H*-xanthene-1,3,9(2*H,4H)*-trione (**51**) from the DPPH assay.

Concentration	Absorbance					Inhibition rate (%)
	1st	**2nd**	**3rd**	**Mean**[1]		
240.0	1.1508	1.1648	1.0902	1.1353 ±	0.0397	19.67
120.0	1.1324	1.4043	1.1180	1.2182 ±	0.1613	13.79
60.0	1.2996	1.2344	1.2036	1.2459 ±	0.0490	11.84
30.0	1.2273	1.2770	1.2341	1.2461 ±	0.0269	11.82
15.0	1.3154	1.2267	1.2158	1.2526 ±	0.0546	11.36
7.5	1.2773	1.2673	1.2344	1.2597 ±	0.0224	10.86
2.5	1.4157	1.2708	1.3334	1.3400 ±	0.0727	5.18
0.0	1.3520	1.3301	1.2574	1.4132 ±	0.1254	0.00

[1] Each value was obtained by calculating the average of three experiments ± standard deviation